PROTEUS

ADAPTIVE MICROFLUIDIC - AND NANO - ENABLED SMART SYSTEMS FOR WATER QUALITY SENSING

WP2-Smart Systems co-design and sub-part specifications

D2.1

First version of smart system co-design

Author/Editor: **UNINOVA**

June, 26th 2015

www.proteus-sensor.eu

This project has received funding from the European Union's H2020 Programme for research, technological development and demonstration under grant agreement No 644852

Editor:	João Pedro Oliveira, UNINOVA	
Deliverable nature:	R-Report	
Dissemination level:		
Contractual/actual delivery date:	M09	M10
Suggested readers:	Consortium partners	
Version:	V1.1	
Keywords:	System Design, CNT, MEMS, CMOS SoC, Energy Harvesting, Operational System Software (OSS), Smart algorithms, Packaging, Safety	

Abstract

The outcome of the use case analysis scenarios carried out for the water monitoring ecosystem has produced a set of requirements that confirmed the need for the design of a complex and heterogeneous system via the Proteus project. This is the objective of work-package WP2, which aims at providing the co-design of the overall smart system, building the system architecture with clear design of the heterogeneous building blocks (hardware and software) and of the interfaces between them (routing, bonding, packaging).

The diversity of the technologies as well as the required interactions between them potentiate the risk of failure, which has to be minimized by reaching a high degree of consistency during the conception phase. This is this subject of this deliverable, in which a full system overview is provided, exposing the proposed technologies to set the specifications for effective interactions between them. The outcomes of this deliverable feed the specification sets that are needed for both hardware (WP3) and software (WP4) implementation.

Due to the complexity of the proposed system and considering the limitations of the number of timeslots available for CMOS chip fabrication, two run/versions were included in PROTEUS project plan. Besides giving an overall description of the complete system, this deliverable focus on the system design for the first version.

Disclaimer

This project has received funding from the European Union's Horizon 2020 Programme for research, technological development and demonstration under grant agreement n° 644852.

Copyright notice

Revision History

Revision	Date	Description	Author (Organisation)
V0.1	26/06/2015	Creation	João P. Oliveira (UNINOVA)
V0.2	07/10/15	Merging contributions	All partners
V0.3	21/10/15	Update	João P. Oliveira (UNINOVA)
V0.4	14/10/15	Added Vortex Piezoelectric Generator info Update/revision	F. Cottone (NiPS) B. Lebental (IFSTTAR)
V0.5	20/11/15	Update for final revision	João P. Oliveira (UNINOVA)
V0.6	03/12/15	Update for final revision after quality revision from IFSTTAR and EGM	B. Lebental (IFSTTAR) F. Le Gall (EGM) João P. Oliveira (UNINOVA)
V0.8	12/12/15	Final updates from partners (answers to internal reviewers' comments)	T. Bourouina (ESIEE) F. Bellouard (Ponsel) F. Cottone (NiPS) P. Vachleas (Wings)
V1	14/12/15	Releasable document	João P. Oliveira (UNINOVA)
V1.1	14/12/15	Releasable document, public version	B. Lebental (IFSTTAR) T. Bourouina (ESIEE)

Table of content

Executive summary

The outcome of the use case analysis scenarios carried out for the water monitoring ecosystem has produced a set of requirements that confirmed the need for the design of a complex and heterogeneous system for the Proteus project. This is the objective of work-package WP2, which aims at providing the co-design of the overall smart system, building the system architecture with clear design of the heterogeneous building blocks (hardware and software) and of the interfaces between them (routing, bonding, packaging).

Considering the multi-parameter monitoring requirements, which imply a multi-sensor approach, the design of a System on Chip (SoC) in a standard CMOS technology and the use of CNT and MEMS sensors contribute to reducing the price and size of the probe. However, the probe has also to be self-powered and smart if an effective maintenance cost reduction is also targeted. The system probe thus also includes elements for energy harvesting and embeds smart algorithms, for example for efficient energy management. Additionally, considering the environment where the probe is installed, the design process tackles the final packaging as well as the production requirements and compatibility issues, like electromagnetic interference or galvanic isolation.

The diversity of the technologies as well as the required interactions between them potentiate the risk of failure, which has to be minimized by reaching a high degree of consistency during the conception phase. This is the goal of this deliverable, in which a full system overview was done, exposing the proposed technologies in order to set the specifications for effective interactions between them. Building upon requirements expresses in D1.2, the outcomes of this deliverable feed the specifications set that is needed for both hardware (WP3) and software (WP4) implementation.

Due to the complexity of the proposed system and considering the limitations of the number of timeslots available for CMOS chip fabrication, two versions were included in PROTEUS project plan. Besides giving an overall description of the complete system, this deliverable describes the design aspects of the first version of the PROTEUS system. At the end a cross-reference table between the requirements gathered in D1.2 and the present document is given.

1 Proteus Node Architecture

The Proteus Node (PNODE), shown in Figure 1, involves the mix of several technologies. Regarding to the hardware, the core functionalities depend on the interaction between three major sub-blocks: the CMOS processing chip, the Sensor chip and the Energy Harvester/Power Management Unit (EPMU). The first version of the PNODE system, which is the subject of this deliverable, is not only focused on testing the interaction between the CNT and MEMS sensors and the analog/digital signal processing circuitry included in the CMOS chip. It also intended, with this version, to evaluate the energy harvester sources and the respective power management. Finally, the coordination and cognitive processing of the acquired information taken from the sensors needs the implementation of smart algorithms, which will also be subject of evaluation.

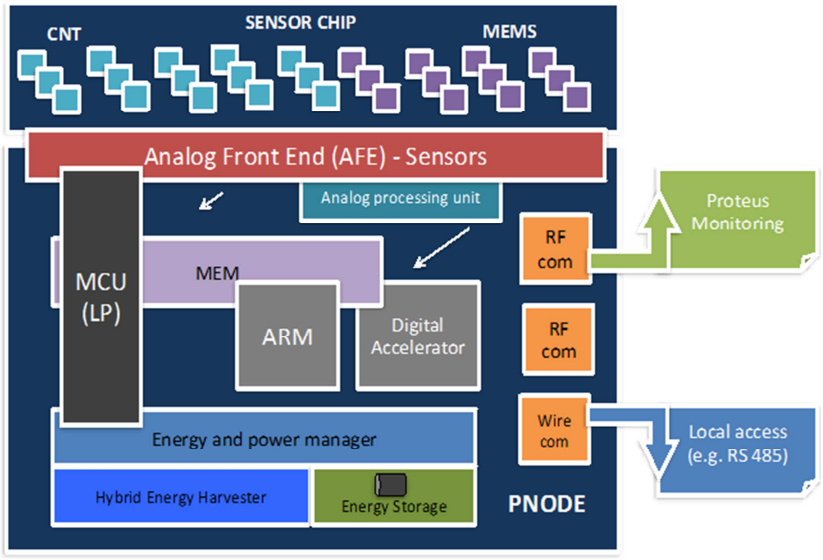

Figure 1: General system overview of the PNODE.

The overall architecture of the PNODE, which is depicted in Figure 1, targets the implementation of a multi-sensor probe able to measure and process several chemical and physical parameters. Moreover, it reflects the requirement of being self-powered, which is ensured by the energy harvesters.

The sensors act as transducers from physical to electrical domain. When correctly biased, they output voltage and/or current signals. These are essentially analog signals (i.e., continuous in amplitude and time), although being significantly weak. Therefore, an analog front end (AFE) is used for the sensor-interfacing stage, to amplify and pre-process the signal before the digitization, which is done by an analog-to-digital converter (ADC). The resulting digital data is further (if needed) processed by the digital part, which may include a direct memory access (DMA) scheme, a digital hardware accelerator (ACC), the microcontroller (MCU) and memory (MEM). The latter is responsible for the operation of the PNODE, including the control of the power duty cycling strategy and algorithms via the energy and power management unit (EPMU). The energy for the device operation is collected by the harvester units and stored in a short-term energy buffer (supercapacitor) and/or long-term energy storage (battery). In order to execute advanced smart algorithms the PNODE may also need the integration of additional digital processing units, e. g., ARM microprocessor. Further improvements in computational energy efficiency are also expected by the use of dedicated digital logic, ACC, to execute special functions or by using dedicated analog processing units.

One of the final goals of Proteus is reaching a high level of integration thus reducing the number of total external components and increasing the level of compactness. This reflects the need to integrate the system electronics in a single chip, known as a System on Chip (SoC). Moreover the same strategy is required for the implementation of the multi-sensor block through a Sensor Chip configuration.

Considering the overall complexity, the project plan includes a minimum of two runs/versions. Attending to the high level of interaction between the large number of modules (hardware and software) it has been identified that the first version of the PNODE, which is the subject of this deliverable, should reflect the need of intensive testing of each individual system blocks (either hardware or software) and also to characterize and verify the interactions between them. A strong focus concerns the interactions between the CNT sensors, the MEMS sensors and the analog/digital signal processing circuitry designed and included in the CMOS chip.

Henceforth, the first version of the PNODE will be based in a mixed configuration in which the most relevant analog signal acquisition, conditioning and digitalization steps are done inside the CMOS chip and the remaining digital processing is performed by an external MCU installed in dedicated Support PCB board. The later also provides wireless communications capabilities (short and long range), energy storage and interface circuitry for the hybrid energy harvester. A support PCB board is thus to be designed to connect the CMOS and Sensor chips.

It also intended with this version to evaluate the energy harvester sources and the respective power management. The coordination and cognitive processing of the acquired information taken from the sensors needs the implementation of smart algorithms, which are supported on energy aware software modules.

Please note that in the second version of the chip shown in Figure 2, to be described in details in a later deliverable, the digital building blocks will be fully integrated into the CMOS chip, including the power management and energy harvesting circuitry.

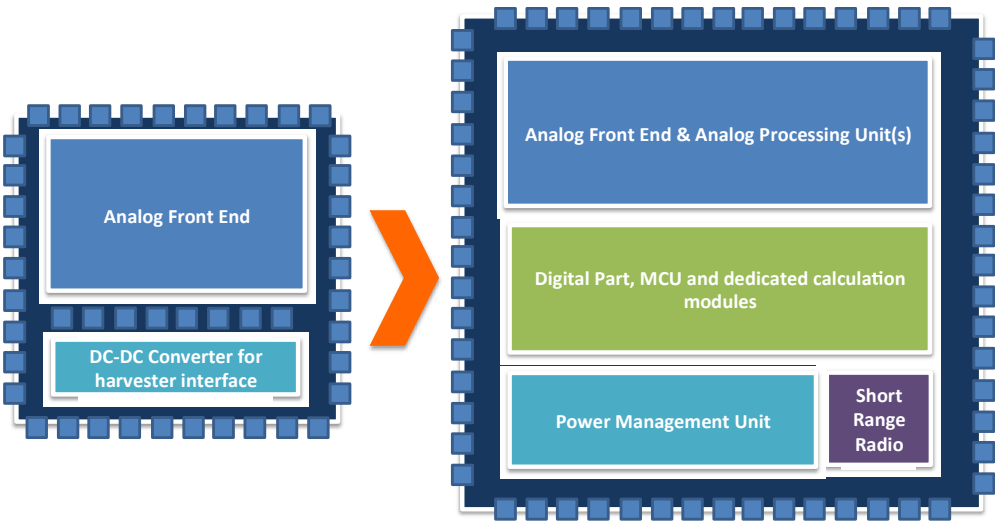

Figure 2: Evolution from first version to second version of the CMOS chip SoC.

Based on these considerations, the proposed block diagram of the first PNODE version is shown in Figure 3. A Printed Circuit Board (PCB) connects to the capsule board. The latter provides the connectivity between the Sensor Chip and the CMOS Chip.

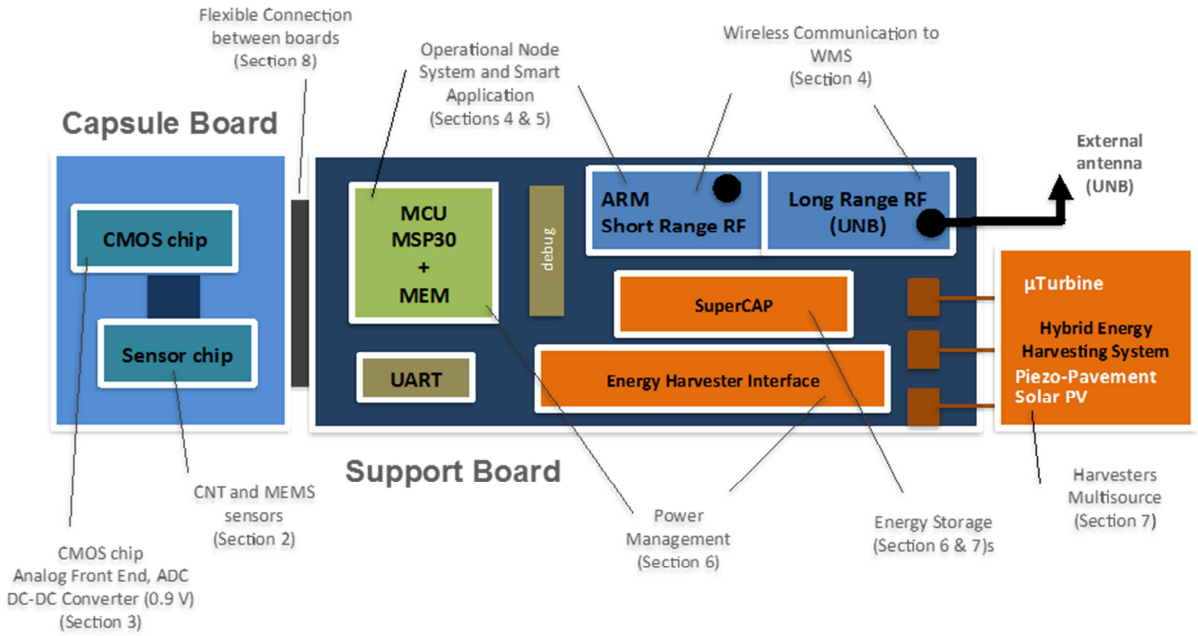

Figure 3: First Version of the electronic board: CMOS chip and sensor chip assembled into a capsule board, itself connected to a support board.

2 Multi-parameter Sensor Chip

The compact multi-parameter sensor chip will result from microfabrication and nanofabrication technologies involving silicon and glass as the substrate materials. The multi-parameter sensor chip will be obtained from processed wafers and subsequently diced into individual chips whose lateral dimensions will not exceed 1 cm and whose thickness will be less than 2 mm.

Our ultimate goal is to implement on the same chip 4 different types of physical sensors and 5 different types of chemical sensors. The typical content of a single chip is the following:

- flow-rate sensors
- conductivity sensors
- temperature sensors
- pressure sensors,
- chemical sensors of various types

More details on the multi-sensing chip are kept confidential, as a patent application is pending.

3 Mixed-mode CMOS chip

3.1 Overall Design Strategy

To accommodate all the functions needed to interface with all the sensors described previously, to interface with the energy harvesting unit and also to be able to perform digital and analog computational tasks associated with a set of cognitive algorithms, the final Proteus CMOS SoC (System on Chip), Figure 4, needs to integrate a significant number of processing blocks. For the analog domain, these include low noise amplifiers (with programmable gain), signal routing matrix, programmable filters, peak detector, high dynamic range Analog-to-Digital (ADC) and Digital-to-Analog (DAC) converters. For the digital domain, the blocks needing to be integrated ranges from a Micro Controller Unit (MCU) and/or small processor units (e.g., ARM based) to dedicated digital processing units, including memory, look-up tables, clock/phase generators.

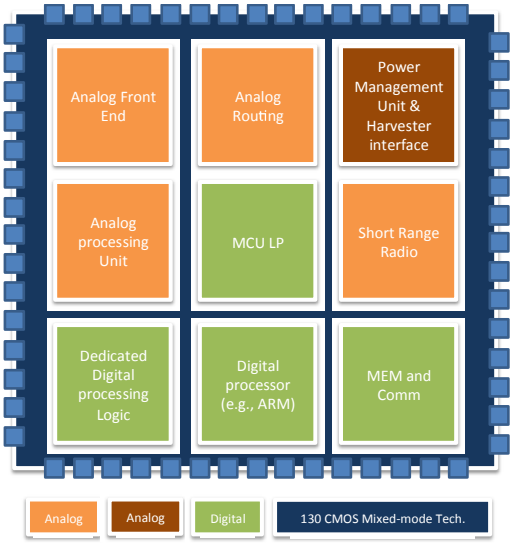

Figure 4: Overview of the Proteus SoC concept.

Over the past 2-3 decades, the downscaling of the CMOS technology has been done to reduce the size and to improve the performance (speed) of the digital processors, making it the dominant and cheapest IC technology, nowadays. Meanwhile, the analog signal processing circuitry had to be adapted and developed in order to operate in this digital optimized technology. For example, new switched-capacitor techniques explores the benefits of using MOS transistors with transition frequency approaching 100 GHz range.

The required design of the Proteus System on Chip (SoC) will include both digital and analog circuitry, which will share the same silicon substrate. As a consequence, several techniques have to be tuned under this mixed analog and digital design. The selected CMOS technology is a P-type substrate one, with 8 metal layers, 130 nm CMOS node. It constitutes an appropriate trade-off between cost, performance and technology maturity and yield, when considering PROTEUS goals.

Despite the maturity of the technology, the mixing of such high number of processing blocks in the same silicon chip and the limited number of fabrication runs available from the silicon foundry, still make the chip design a challenge. As a consequence, it has been elected that the SoC development has to be divided into intermediate phases. The corresponding design strategy guidelines are as follows:

- All the circuits have to be designed in a standard CMOS digital technology, thus not requiring additional extra fabrication steps (which are costly).

- To optimize power consumption, extensive use of low-voltage circuit techniques including:
    - Use of a multi voltage supply approach for powering each of the integrated building blocks.
    - Use of the active devices in weak inversion thus enabling the reduction of the voltage supply.
    - Use of circuit topologies that can operate with low gain amplifiers.
    - Wherever possible replace active configurations by passive counterparts. The degradation of performances can be compensated, to a certain extent, by implementing a digitally- assisted analog processing approach.
    - Each building block has to include power and low power operational modes, to support operation with efficient duty-cycling..
- To interface with the Energy Harvester, integration of a power/energy management unit capable of optimizing the use of the available energy, and able to deliver the proper voltage supply for the chip. Therefore it should include a flexible DC-DC converter.
- Considering the low amplitude and low frequency signal obtained from the sensors:
    - Use of flexible/reconfigurable analog front-end for the signal conditioning and digitization, including, programmable sample-hold amplifiers, filters and ADCs.
    - Use of differential signal processing to reduce effects of common mode noise and interferers. Additionally, even order distortion is strongly attenuated.
    - Use of current biasing for the sensors instead of a voltage approach. The current biasing is set by a current Digital-Analog converter, which facilitates the adjustment of the dynamic range.
- The ultimate goal being the implementation of the system on chip, it was strategically considered that the first version of microsystem should enable a full characterization of each individual analog building block and their interactions with the sensors and energy harvesters.

Before going into the details of the chip architecture, next a set of considerations are given to expose the technical principles about the interface and acquisition of the sensor signals. As stated in Section 2, the common transduction scheme among the selected CNT and MEMS sensors used in this project involves the variation of the sensor resistance, except the conductivity sensor where an impedance based principle is used instead. This variation can be converted into an electrical signal with a corresponding variation of its current, voltage, frequency, time pulse positioning or pulse delay.

Excluding the conductivity sensor case, the signal generated from the remaining sensors are characterized to be very low frequency, have a considerable dynamic range with signals that can be very weak in nature. The general strategy for this first version is to bias the sensor with a programmable current source and acquiring the resulting voltage that appears across the sensor terminals. Under these conditions the overall resolution of the resistance variation measurement is not only determined by the minimum detectable step (V_{LSB}) of the Analog-To-Digital Converter (ADC) but can also be controlled by the input biasing sensor current.

CNT and temperature Sensor (MEMS)

Electrically, both CNT and MEMS temperature sensors are variable resistors. By using a current biasing approach shown in Figure 5, the use of Wheatstone can be avoided. The output voltage, before being processed by the ADC, is given by the programmable source current **Ibias** times the value of the resistor (including baseline level plus the variation). Moreover, this topology can extend the overall dynamic range since for N bits ADC and if the dynamic range of the current source is M bits, the dynamic range of the readout interface is N+M bits. Additional bits of the current source are used for calibration purpose.

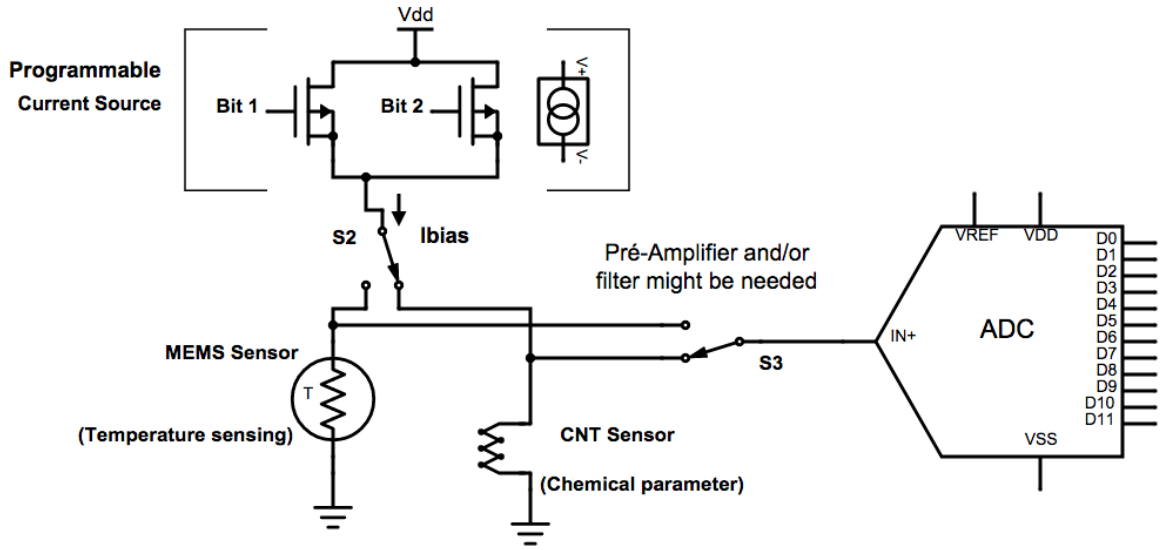

Figure 5: Interface for the CNT and Temperarure (MEMS) sensor.

MEMS Pressure Sensor

As demonstrated in Section 2, the various MEMS elements that compose the pressure sensor are disposed in a Wheatstone bridge structure. Traditionally, this type of structure is biased by a constant voltage source. However, similarly to the previous case, in our case the bridge is biased by a programmable current source, as shown in Figure 6. This facilitates the calibration phase and improves the final dynamic range of the readout circuitry. Moreover, the low linearity error level is not degraded, when compared with voltage biasing version.

Considering Figure 6, it is easy to obtain that the output differential voltage is given by the programmable source current **Ibias** times the value of the variation of the resistance, i.e., Vout = I_{bias}*ΔR [volt]. Depending of the level of this differential signal voltage, amplification and filtering might be applied before being digitalized by the ADC

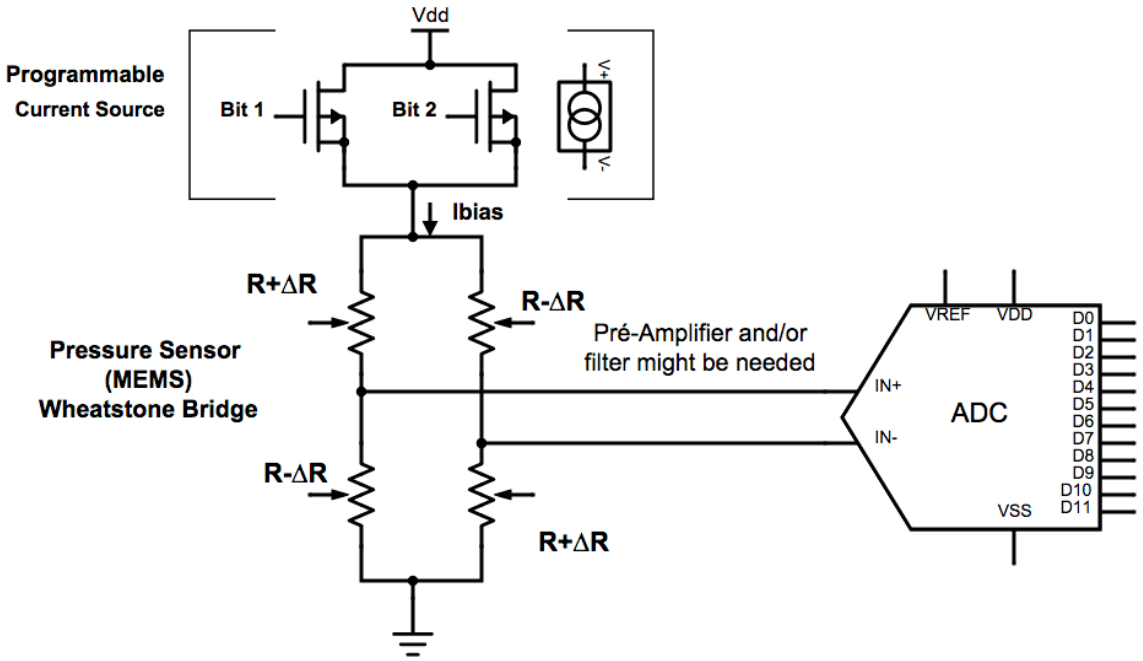

Figure 6: Interface for the MEMS based Pressure sensor.

MEMS Flow sensor

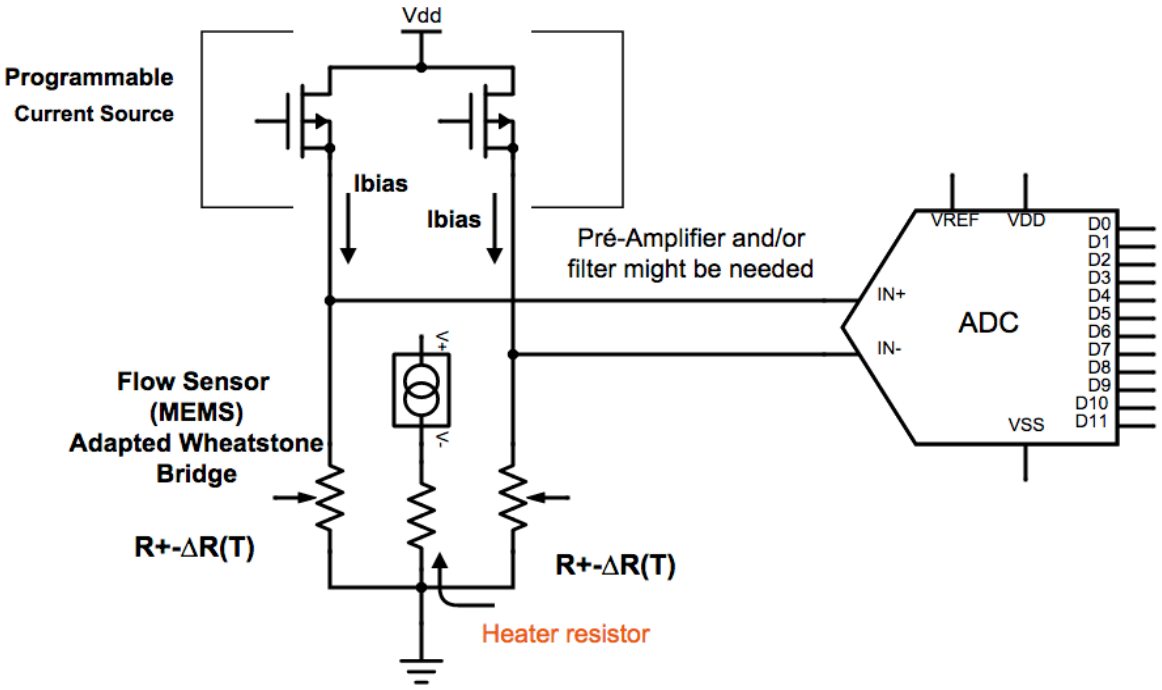

Figure 7: Interface for the MEMS based Flow sensor.

For the MEMS Flow Sensor readout setup, a modified version of the Wheatstone was developed. The top reference resistors of the classical structure were replaced by two programmable current sources which guaranties better controllability and better operation with low voltage supply.

Considering Figure 7, it is easy to obtain that the output differential voltage is given by the programmable source current **Ibias** times the value of the variation of the resistance, i.e., Vout = I_{bias}*ΔR [volt]. Depending of the level of this differential signal voltage, amplification and filtering might be applied before being digitalized by the ADC

MEMS Conductivity Sensor

As explained in Section 2, the capacitive nature of the frequency response of the conductivity sensor suggests proceeding with a dynamic measurement type, to determine indirectly the value of the impedance from which it is possible to extract the water conductivity. The configuration developed is represented in Figure 8. Here, a sinusoidal signal generated by a voltage or current Digital-to-Analog Converter (DAC) is injected in the sensor and resulting output signal voltage is acquired by the ADC. Despite not being represented in Figure 8., preceding the ADC a bandpass filter is used to prepare the signal for digitalization.

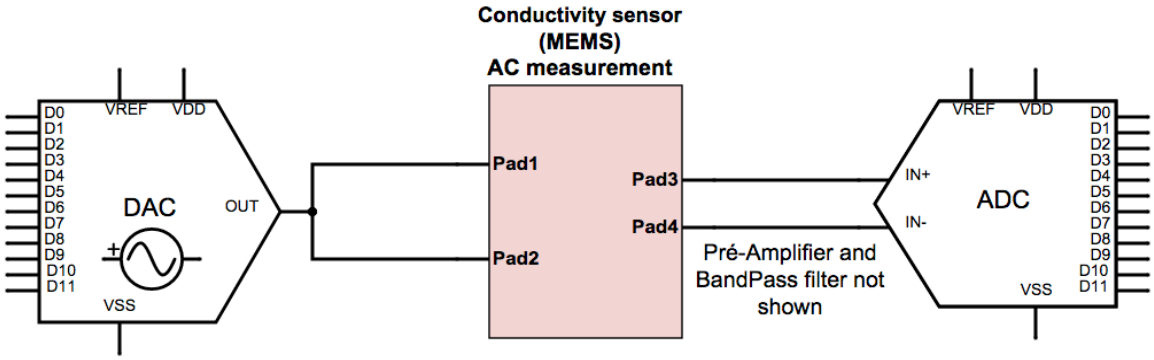

Figure 8: AC measurement interface for the MEMS based Conductivity sensor.

3.2 Chip architecture

As discussed previously, the first version of the CMOS chip focuses on the implementation and testing of the major analog building blocks and of their interactions with the set of MEMS and CNT sensors. The chip block diagram is included in Figure 9 and it comprises:

- Dedicated PADS (analog input/ouput-I/O) to connect directly to each of the sensor types (CNT and MEMS). Single-ended or differential sensors should be supported.
- An input analog switching matrix acting as an analog multiplexer.
- Analog processing block (APB), in which the signal is amplified and conditioned prior to be digitized by the ADC.
- Sigma-Delta Analog-To-Digital Converter (ADC), with a serial digital output

- A single DC-DC converter delivering 0.9 V output voltage
- A shift register to receive the configuration vector set by the external microcontroller

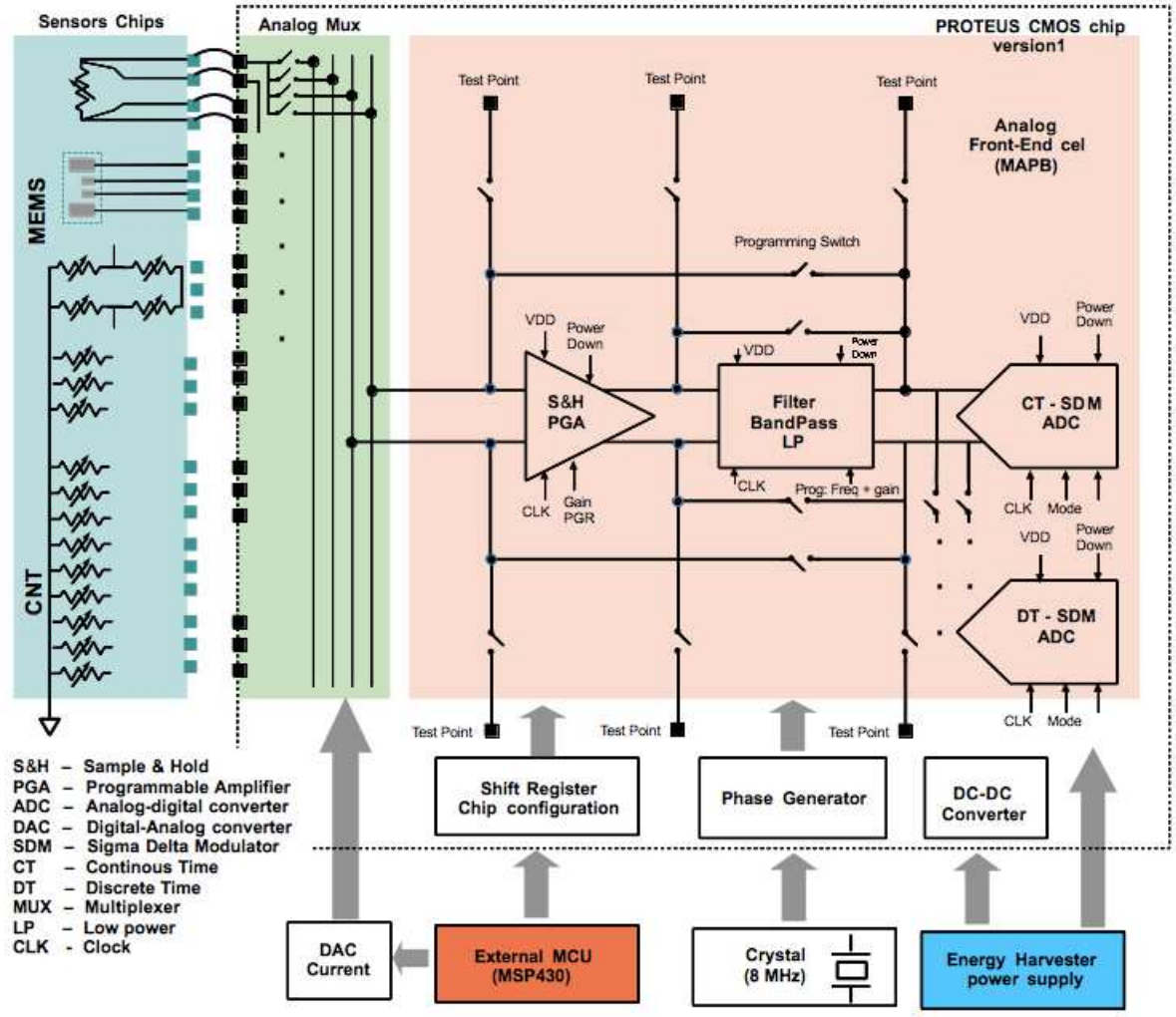

Figure 9: Block diagram of the CMOS chip 1st version.

3.3 Analog Signal Routing

A simplified strategy of the analog signal routing block is used in this first version to save area and complexity. It translates into the following design considerations:

- Implement an analog multiplexer at the input to interface with the sensors;
- Inside each mixed-analog processing block (MAPB), the signal can be rerouted between sub-blocks;
- A shift register/memory is used to program the matrix and MAPB, that is, to configure the chip. In this version when the power is off the matrix set is lost.

The cell unit of this routing signal fabric is an analog switch. Considering the characteristics of the PMOS and NMOS devices available in the CMOS technology in general, one of the simplest ways to achieve a low and flat ON-resistance characteristic for a switch is by using a complementary configuration like the one shown in Figure 10, also known as “gate transmission”.

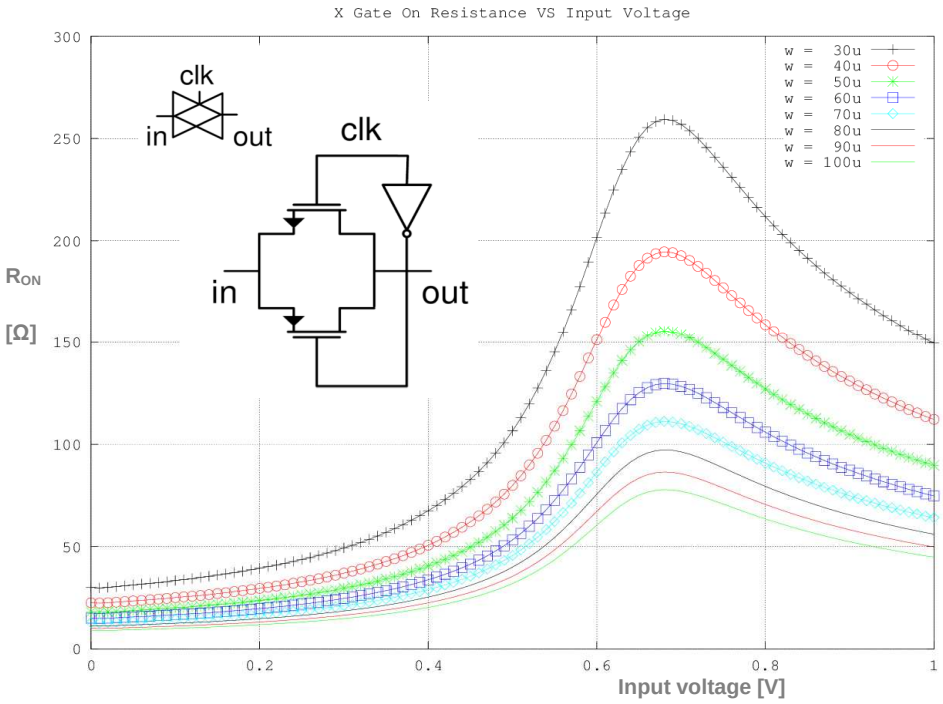

Figure 10: Transmission gate "ON" resistance (Ω) versus input voltage in volt.

When both transistors are conducting with a low voltage between their drain and source terminals (as it is intended for a switch), the total switch conductance is simply the parallel of the two transistor output conductance, determined in the triode region, by

$$R_{ON} = \frac{1}{g_{ds,PMOS} + g_{ds,NMOS}} = \frac{1}{\frac{W_p}{L_p}\mu_p C'_{ox}\left(V_{SG,PMOS} - V_{tp}\right) + \frac{W_n}{L_n}\mu_n C'_{ox}\left(V_{GS,NMOS} - V_{tn}\right)} \quad [\Omega] \quad \textit{Eq. 1}$$

where W_i and L_i are the width and length of the transistors, μ_i is the carrier mobility the channel, V_{ti} is the threshold voltage, and V_{GSi} is the gate to source voltage. The V_{GS} (and V) voltage is determined by the clock (CLK) signal and the input voltage V_i.

The implementation details, namely those related with device sizing, are the subject of work-package 3. However, the target requirements are summarized in *Table 1*.

Table 1: Target requirements for the switches.

Block	Switch type	SNR	On resistance	VDD	Bandwidth
Input Mux	Transmission gate	> 60 dB	< 1kΩ	0-1.2V	> 20 kHz
Inside the MAPB	Transmission gate	> 60 dB	< 1kΩ	0-1.2V	> 20 kHz

3.4 Analog Signal Amplifier and Sample & Hold

The weak input signal must be amplified and sampled by a sample and hold (S&H) before being digitalized. Moreover, this operation must be accomplished with low noise and high level of linearity. It is well known that MOS devices have a low frequency noise level that cannot be neglected. This is mainly due the flicker noise which, for a field effect transistor (FET), has frequency corner located at a higher frequency when compared with other type of active transistors like the bipolar one. In order to reduce this contribution, a correlated double sampling or chopping technique is added to the structure of the amplifier and sample and hold (S&H). The circuit topology is based on a typical switched capacitor (SC) amplifier, which is also used as a sample and hold. The circuit schematic is similar to the one used in the switched-capacitor sigma-delta ADC presented in next section.

The implementation details, namely, those related with the device sizing are the subject of work-package 3. However, the target requirements are summarized in *Table 2*.

Table 2: Target requirements for the programmable gain S/H amplifier.

Amplifier / S&H	VDD Voltage supply	SNR / DR	Bandwidth	Special techniques	Programmability
SC type	0.9 -1.2 V	> 60 dB	Up to 20 kHz	Chopping to reduce noise effects	Voltage Gain up to 40 dB

3.5 Analog-To-Digital Converters

Among all type of ADCs, the Sigma-Delta Modulator (SDM) topology has gained a significant relevance due to its robustness under Process-Voltage-Temperature (PVT) variations and to its flexibility enabling it to be designed under low-voltage constraint.

The SDM ADC[1] samples the input signal at a much higher rate than the one requested by the Nyquist theorem. The excess of sampling rate is characterized by the Oversampling Ratio (OSR), which relates the sampling frequency and the signal bandwidth. Oversampling is used to improve the input dynamic range, which can be further enhanced by introducing a feedback loop in the ADC. Combining these factors the ADC experiences a noise shaping effect, resulting in a higher Signal-to-Noise ratio (SNR) given by

$$\mathrm{SNR}_{\mathrm{dB}} \approx 6.02\mathrm{N}_{\mathrm{bits}} + 1.76 + 10\log\left(\frac{2\mathrm{L}+1}{\pi^{2\mathrm{L}}}\right) + (2\mathrm{L}+1)\cdot 10\log(\mathrm{OSR}) \qquad \textit{Eq. 2}$$

where N_{bits} is the number of bits of the internal quantizer and L is the order of the ADC. Considering the ADC as a black-box, the effective number of bits of the full ADC is determined by the $N_{bits,effective} = (SNR_{dB}-1.76)/6.02$, meaning that when compared to Equation 3, the sigma-delta loop improves the overall resolution.

[1] Richard Schreier and Gabor Temes, “Understanding delta-sigma data converters”, Wiley-IEEE Press, 2004

Two types of SDM ADCs will be evaluated in terms of their performances, namely, resolutions and power consumption. Both ADC are based on a second-order configuration, i.e., with two integrators in the loop. Their main difference is the type of integrator in the sigma-delta loop.

In SDM #1, the integrator is based on a switched capacitor configuration and therefore has a discrete-time operation. The architecture, shown in Figure 11, is based on a 4-bit 2nd order sigma-delta modulator. Instead of using a single comparator and 1-bit DAC, this multi-bit approach enables to lower the OSR considering the input-required minimum bandwidth of 20 kHz. The lookup table is used for calibration/correction purposes.

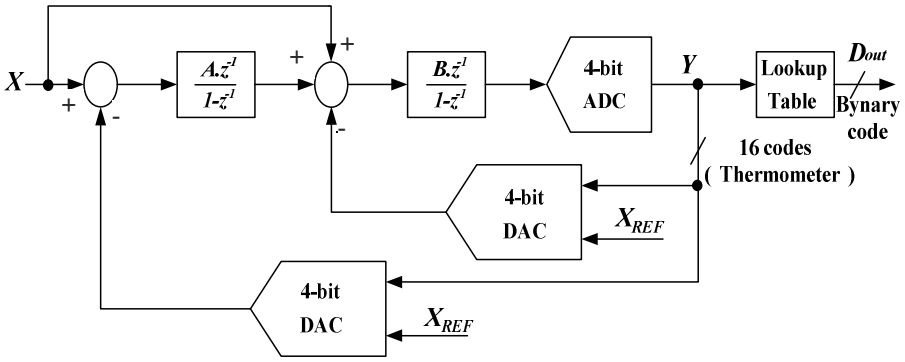

Figure 11: Switched-Capacitor based SDM ADC.

Figure 12 show the complete electrical schematic of the 4-bit SDM ADC that was selected for the project. It uses two discrete-time switched-capacitor integrators, a 4-bit quantizer and 4-bit switched DAC. The first integrator has a chopper input sampling network to reduce the effect of the flicker noise.

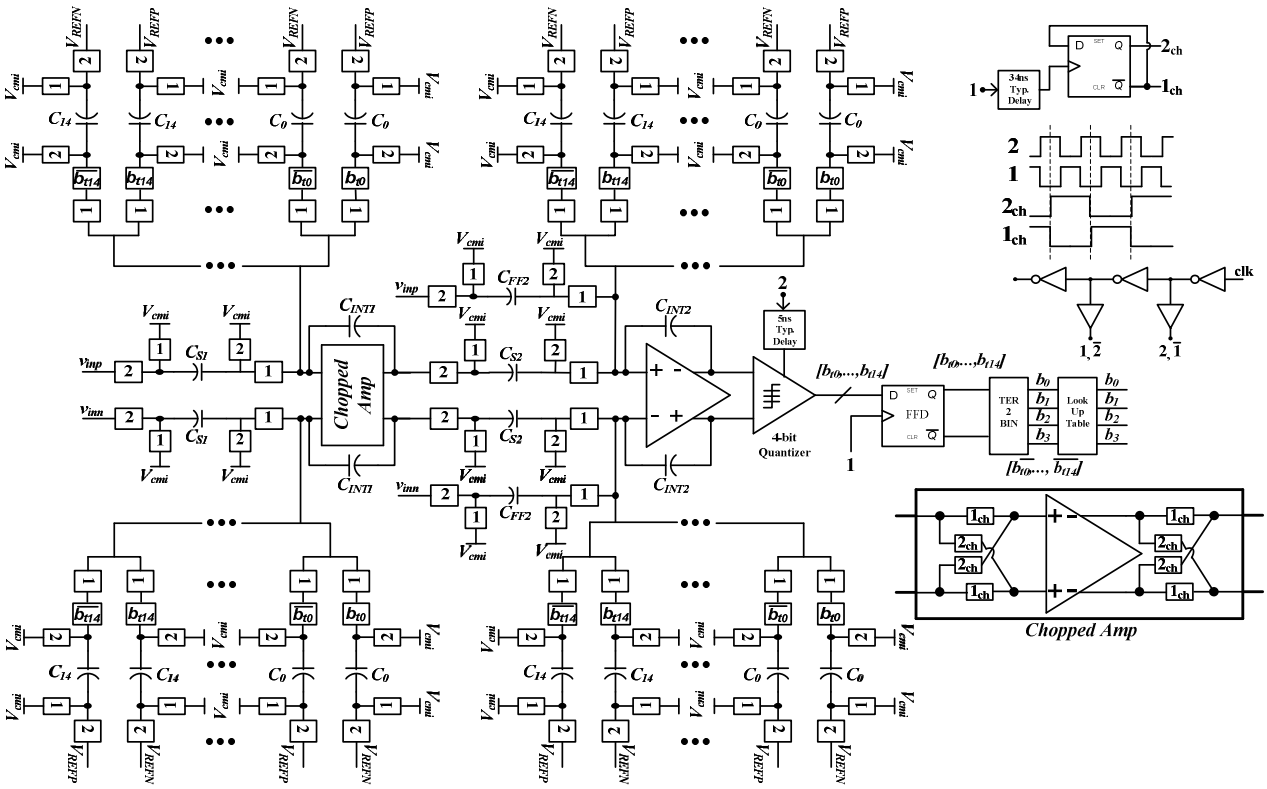

Figure 12: Complete electrical schematic of the second-order 4-bit □□M.

As a preliminary design, for a nominal power supply of 1.2 V, the full ADC reaches a peak SNR of 75 dB (corresponding to an effective number of bits of 12 bits) for a bandwidth of 20 kHz and a full-scale of 1 V_{pp} (differential, 0 dB_{FS}). With an OSR of just 32 (F_{CLK} = 1.28 MHz), the ADC power consumption is lower than 200 µW.

For the second ADC, a continuous time integrator is used instead. Moreover, an aggressive approach is followed to reduce the overall power consumption; it consists of using a passive-based continuous time integrator. The block diagram is depicted in Figure 25: it can be observed that the ADC is based on a 2nd order architecture with a feedforward path. Moreover, this structure can be implemented with passive integrators (e.g., without the need of power-hungry active amplifiers) thus reducing the power consumption.

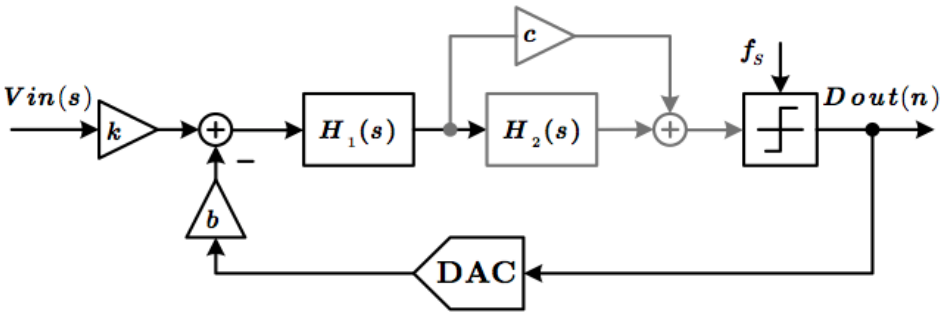

Figure 13: Diagram of the Continous-Time SDM ADC.

In the case of a passive SDM[2] the only gain is the comparator gain. This means that if more than one feedback path is used, the inner feedback path will have most of the processing gain of the comparator. Therefore, in order to have a stable loop with only one feedback path it is necessary to add a zero to the loop gain. This can be achieved by adding a resistor in series with the capacitor in the second RC circuit, as shown in Figure 26.

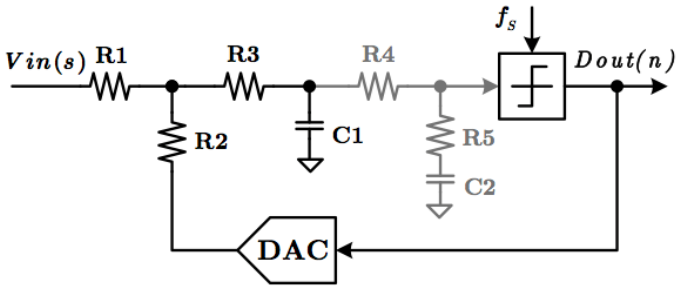

Figure 14: Circuit schematics of the Continous-Time SDM ADC.

For the design of the loop filter, a tool based on a Genetic Algorithm modified for passive CT SDM was used. In this tool, an initial randomly population of N chromosomes is created. Each chromosome, which contains the values of the resistors and capacitors used in the modulator, is evaluated and its total fitness is calculated based on the desired specifications.

[2] João Melo et al., "A low power 1-MHz continuous-time ΣΔM Using a passive loop filter designed with a genetic algorithm tool," in Circuits and Systems (ISCAS), 2013 IEEE International Symposium on , vol., no., pp.586-589, 19-23 May 2013

The electrical schematic of the differential 2nd order passive CT SDM with feedforward structure is shown Figure 27, where the capacitors are implemented using MOS devices with their drain and source terminals shorted (MOSCAP). The latter configuration enables to implement higher capacitances values using less chip area. .

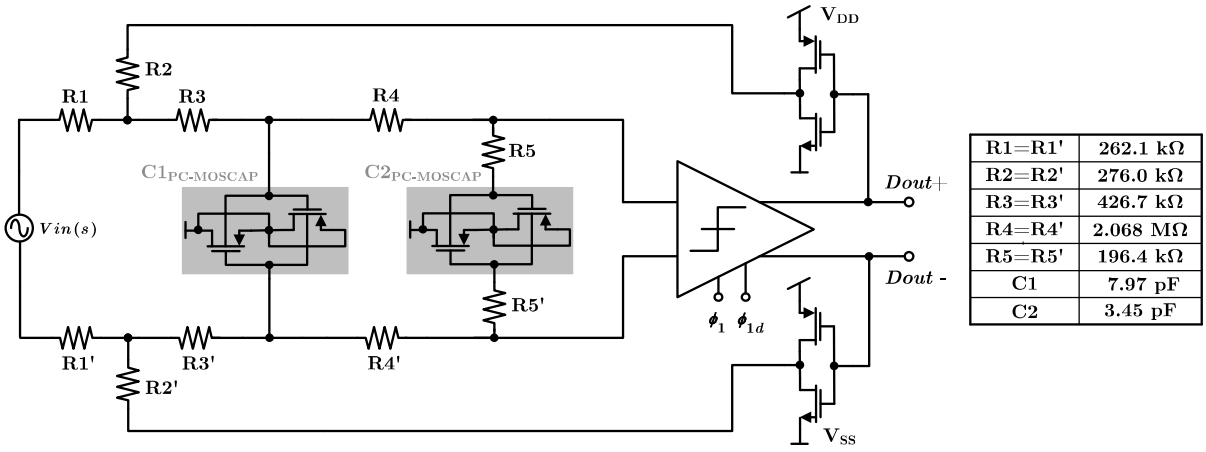

R1=R1'	262.1 kΩ
R2=R2'	276.0 kΩ
R3=R3'	426.7 kΩ
R4=R4'	2.068 MΩ
R5=R5'	196.4 kΩ
C1	7.97 pF
C2	3.45 pF

Figure 15: Continuous-Time Passive Sigma-Delta ADC.

The comparator used in the SDM is shown in Figure 16. It consists of a differential input stage, two regenerative flip-flops, and a set-reset (S-R) output latch built with two NAND gates. The input stage is important to reduce the input-referred offset of the regenerative flip-flops, which is too big (tens of mV) for the purpose of this work.

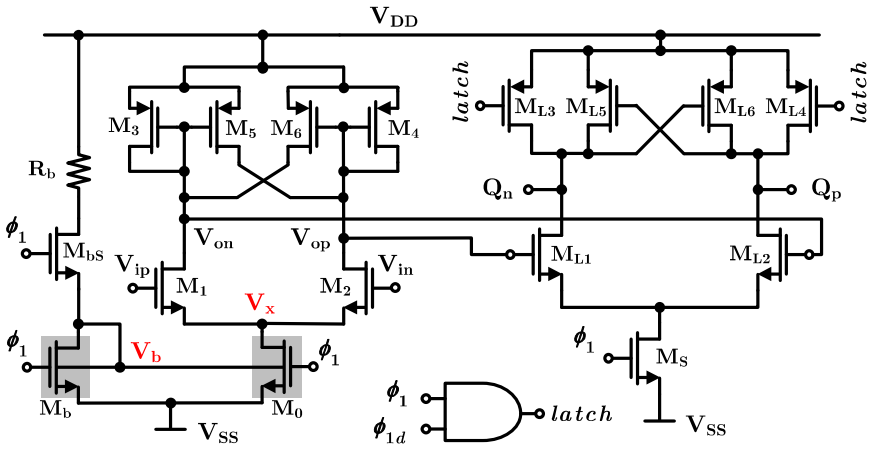

Figure 16: Low-voltage comparator.

In order to validate this new ADC configuration, which will be specially tuned for the project, a preliminary evaluation of the design was performed. Its results are shown in Figure 17 and Table 3. The dynamic range is more than 60 dB and the power consumption is at level of 32 fJ per conversion.

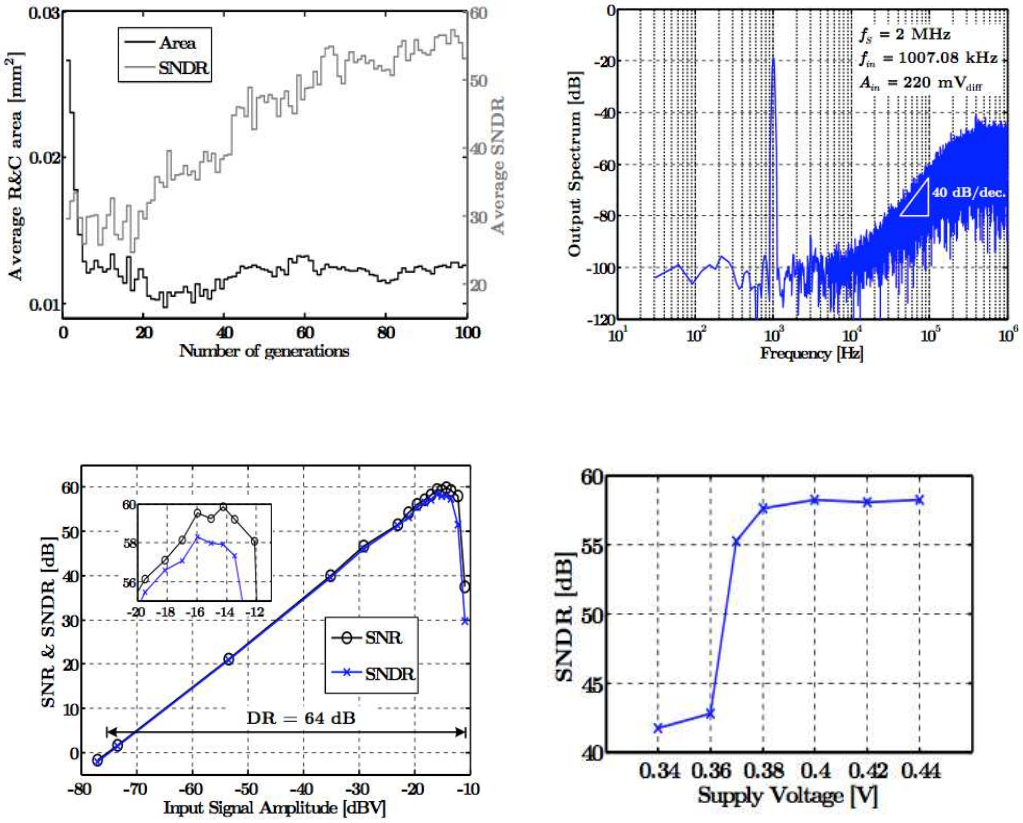

Figure 17: Characterization of the passive CT SDM ADC.
Table 3: Characterization of the passive CT SDM ADC.

Technology [nm]	130
Supply Voltage [V]	0.4
Clock Frequency [MHz]	2
Signal Bandwidth [kHz]	10
Power Consump. [uW]	0.41
Peak SNDR [dB]	58
Dynamic Range [dB]	64
Area [mm^2]	0.02‡
FoM$_1$ [dB]	168
FoM$_2$ [fJ/conv.-step]	32

$$\mathrm{FoM}_2 = \frac{\mathrm{P}}{2 \cdot \mathrm{BW} \cdot 2^{\mathrm{ENOB}}}$$

$$\mathrm{FoM}_1 = \mathrm{DR}_{\mathrm{dB}} + 10\log\frac{\mathrm{BW}}{\mathrm{P}}$$

The implementation details, namely those related with the device sizing, are the topic of work-package 3. However, the target requirements are summarized in *Table 4*.

Table 4: Selected specifications for the ADCs.

SDM	VDD	SNR / Num Bits	Bandwidth	OSR	Energy per conversion step	Programmability
CT-SDM	0.9	70 dB / 10-12 bits	Up to 20 kHz	< 128	< 100 fJ/conv	Band and resolution by changing the clock frequency.
DT-SDM	1-1.2	70 dB / 10-12 bits	Up to 20 kHz	< 128	< 100 fJ/conv	Band and resolution by changing the clock frequency

3.6 Programmable Analog Signal Filtering

The programmable analog filter architecture that was selected for the project is based on a discrete-time (Z-Domain[3]) signal processing approach. It uses a switched-capacitor (SC) network with low gain amplifiers, in order to avoid the use of power hungry high gain amplifiers with large bandwidth. Moreover, the intrinsic SC operation gives a high level of programmability, not only by changing the capacitance values but also by controlling the clock frequency.

The single-ended configuration of the band-pass SC Sallen-Key based topology[4] is shown in Figure 30, which needs only two complementary clock phases, Φ1 and Φ2. An additional capacitor (C3) was added to the circuit to facilitate the process of compensating the input parasitic capacitance of the amplifier.

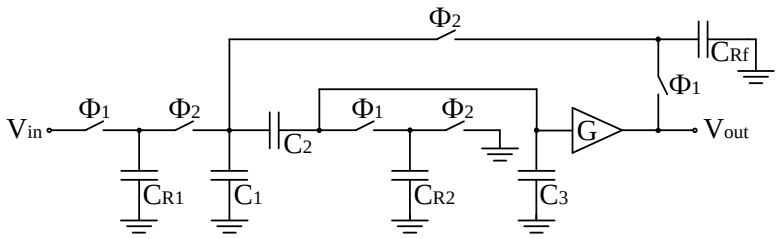

Figure 18: Band-pass SC biquad filter in single-ended configuration.

Applying a charge conservation analysis[3] and considering that the circuit output is sampled at the end of phase Φ1, the transfer function in Z-domain is given by

$$H(z)=V_{out}(z)/V_{in}(z) = G\cdot(z\text{-}1)\cdot d / (a\text{-}bz+ cz^2\ ) \qquad \text{Eq. 3}$$

where coefficients **a**, **b**, **c** and **d** are direct functions of the capacitance values. Therefore, the programmability of the filter frequency response is obtained by changing the values of the capacitors. Actually, in order to cancel the even harmonics and reduce the distortion due to charge injection from the switches, the differential configuration has to be used instead of the single-ended one (*Figure 19*). Assuming that in this configuration the voltage drop across the capacitors is two times larger than in the single-ended configuration, the capacitors must have half the capacitance of the single-ended capacitors.

[3] Alan V. Oppenheim, Alan S. Willsky, and S. Hamid Nawab. 1996. Signals &Amp; Systems (2nd Ed.). Prentice-Hall, Inc., Upper Saddle River, NJ, USA

[4] Hugo Serra et al, "A Switched-Capacitor Band-Pass Biquad Filter Using a Simple Quasi-unity Gain Amplifier", Springer Volume 394 of the series IFIP Advances in Information and Communication Technology pp 582-589, 2013

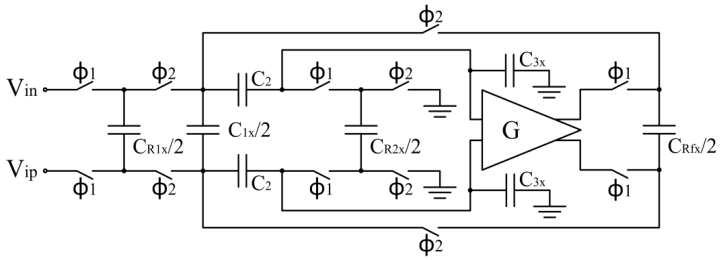

Figure 19: Band-pass SC filter in differential configuration.

The low gain and low power amplifier used in the filter is based on a voltage combiner configuration, with common source and common drain stages. The circuit is depicted in *Figure 20*.

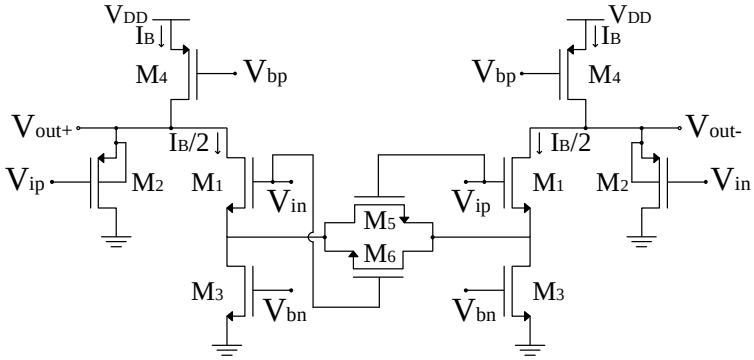

Figure 20: Low gain, low power amplifier based on a voltage combiner structure.

To illustrate the feasibility of the topology, a preliminary design proof was performed. The frequency responses of the prototype filter, ideal circuit, and real circuit of the second-order bandpass filter are shown in *Figure 21*. The attenuations at the filter bandwidth, as well as the amplifier parameters and IM2 (second order) distortions are shown in *Table 5*.

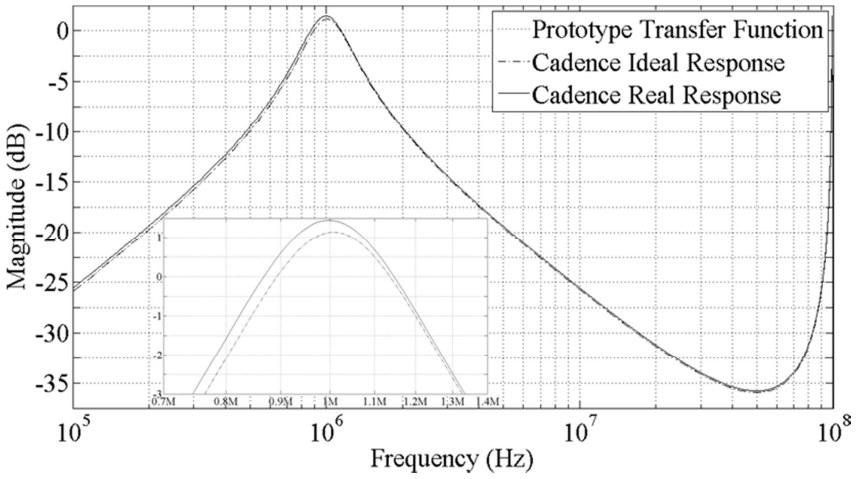

Figure 21: Band-pass SC filter in differential configuration.

.

Filter Attenuation @ Filter Bandwidth			Voltage-Combiner Amplifier		IM2 @ 200 mV_{pp}	
Prototype [dB]	-2.58	-2.29	**DC Gain [dB]**	2.90	**Real**	
Ideal Circuit [dB]	-2.58	-2.29	**Power [µW]**	244.33	**Circuit**	-52.11
Real Circuit [dB]	-2.07	-2.17	**GBW [MHz]**	349.8	**[dB]**	

Table 5: Filter simulation results

The type of response can be changed by modifying the circuit topology, as illustrated in *Figure 22*, where a low-pass filter is represented.

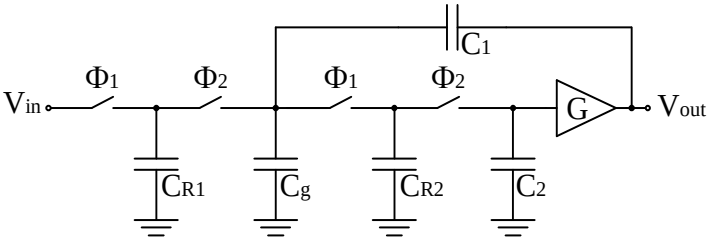

Figure 22: Low-Pass SC biquad filter in single-ended configuration.

To illustrate the operation of the low-pass biquad, a preliminary design proof for a cascade of 3 low-pass biquad (resulting in a 6th order filter) is shown in *Figure 23*. *Table 6* summarizes the results obtained for this particular case.

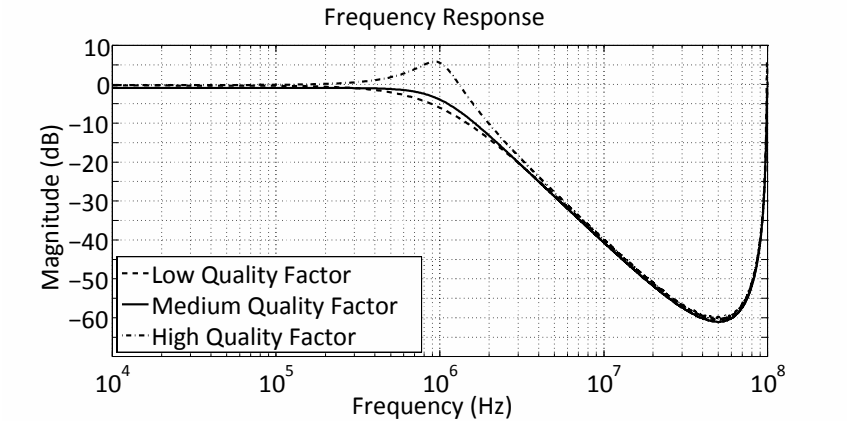

Figure 23: Frequency response of the sixth order low pass SC filter..

	Sect. 1	Sect. 2	Sect. 3	Cascaded
Filter Attenuation @ Cutoff Frequency				
Prototype (dB)	-5.711	-3.002	5.728	-2.985
Ideal Circuit (dB)	-6.024	-3.947	5.535	-4.436
Real Circuit (dB)	-6.012	-3.953	5.514	-4.487
Error (%)	0.200	0.152	0.381	1.137
Total Harmonic Distortion @ 600 mV_{pp}				
Real Circuit (dB)	-58.44	-46.13	-46.13	-42.06
Amplifier Circuit				
DC Gain (dB)	-0.313	-0.946	-0.193	-1.452
Power (mW)	0.491	1.084	2.949	4.523
GBW (MHz)	258.1	259.0	223.9	-

Table 6: Low-pass biquad simulation results and amplifier specifications, namely, for the Gain-Bandwidth Product (GBW)

The implementation details, namely those related with the device sizing, are the subject of work-package 3. However, the target requirements are summarized in *Table 7*.

Table 7: Target requirements for the programmable filter.

Filter	VDD Voltage supply	SNR	Bandwidth	Type	Programmability
SC biquad	0.9 V	70 dB	Up to 10 kHz	Band-pass	Central frequency

3.7 Power unit: the DC-DC Converter

As a part of the power management unit (EPMU), the DC-DC converter is an important block since it converts a variable input voltage provided by a supercapacitor, into a stable output voltage. The most suitable configuration for full integration uses switch capacitors[5] instead of inductors since the later ones occupy a too large amount of chip area. The selected converter, shown in Figure 24, is composed of two “flying” PMOS capacitors (C1 and C2) and nine MOS switches (1..9). This is the result of merging three converters in a single one. Therefore, the converter has three states (1/2, 2/3, and 1/1) of operation with two-phase clock, with phases Φ1 and Φ2. Auxiliary circuits, such as a phase generator, a state machine, switch drivers and a start-up circuit, carry out the changes between states as well as the clock phases. This converter is able to produce a stable 0.9 V output voltage for a input voltage variation between 0.9 V to 2.3 V, with an output power of 20 mW, corresponding to an energy efficiency of 76.0%, 70.7%, and 68.2% in the 1/2, 2/3, and 1/1 sates, respectively.

[5]Ramadass, Y.K.; Fayed, A.A.; Chandrakasan, A.P., "A Fully-Integrated Switched-Capacitor Step-Down DC-DC Converter With Digital Capacitance Modulation in 45 nm CMOS," in Solid-State Circuits, IEEE Journal of , vol.45, no.12, pp.2557-2565, Dec. 2010

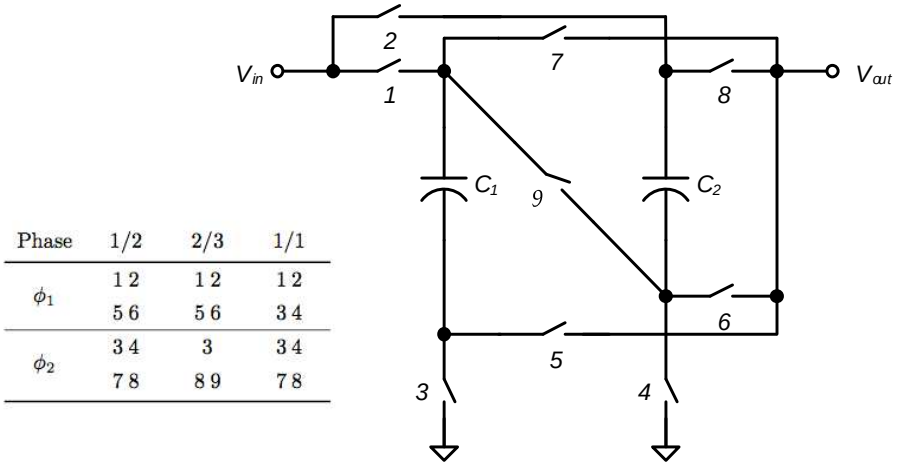

Phase	1/2	2/3	1/1
ϕ_1	1 2 5 6	1 2 5 6	1 2 3 4
ϕ_2	3 4 7 8	3 8 9	3 4 7 8

Figure 24: DC-DC converter topology.

The selection of the appropriate operation modes for the DC-DC converter is determined by a dedicated state machine with block diagram shown in Figure 25. The input voltage is compared with a stable reference generated by the bandgap and triggers the corresponding operational state.

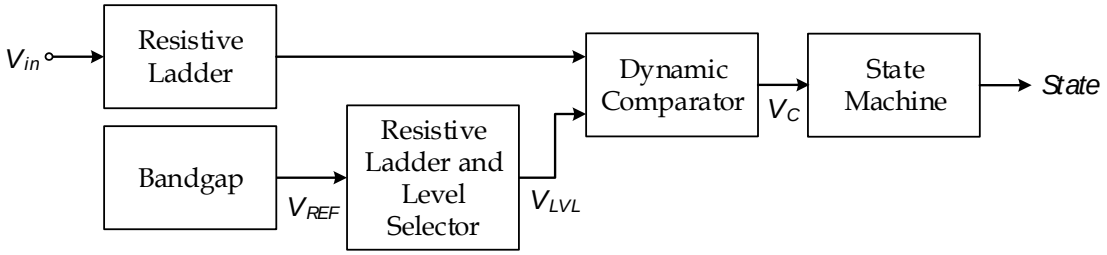

Figure 25: DC-DC converter.

The efficiency achieved by the converter depends on the correct phase generation in order to precisely define the level of overlap supported by the circuit. A dedicated phase controller, shown in Figure 26, delivers the needed phases for each operation state. It is composed of an Asynchronous State Machine (ASM) which implements the state diagram described in Figure 27.

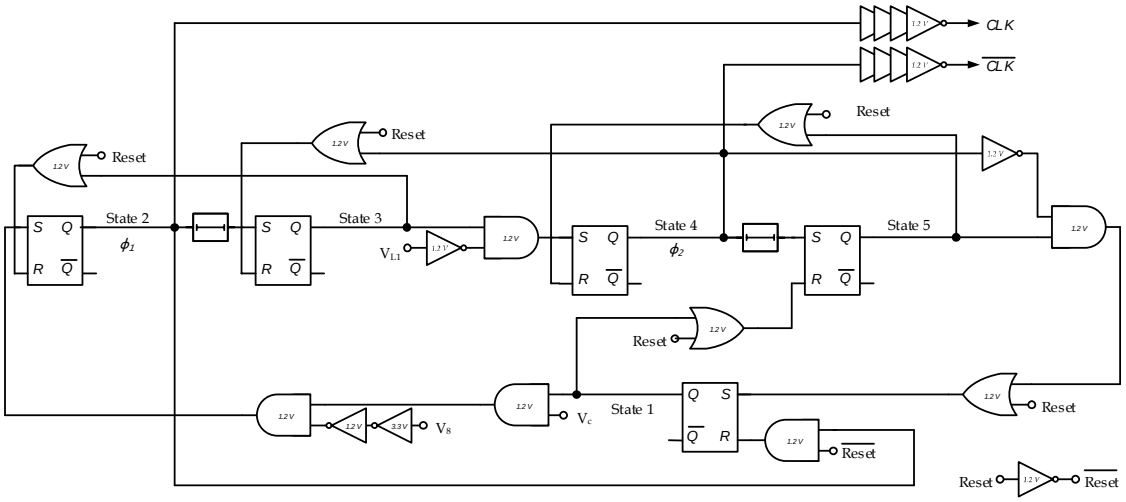

Figure 26: Clock Phase controller.

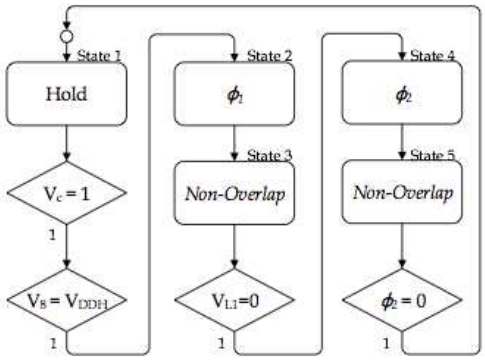

Figure 27: Clock Phase state diagram.

To illustrate the operation of the converter design for the Proteus project, a preliminary configuration in the selected 130-nm CMOS technology was evaluated using MOS capacitors to implement the flying capacitors. As an example, limiting the total area for the capacitors to 1 mm^2 results in a maximum capacitance value of 9.6 nF (C_1 = C_2 = 4.8 nF). With this level of capacitances, the estimated output capability is 20 mW, for an output voltage of 0.9 V. Figure 28, show the electrical simulation of the converter, where the state transition is clearly observable.

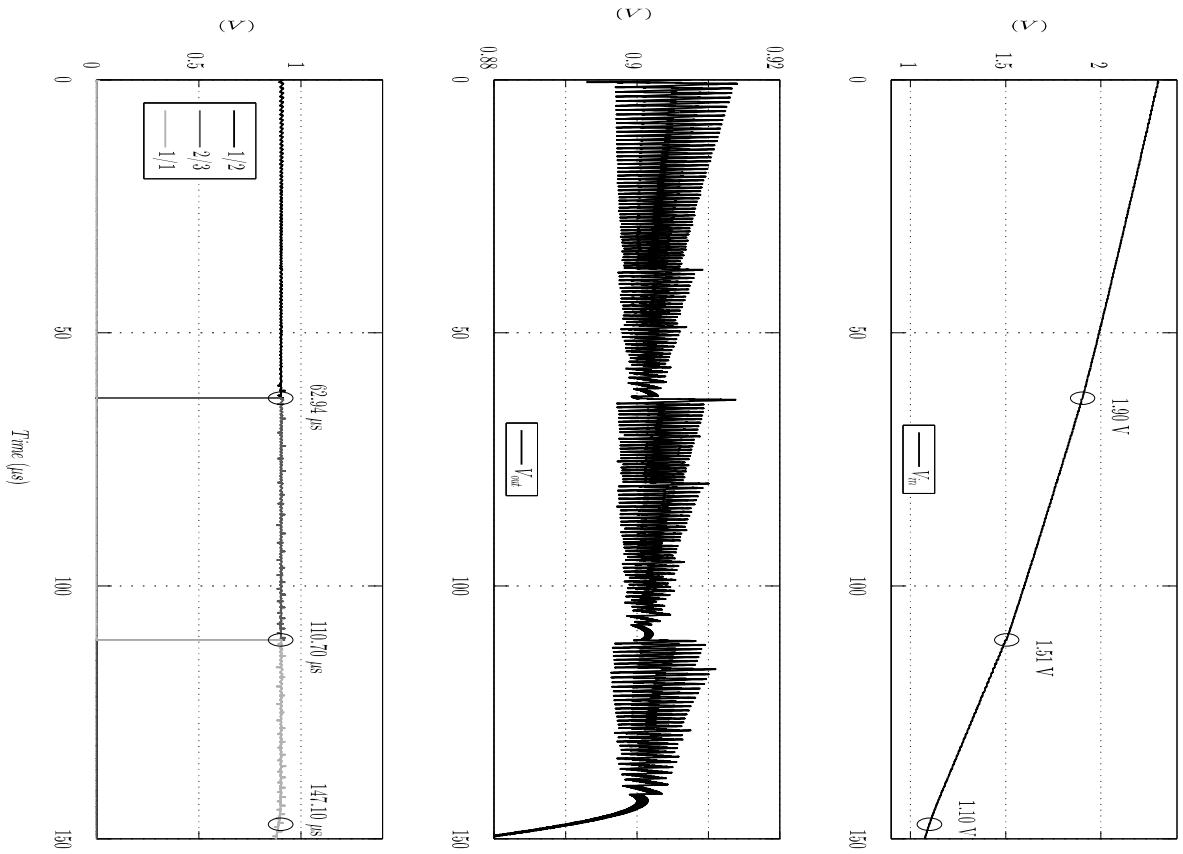

Figure 28: DC-DC converter output voltage.

The implementation details, namely those related with the device sizing, are the subject of work-package 3. However, the target requirements are summarized in *Table 8*.

Table 8: Target requirements for the DC-DC converter.

DC-DC	Input source	Nominal Output voltage	Ripple	Special techniques	Programmability
SC type	0.9 -2.3 V	0.9 V	< 20 mV	Chopping to reduce noise effects	Autoset

4 System Software: operation and smart application levels

It has been identified two software planes in the project: the operational one and the smart application level.

4.1 Node management

This section addresses the control/operational plane of the PNODE. To that respect, a state machine is designed that needs to be implemented in software, which in this first version will be run outside the CMOS chip in MCU. The purpose of the operational system software is to address the required **reactive capabilities** of the PNODE, thus the reaction to triggers either by the Water Management Service (WMS) through commands or by the measurements in PNODE level (of both sensing parameters e.g. flowrate, pressure, etc and paramaters related to the PNODE internal system operation e.g. energy and memory footprint, etc.).

4.1.1 Reminder of D12 requirement analysis

Based on the use cases that were identified in Deliverable D1.1 and the subsequent requirements analysis of Deliverable D1.2, 6 different modes of operation for the PNODE, which are represented as states in the state machine, are identified:

1. **Regular Measurement mode**: regular measurements are taken from primary sensors. Values can be taken/memorized with minimal processing. However it can also perform more elaborated (smart algorithmic based) processing, for example, to aggregate data, detect alerts, etc.

2. **Alert Measurement mode**: when in alert mode, measurements are taken from primary sensors with increased frequency, while secondary sensors may be also activated, and data is prepared to be sent more frequently. The Alert state comprises 2 substates, i.e. Alert and Alarm, which have different Monitoring Profiles as described in D1.1 and recapped in the form of functional requirements in D1.2, and 1 additional substate, i.e. Extrapolation.

    - Alert substate is evoked when at least one measurement is between the alert and the alarm thresholds.

    - Alarm substate is evoked when at least one measurement passes the alarm threshold.

    - Extrapolation substate is evoked when there is need for predicting the current or future value e.g. due to malfunction or irregular (out of range) measurement, large variation or large noise or unexpected rate of change, the latter cases leading to more smart processing and need to communicate with WMS.

3. **Control/signalling mode**: when in control/signalling mode, the PNODE receives configuration messages from the WMS comprising e.g. parameterization.

4. **Communication mode**: in this mode, the PNODE is transmitting data (keep alive signals and sensing data). An ACK is received from the WMS. The WMS may be able to use this ACK to send a control command to the device.

5. **Sleep mode**: the device enters into this mode every time it does not have anything to do. No measurements/processing/transmission, but waiting for control commands. This state is essential to extend the autonomy.

6. **Panic state**: running out of energy "very soon". The device must proceed with data transmission and transition to Sleep mode.

Transitions from one mode to the other is triggered by commands (imposed by WMS) or events (either node-related or environment-related).

The PNODE must be able to respond to 4 commands (Start, Send, Update, GoToSleep):

1. **Start**: The WMS sends this command in order to set the PNODE from the Sleep state to the Regular state.

2. **Send**: The WMS sends this command in order to set the PNODE to the Communication state, so that the PNODE transmits on demand the last data from all sensor elements that are relevant to the defined use case.

3. **Update**: The WMS sends this command in order to set the PNODE to the control/signalling state in order to process a configuration message from the WMS comprising e.g. parameterization of the software.

4. **GoToSleep**: The WMS sends this command in order to set the PNODE to the Sleep state.

The PNODE must respond to 6 basic trigger events (AlertLevelReached, TimeToTransmit, UpdateCompleted, TransmissionCompleted, NoAlertAfterX, NoEnergy), plus to one composite, more complex, event (Malfunction| LargeVariation| LargeNoise| UnexpectedRate) the latter leading to more smart processing. These act as inputs to the states provoking the transition from a state to another, while having additional effects (outputs of the transition). Detailed description of the triggers:

1. **AlertLevelReached**: This trigger event is true when either at least one measurement is between the alert and the alarm thresholds (AlertThresholdBypassed) or at least one measurement passes the alarm threshold (AlarmThresholdBypassed).

2. **TimeToTransmit**: This trigger event is true when it is time for either a transmission in regular or alert state or for a keep alive signal.

3. **UpdateCompleted**: This trigger event is true when the PNODE has completed the updates that are instructed by the previously received "Update" command.

4. **TransmissionCompleted**: This trigger event is true when the PNODE has completed the transmission of either measurements in a regular or alert state or a keep alive signal.

5. **NoAlertAfterX**: This trigger event is true when all measurements (from the parameters that are relevant to the defined use case) are not passing the alert or alarm thresholds, having an observation window in time of X.

6. **NoEnergy**: This trigger event is true when the energy level of the PNODE reaches the lowest level.

7. **ExtrapolationRequired**: This trigger event is true when there is need for predicting the current or future value e.g. due to malfunction or irregular (out of range) measurement, large variation or large noise or unexpected rate of change.

8. **ExtrapolationNotRequired**: This trigger event is true when there is no further need for predicting the current or future value.

In Figure 29, the PNODE state machine with its state transitions is illustrated.

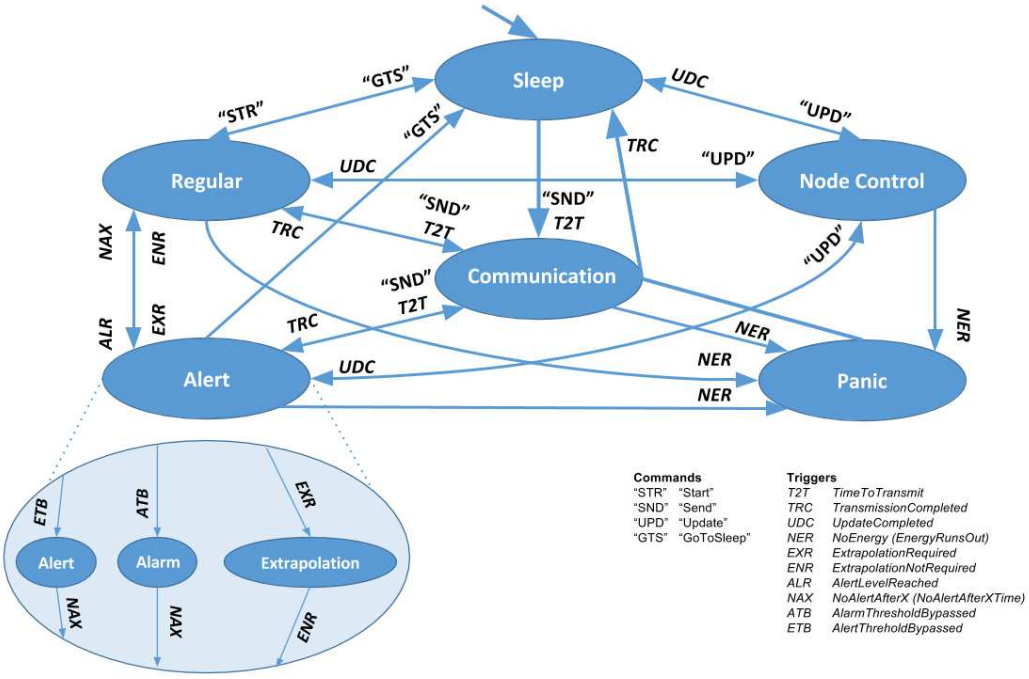

Figure 29: PNODE state machine and state transitions.

The current system state of the PNODE can be defined at any time by the triple {use case, current state, previous state}.

Below we provide the state transmission table, Table 11, for the system. In Command or event column and in quotes, we consider a command received by the PNODE from the WMS.

Table 9: PNODE state transmission table

Modes of operation	Command or event	Next modes of operation	Output (action the node must carry out)
Sleep	"Start"	Regular	Activate primary sensors
Regular	"GoToSleep"	Sleep	Deactivate primary sensors Put the sensor in sleep mode
Regular	TimeToTransmit	Communication	Keep alive signals Data sent to WMS
Regular	AlertLevelReached	Alert	Increase measurement frequency Change TimeToTransmit (communication periodicity) May activate secondary sensors if requested by use case and/or possible with energy budget
Regular	ExtrapolationRequired	Alert	May predict next expected measurements May/Must go to Communication mode to send warning
Alert	ExtrapolationNotRequired	Regular	-
Alert	NoAlertAfterX	Regular	Decrease measurement frequency Deactivate secondary sensors in case of previous activation
Alert	"GoToSleep"	Sleep	Deactivate primary sensors Deactivate secondary sensors in case of previous activation
Alert	TimeToTransmit	Communication	Data sent to WMS immediately
Node control	UpdateCompleted	Previous state (Sleep, Regular, Alert)	Return to previous state
Communication	TransmissionCompleted	Previous state (Sleep, Regular, Alert)	Return to previous state
Communication	TransmissionCompleted and previous state is Panic	Sleep	Go to Sleep to charge
Sleep Regular Alert	"Update"	Node control	Over the air parameterization (define threshold, alert levels) Over the air programming
Sleep Regular Alert	"Send"	Communication	Data sent to WMS immediately
Regular Alert Communication Node control	NoEnergy (Energy runs out)	Panic	Go to Communication mode to send warning (and data) to WMS

The sensing parameters are defined on D1.2. Each of them will have the following attributes {Name, Criticality, Minimum, Maximum, CurrentValue, Precision, MinAlarm, MinAlert, MaxAlert, MaxAlarm, MeasurementFrequency, TimeToTransmit}, where:

1. **Name**: The literal name of the parameter e.g. pressure, flowrate, etc..

2. **Criticality**: A logical value depicting if the parameter is critical or non-critical in the specific use case.

3. **Minimum**: The lowest bound of the typical range of operation, thus the minimum value of the parameter.

4. **Maximum**: The highest bound of the typical range of operation, thus the maximum value of the parameter.

5. **CurrentValue**: The current measurement value of the parameter.

6. **Precision:** The precision of the parameter, however this property may be reconsidered to be deleted if not used in the state machine.

7. **MinAlarm:** The minimum alarm threshold, that when a measurement value of the parameter is below this threshold, an alarm is triggered.

8. **MinAlert:** The minimum alert threshold, that when a measurement value of the parameter is between the minimum alert threshold and the minimum alarm threshold, an alert is triggered.

9. **MaxAlert:** The maximum alert threshold, that when a measurement value of the parameter is between the maximum alert threshold and the maximum alarm threshold, an alert is triggered.

10. **MaxAlarm:** The maximum alarm threshold, that when a measurement value of the parameter is above this threshold, an alarm is triggered.

11. **MeasurementFrequency:** The periodicity of measurements of the parameter depending on the use case, parameter name and criticality, expressed in time interval between measurements.

12. **TimeToTransmit:** The periodicity of transmission of the parameter's measurement to the WMS depending on the use case, parameter name and criticality, expressed in time unit scheduled for the next transmission.

Criticality, Minimum, Maximum, Precision, MinAlarm, MinAlert, MaxAlert, MaxAlarm, MeasurementFrequency and TimeToTransmit of each parameter are defined in D1.1 and summarized in the D1.2 functional requirements table (FR01 to FR15).

As a summary, the PNODE will be able to detect by itself (without off-node processing) an alert or alarm based on sensors' measurement and thresholding. Alert and alarm levels are defined either by the observable passing a fixed threshold or by the observable passing the "average or trend of last measures, for an integration time of 5 minutes". If the PNODE has entered Alert state, it returns in Regular state if no violation of all Parameters' thresholds is observed.

When all the critical parameters are in their regular range of operation (between low and high alert levels), critical parameters will be acquired once per minute, non-critical parameters, once every 5 minutes. When a single parameter (critical or not) enters a non-regular level (above or below alert level) all the correlated parameters parameters will be acquired once every 30s and the non-critical

parameters will be acquired once every 2 min. All the collected data will be transmitted to the WMS once a day. If a critical or non-critical parameter passes alarm threshold for 4 consecutive measurements, the information about this parameter and the correlated ones plus the last measurements before alert/alarm will be transmitted immediately to the WMS. If a critical parameter remains above alert threshold for 10 consecutive measurements, the same information will be transmitted immediately to the WMS. If a non-critical parameter remains above alert threshold for 15 consecutive measurements, the same information will be transmitted immediately to the WMS.

4.1.2 Correlation between parameters

The D1.2 introduces the notion of correlated parameters. The correlations may be retrieved by the cross-relation table of Figure 30 that illustrates the degree of dependence between parameters in a qualitative format. Please note that the relation is not bi-directional and the table is not symmetric. In any case, the correlation among parameters will be parameterized and reconfigurable.

Parameters (column below) and their dependence to each other (lines)	Temperature	Flowrate	Pressure	pH	Chlorine	Conductivity	Dissolved oxygen	Nitrates	Redox potential	Chloride	Calcium	Magnesium	Hardness	Salinity
Temperature		-	-	-	-	-	-	-	-	-	-	-	-	-
Flowrate	-		+++	-	-	-	-	-	-	-	-	-	-	-
Pressure	-	+++		-	-	-	-	-	-	-	-	-	-	-
pH	+	-	-		-	-	+	-	-	-	-	-	-	-
Chlorine	-	-	-	++		-	-	-	-	+	-	-	-	-
Conductivity	+++	-	-	-	+		+	++	++	+++	+++	+++	+++	+++
Dissolved oxygen	-	+	+	-	-	-		+	-	-	-	-	-	-
Nitrates	-	-	-	-	-	-	+		-	-	-	-	-	-
Redox potential	-	-	-	++	++	++	++	++		++	++	++	++	++
Chloride	-	-	-	-	+	-	-	-	-		-	-	-	+++
Calcium	-	-	-	-	-	-	-	-	-	-		+	-	-
Magnesium	-	-	-	-	-	-	-	-	-	-	+		-	-
Hardness	-	-	-	-	-	-	-	-	-	-	+++	+++		-
Salinity	+	-	-	+	+	+	+	+	-	+++	+	+	+	

Temperature dependence

In case of leakage ONLY, both parameters decrease simultaneously (downstream); flowrate increase and pressure decrease (upstream)

Figure 30: - Cross-relation table between parameters

4.1.3 Reconfigurability

It is important to say that the PNODE will be reconfigurable. First, all Monitoring Priorities, Requirements, Control levels, Monitoring and Transmission profiles for each use case (Drinking water, Rain water, Waste water) together with other operator-defined parameters, e.g. frequency of keep alive signals, will be parameterizable through a header file before being loaded to the MCU at boot-up. Then, WMS can set use case and issues commands for over the air parameterization of some definitions of some operator-defined parameters.

Some of the basic sub-functionalities of the PNODE, as stated in D1.2 section 8.3, e.g. the Write function, the Reading function, the Average function, the Threshold function, the Derivative function can be given by the Analog Front-End API or by dedicated digital circuit domain, so as to reduce energy consumption, as well as the Transmission function, the Receive function and the Data modulation function by the Communication API. The Analog Front-End API will also decouple signals from sensors based on corresponding issued commands of the operational system software, thus the signal coming from each sensor can be routed and independently processed. It will also allow the configuration of the sensor elements, e.g. the activation/deactivation of primary and secondary sensors, the increase/decrease of the periodicity of measurements etc.

4.2 Communications

In the context of PROTEUS, communications will be used to both extract sensor data from the PNODES and to exchange control commands between PNODES and water management software. Communications technologies to be used in by PNODES must be able to address two issues: the very limited energy available in the PNODE and the electromagnetic attenuation produced by the deployment environment. As PNODEs must be energetically autonomous, the power consumption of the chosen communication technology must be compatible with the power generated by the energy harvesting system. Regarding to the electromagnetic attenuation, the majority of the attenuation on the communication signal is expected to be due to the construction material used to build the visit boxes where the PNODES will be deployed, identified in the subsection 9.2 of D1.2 named "Constraints on Communication". Since most of the visit boxes are located in urban environment, several other sources of electromagnetic attenuation and interference may be present (such as buildings, vehicles, etc.). Electromagnetic attenuation is an important aspect of study since it as direct impact in the effective range of communication technologies.

Both aspects (energy consumption and effective range) will be key parameters for the selection communication technology that will be used for communication with PNODES. Therefore, the selection of the communication technologies will require the execution of communication field trials on the real world conditions, as described on section 9.2 of D1.2. Such tests will have as main focus the quantification of the real power consumption on the deployment conditions, and how it varies with different network loads and communication ranges.

4.2.1 Testing Conditions

For an accurate assessment of the most appropriate communication technology to be used in PNODES, tests must be executed in an environment as close to reality as possible. In PROTEUS context, the deployment will require devices to be place inside visit boxes and manholes made of concrete and covered by cast iron covers as represented in Figure 31. The deployment of devices in those conditions requires a considerable amount of time. Moreover, each time that a new communication technology needs to be tested, radio modems on testing devices must be changed. This type of tests requires cast iron cover to be frequently opened and closed, operations that must be performed by authorized personnel. To make things worse, most of these visit boxes and manholes are located on roads, where the access to them imposes traffic limitations.

Figure 31: Concrete Manhole and Cast Iron Cover

A large amount of communication technologies is available on the market, differing on many aspects as: the communication protocols used (e.g. Wi-Fi, ZigBee, BLE, LORA, etc.), the radio frequencies used (e.g. 2.4 GHz, 868 MHz, etc.), and the hardware technologies used by the manufacturer. Therefore, in order to save time and less the burden on the traffic, a prior set of tests is needed in a simulated environment in order to identify the most promising technologies to be then tested in a real world environment.

The results of the tests in communication technologies may affect the network architecture and the deployment strategy of the network elements. These depend mostly on the effective communication range achieved for the power available. Two approaches were defined based on the communication range:

- Short-range Communication – This approach considers that PNODES have a communication range of a few meters. In this approach, a PNODE inside a visit box is able to exchange messages with a gateway deployed a few meters away on the surface, for example in a lamp post. Due to the very limited communication range, one gateway will only communicate with one or very few PNODES. These gateways will also be equipped with a module that can connect to the Water Management Service (WMS).
- Long-range Communication – In this approach PNODES are expected to be able to communicate to a distance of many meters or few kilometres. Each gateway will be able to exchange messages with many PNODES. The further the communication range achieved, the lesser will the number of gateways that needs to be deployed. In the optimal case, few gateways deployed in high structures (such as the water towers identified in D1.2) will be enough to cover all of SMAS water network.

4.2.2 Testing Methodology

A methodology was defined to run automated field tests using Wireless Sensor Networks communication technologies, being developed in the context of a master thesis supervised by UNPARALLEL INNOVATION, Lda. This methodology defines a set of parameters that can be configured in order to define a range of tests to be executed. These parameters are:

- **Communication Technology** – refers to technological specific aspects, such as the communication protocol and the radio characteristics;
- **Communication Distance** - specifies the distance between distance between the antennas during the tests;
- **Communication Environment** – characterises the environment where the tests were executed (e.g. executed indoor or outdoor, with line-of-sight or with obstacles in the communication path)
- **Payload** – specifies the size of the messages used in the tests;
- **Communication Type** – defines the communication role of the device under study (receiver, transmitter, receiver and transmitter);
- **Power Level** – specifies the power level applied to the antenna's amplifier;
- **Duty Cycle** – defines the ratio of time that radio interface is turned on over a completed on-off period

There parameters can be aggregated in two groups: one corresponding to parameters related with the software configurations – Payload, Communication Type, Power Level and Duty Cycle; and others related with the physical configurations of the deployment, affecting physical aspects of both the

environment and the hardware used in the tests – Communication Technology, Communication Distance, and Communication Environment.

The parameters that correspond to software configurations will be used by an automation algorithm. This algorithm calculates all the possible combinations of configurations and automatically generates the code corresponding to each different testing configuration. This process is represented in Figure 32**Erreur ! Source du renvoi introuvable.**, where different values of Communication Type, Duty Cycle, Payload and Power Level are introduced into the automation approach that will generate all the possible tests.

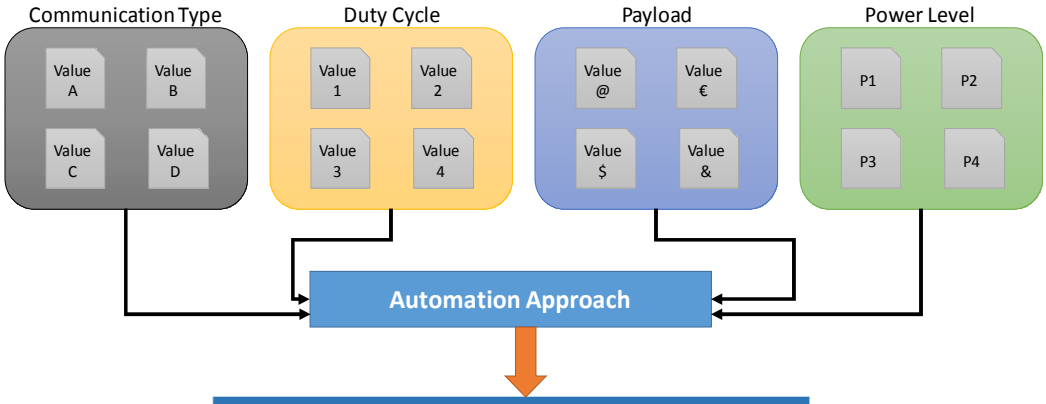

Testing Specifications				
#	Communication Type	Duty Cycle	Payload	Power Level
1	Value A	Value 1	Value@	P1
2	Value A	Value 1	Value@	P2
3	Value A	Value 1	Value@	P3
4	Value A	Value 1	Value@	P4
5	Value B	Value 1	Value@	P1
…	…	…	…	…

Figure 32: Approach for software automation.

The testing deployment consists in the setup of three devices, where two devices will have a communication role and third will be equipped with a current sensor in order to monitor the power consumption of one communication device. This deployment is represented in the diagram presented in Figure 33. The communication devices are categorized in **Coordinator Device** and **End Device**. The first device receives the software configurations of the test to be executed and transmit them to the End device before the test execution. The **Auxiliary Device** will be used to sense the current in the End device, which will be used to compute the power consumption of the End device during the tests.

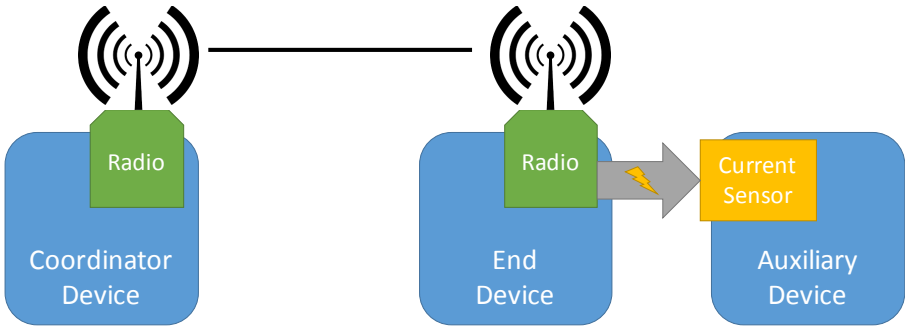

Figure 33: Deployment Diagram

The Coordinator device will inform the End device about the test configuration during the setup stage of the test. This information is transmitted by a configuration message, whose structure is represented in Figure 34. The first parameter of this message is the Communication Type, where: value 1 corresponds to the scenario where the coordinator sends messages and the end acts only as receiver; value 2 corresponds to the scenario where the coordinator acts as a receiver and the end device assumes the role of message transmitter; and value 3 where both coordinator and end devices act as transmitter and receiver, one at a time.

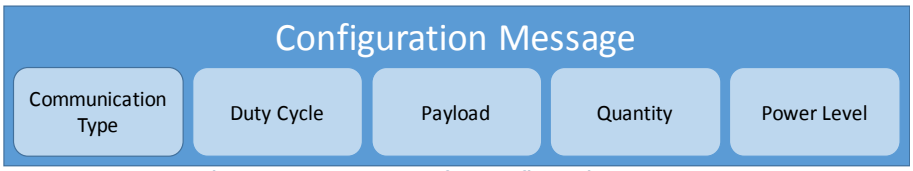

Figure 34 – Structure of a Configuration Message

The second value represents the Duty Cycle, which can be used to determine the sequencing between two consecutive transmissions. The third value is the Payload parameter, used to define the number of bytes that each testing message will have. The fourth parameter is the Quantity that specifies the amount of times that the test will be executed. The fifth and last value corresponds to the power level applied to the antenna amplifier. It was defined that the highest power level corresponds to the value 4 and the lowest power level corresponds to the value 0.

The interaction between the devices used in the testing deployment will depend on the Communication Type under test. As this testing methodology considers three different Communication Types, three flows of interactions can be observed. These interactions are represented by diagrams in Figure 35, Figure 36, and Figure 37. In Figure 35 are represented the flow of messages for the communication type where the coordinator device has the role of sending the test messages and the End device only receives messages. This type of test has the purpose of computing power consumption when the device is working in receiver mode. This test starts with the definition of the test parameters by the user and its configuration on the Coordinator Device. Then, the coordinator sends the Configuration Message, presented in Figure 33, to the End Device. After processing ths message, the End Device sends the signal to the Auxiliary Device to start the power consumption monitoring process, as well as an acknowledge (ACKc) to the Coordinator Device.

Achieving this point, the devices will start the real test assuming the Coordinator device the Transmitter Role (Tx) and the End device the Receiver Role (Rx). This test execution implies the exchange of a pre-defined number of test messages, this number being defined in the received Configuration Message. At the end of the testing loop, the Coordinator will transmit to the End device a message indicating the End of Test, being the End device oblige to reply with a message (ACKe) to

the Coordinator device finishing the one test process. During the end of test sequence of messages, the End Device must also send a signal to the Auxiliary Device to finish the power consumption monitoring process.

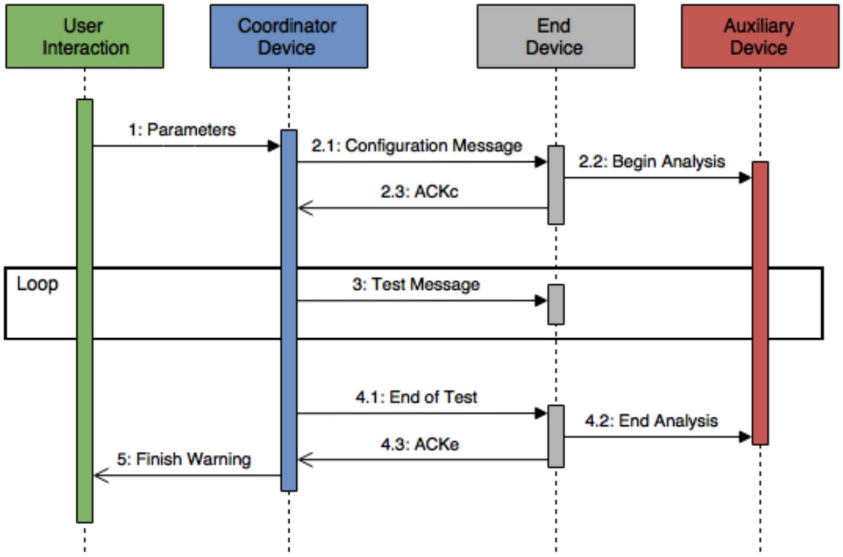

Figure 35 – Receiver Diagram

In Figure 36 is presented the diagram corresponding to the scenario where both devices transmit and receive messages. The flow of messages in the test is similar to the previous one, differing only by the content of messages transmitted during the testing loop. Following a test transmission from the Coordinator, a transmission from the End device will occur, being the coordinator tasked with the reception of test messages and the End device responsible for its transmission. Finishing this transmission from the End device, both devices restore their primarily role.

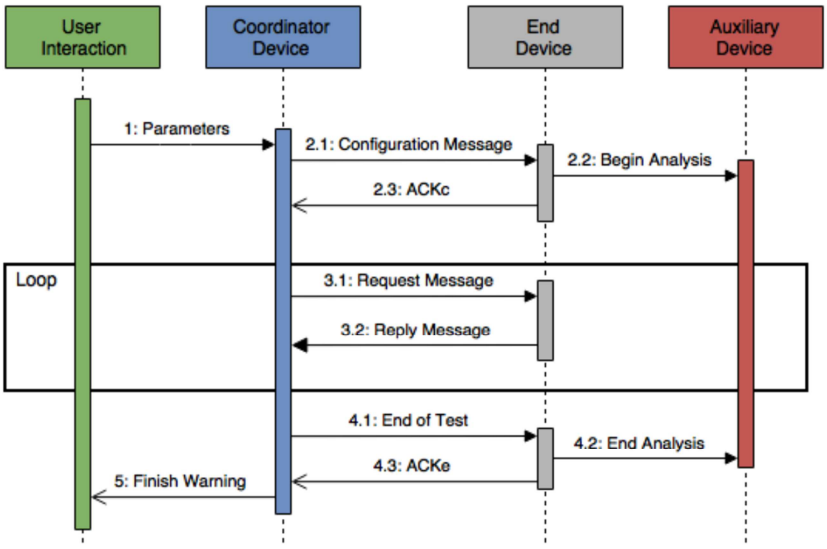

Figure 36 – Request-Reply Diagram

The diagram corresponding to the scenario where the End Device assumes the transmitter role is presented in Figure 37. This setup allows computing of the power consumption during transmissions. The device that begins the testing loop transmission must end it with the transmission of the End of Test message, this case is no different being this task done by the End device. Followed to this device

communication, the device in question is responsible for the command transmission that disengages the Auxiliary device and also for the End of Test message transmission to the coordinator device.

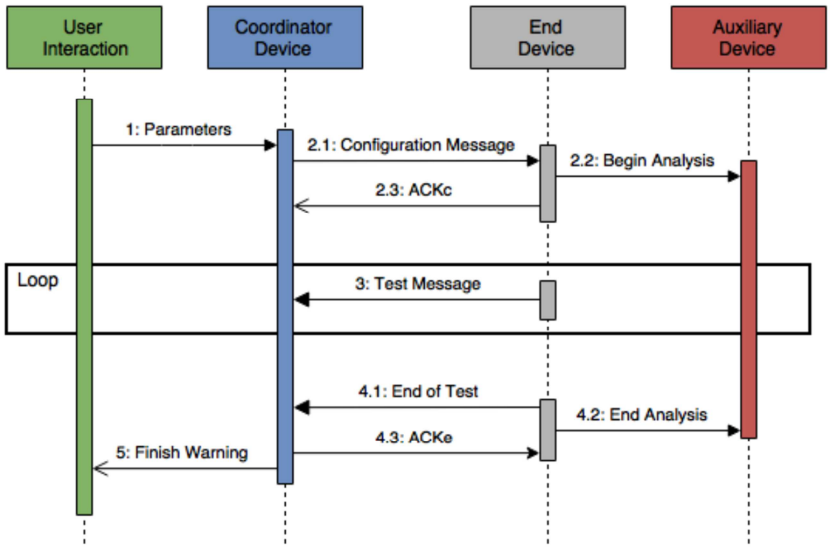

Figure 37 – Transmitter Diagram

More details about the behaviour of the devices that must be implemented can be found in appendix 1. In this appendix, the internal actions of each device are described in detail, this description being supported by state machines diagrams.

4.2.3 Initial Communication Approach

The first version of PROTEUS chip will be accompanied by a support board which will be equipped with two communication technologies:

1. One for short-range communications. This is supported on a Bluetooth Low Energy (BLE) chipset (implementation details given in WP3) with low power consumption, operating at the 2.4Ghz ISM band. In the second version of the CMOS chip, the radio module will be based on an Impulse Radio Ultra-WideBand (UWB) technology.
2. One for long-range communications based on an Ultra Narrow Band chipset (implementation detiaks given in WP3) operation at 433 MHz and 800MHz bands. Not being part of the CMOS chip, the inclusion of this technology in the support will enable to reach up to 20 km in rural area and 3 to 5 km in urban area, depending on the conditions of installation. This is achieved by limiting the channel noise power through the use of ultra narrow band radio channels.

Despite the fact that the communication technologies provided in this first version may not be the ones that will be included in the final version of PNODES, the provided technologies will enable initial experiments with network architectures. These technologies will also allow the calculation of rough estimations of the power consumption due to communication, support the development of the Communication API, and support the definition of power saving strategies to optimize the performance of the different communication technologies within the different network architectures.

4.3 Smart Application Software

4.3.1 Methodology

This section addresses the Smart Application Software of the Proteus System (both PNODE and WMS). To that respect, cognitive algorithms are designed that need to be implemented in software, which in this first version, it will be run either outside the CMOS chip but in the MCU and/or normal processor (e.g., ARM) or in a remote PC in the WMS. The purpose of the Smart Application Software is to address the required **predictive and cognitive capabilities** of the Proteus System (both PNODE and WMS).

In the first version of PROTEUS system, the focus will be on the Extrapolation function (D1.2 section 8.3), namely the prediction of the next value of a detectable Parameter.

It is very important to define in the design when extrapolation is required from both a user and system perspective. The current design (of the first run) comprises the following extrapolation needs:

1. To trigger extrapolation depending on some energy availability thresholds (D1.2 section 8.2), so as to see if energy is enough to support the PNODE in Alert state and to send to WMS a warning if required. The rationale is that energy autonomy strongly depends on the number of alerts and the stay of the PNODE in the Alert state; thus, extrapolation can be used to check if an alert is likely to be raised in the short (5 to 15min) term and then if there are the required (e.g. for sensing and communication) energy resources.

2. To trigger extrapolation in case that no reading (malfunction?) or irregular (out of defined operating range) data is received from sensor.

3. To trigger extrapolation in case of large variation or large noise in measurements.

4. To trigger extrapolation when a detectable Parameter increases or decreases with a large rate of change, so as to issue a warning for an emergency.

It is important to say that the extrapolation triggers should not result in too many alert or alarms events, which would result in lack of confidence from the user. Thus, the software deployed should be resilient to regular, expected variations in parameters' measurements which do not imply a problem for water consumption: e.g. it is expected that the conductivity, chlorine, nitrates and even pH have small variations through the day and the pressure is typically constant at every location. However the flow rate is an example of a measurement that must be parameterized in each case, according to its historical data.

As a consequence, the triggers for alert and alarm should have some critical values that should be configurable either before loading the software at boot-up or by over the air parameterization, but the device should be able to eliminate outliers itself, that may result from the wrong point readings. The intention is on the one hand to help the water operator to have quick information and identify critical situation and on the other hand to consider the triggers in a way that saves energy and ensure proper operation. A critical point is that there must always be some energy in reserve for critical cases.

To the aforementioned extrapolation needs, the design will also investigate additional extrapolation requirements, namely:

1. To trigger extrapolation to identify unexpected cross-sensitivity on the node faster that a detailed lab screening (when putting a sensor in a real pipe). Indicative example may be to automatically correlate data from a test sensor with the data from the reference sensors that measure cross-sensitivities, when a supposed constant observable is varying, in order to see if some trends are similar between the observable as measured by the test sensor and the cross-sensitivities as measured by the reference sensors.

2. To trigger extrapolation for online calibration. Indicative example is to find the coefficient of correlation between test sensor output and the real observable, when reference sensors are measuring the observable among others, while the other cross-sensitivities remain uncontrolled (or at least imperfectly controlled, main observable may also vary). A prerequisite of this problem is to extrapolate the patterns of the water flow in the loop based on the reference sensors outputs. More precisely, by means of knowing the data at some points in the network from reference sensors, you extrapolate what happens between these reference points. In a real network, where there are not any reference sensors and no info on the flow is available in the network, when one or more sensors have a drift, you should probably learn at the start of the deployment (when the sensors have just been calibrated), to extrapolate the geographic pattern of the flow in the network (maybe also using physical models of the flow/concentration propagation in the network), and then check in time whether this pattern is respected, use it to deduce which sensor is probably most erroneous, and finally use the data from the other sensors and the extrapolated pattern to correct it.

3. To trigger extrapolation to correlate info from neighbouring sensors (to remove bad points first, to identify geographic trend second), e.g. when there may be important noise in the pipes related to bubble formation.

The second important point in the design is to define where extrapolation should be run; in the PNODE or in the WMS. The current design (of the first run) comprises a distributed processing approach with both in-node processing and in-WMS processing. The in-node processing for extrapolation may be considered either in the MCU or in slave ARM controlled by the master MCU, the latest instructing when it is time for the “heavy” processing to be done. The following potential solutions are currently adopted related to the execution place of the extrapolation:

1. Short term (time) extrapolation in PNODE and long term (time and space) and more precise in WMS.

2. In Regular state, where data is communicated once a day, extrapolation is better to occur in PNODE, since no latest (or all) data exists in WMS. Moreover, communication of data may consume more energy than a simple algorithm to run in the PNODE.

3. If extrapolation is done from a system (related to the operation of the PNODE) perspective (e.g. when triggering extrapolation depending on some energy availability thresholds as explained before), it is better to do in-PNODE extrapolation.

4. If extrapolation is done from a user perspective and data is available to WMS, in-WMS extrapolation is better to be selected; due to resources, it may be also more efficient e.g. pattern prediction instead of value prediction, correlation of data from different nodes etc.

To reduce complexity and resource consumption, the current design considers only one parameter (the more critical one) per use case to extrapolate. Training for extrapolation is very important. To that respect, data availability (from SMAS) is considered. Training is better to be done in WMS for both in-PNODE and in-WMS processing; for in-PNODE processing, after training phase, coefficients may be sent to the PNODE with the command Update (over the air parameterization). Where training occurs may depend on the energy availability and the complexity of the training. If the pattern changes, which may be identified either by recurring failures in extrapolation (reactively) or by checking its validity periodically by comparing real measurements with their predicted values (proactively), then the training process should be repeated.

In the second run (some of these aspects may be reconsidered even for the first run), the design intends to investigate further cognitive functions for the Smart Application Software, as follows:

1. Reaction and prediction with respect to more complex events.

    - In-WMS processing that may involve the collaboration of more than one sensor nodes and more than one sensor parameters.

    - In-PNODE processing when values of some parameters only change if the values of others parameters change too, e.g. patterns and inter-correlations between parameters. This can be used to **reduce the measurement needs**, e.g. if no variation is detected in the values of conductivity then there is no need to measure the concentration of chloride and nitrates as they didn't change, but also to **identify failure of one specific sensor at a given PNODE or to eliminate false values or to understand the behaviour of the measurement**.

    - Trend detection in several forms; this comprises for most cases constant values, for some others constant variations e.g. when there is mixing of water from different sources, in another one 2^{nd} order polynomial behaviour e.g. when one tap is opened or closed, the variation of the flow rate in that point increases or decreases exponentially. Numerical derivative/rate of change can be an alternative for less energy consumption/required memory. This trend detection is also important so as to **eliminate false values or to understand the behavior of the measurement** and the design is desirable to allow some parameterization.

2. Optimization in processing by dynamical switching based on energy and memory availability between processing blocks in PNODE – analog, digital, MCU, ARM – but also between PNODE and WMS.

4.3.2 Cognitive algorithms

Two kinds of algorithms are considered in the first version of the design for the extrapolation function.

The first algorithm is intended for in-PNODE extrapolation and targets short term but fast prediction with small memory usage. It is based on a **linear regression model** receiving up to 3 past values of the measurement as inputs. The regression model is as follows

$$Y_{n+1} = b_1 + b_2 * Y_n + b_3 * Y_{n-1} + b_4 * Y_{n-2}\,, \qquad \text{Eq. 4}$$

where b_x are the trained coefficients and Y_{n-x} is the output x samples ago.

The training for the 4 coefficients that describe the system behavior is performed based on Normal Equation, a method that is fast, with no need to loop and straight forward calculation.

The quality of the trained coefficients is affected by the number of real data we have available as historical data from past measurements and by the use of nonlinear functions on lagged versions of these past measurements. The use of non-linear functions on the lagged versions may achieve better results and cast more accurate predictions. The impact of using non-linear functions is that it increases the performance of the extrapolation, but on the expense of more complexity in computations.

Some indicative examples, on how the number of considered historical data in training affects the regression model, are as follows.

In case of 10 previous values to train the coefficients and forecast the next value for flow rate, the model that described our data (hypothesis model), with an 87.29% correlation between the guessed and the actual value, though we had to use many nonlinear functions, is:

$$Y_{n+1} = b_1 + b_2 * Y_n + b_3 * \log(Y_n * Y_{n-1}) + b_4 * \sqrt{Y_{n-1} * Y_{n-2}} \qquad \textit{Eq. 5}$$

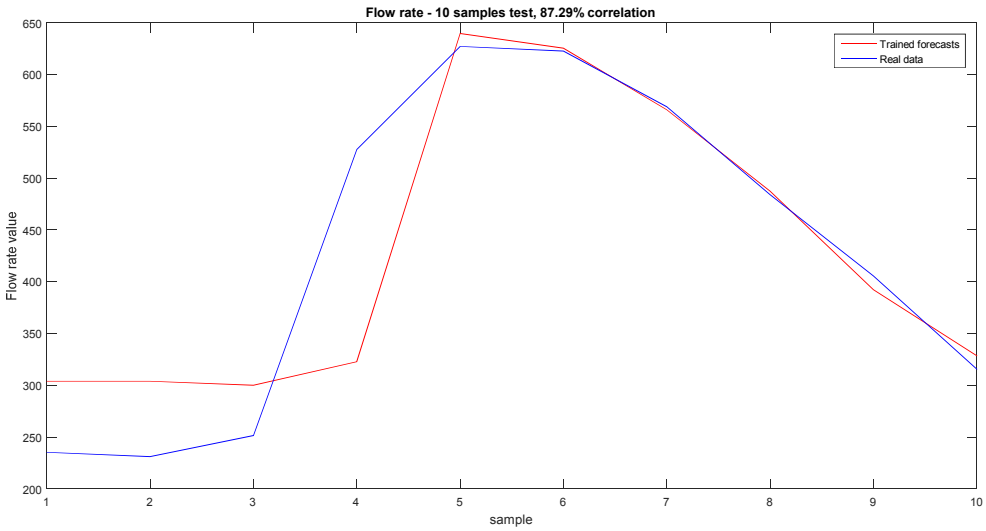

Figure 38: Flow rate prediction using 10 past measurements as input data

When the number of samples for training increases to 30 past measurements. the correlation between the hypothesis model and the real data also increases to 92.21%, but again the model should comprise nonlinear functions to describe our dataset. For this training, more coefficients are used and the hypothesis model is described by the following equation:

$$Y_{n+1} = b_1 + b_2 * Y_n + b_3 * (Y_{n-1} * Y_{n-2}) + b_4 * \log(Y_{n-1}) + b_5 * \sqrt{Y_n} + b_6 * \sqrt{Y_{n-1}} + b_7 * \sqrt{Y_{n-2}} \quad \text{Eq. 6}$$

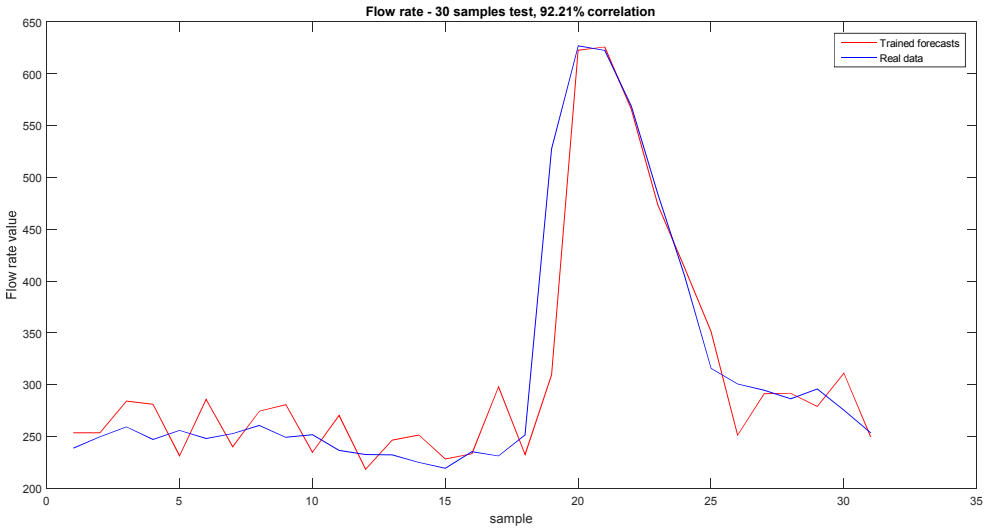

Figure 39: Flow rate prediction using 30 past measurements as input data

In case that the number of past measurements for training increases from 30 to 100 using the same hypothesis model, the improvement in quality of the trained coefficients can be shown clearly in the next figure, achieving a correlation of 93.83%. This identified that improvement is feasible by "feeding" with more data rather than using a more complex model (adding more nonlinear functions). Of course, there is a trade-off, since there is no meaning to use more data for training to achieve a marginal effect on performance, and this fact should be considered in the final selection of model and size of training data.

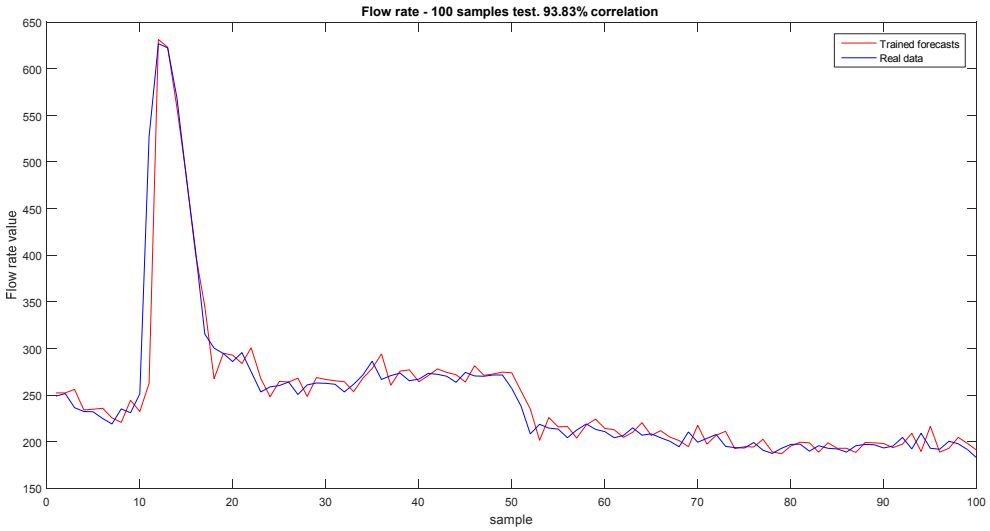

Figure 40: Flow rate prediction using 100 past measurements as input data.

For the previous example with the 100 past measurements for training, we can however select to describe our model with a much simpler expression, without using nonlinear functions, like the one presented in the beginning of the section, namely

$$Y_{n+1} = b_1 + b_2 * Y_n + b_3 * Y_{n-1} + b_4 * Y_{n-2} \qquad \text{Eq. 7}$$

This model achieves a correlation of 93.61%, which is only 0.22% less accurate than the nonlinear hypothetical model but it requires less computations. As anticipated in 4.3.1, training will take place in the WMS and then coefficients will be sent to the PNODE, since this will reduce significantly the computations and the data to be preserved inside the PNODE, thus reducing the required memory requirements of the PNODE.

Finally, in the next figure one can see the effectiveness of the number of data on the quality of the training. If we use 3400 past measurements as training data, then we can achieve a correlation of 98.91%. We can then cast very accurate predictions using the simple model, which was described above.

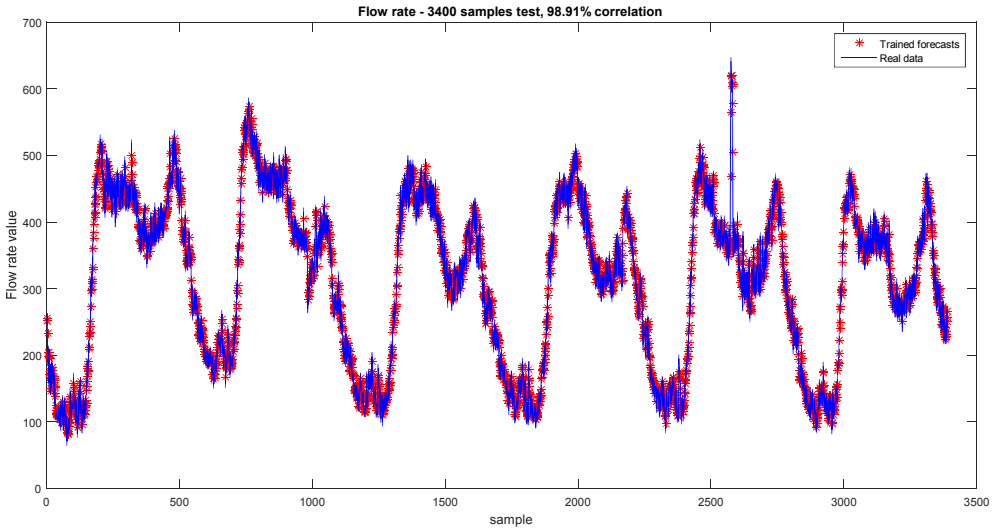

Figure 41: Flow rate prediction using 3400 past measurements as input data.

Our first run design will consider as first option the linear regression model that was presented and which reduces computations for in-PNODE extrapolation, while the training will take place in WMS with a sufficient number of past measurements, and coefficients will be sent after training phase to the PNODE with the command Update (over the air parameterization).

The second algorithm for extrapolation aims at in-WMS extrapolation for long term and extremely accurate prediction with higher memory/data usage and good processing unit.

Neural Networks are exploited for time series prediction and stochastic signals, receiving up to 3 past values of the measurement plus the current measurement as inputs. The training is more demanding in terms of time and processing power and when training is finished, a generated function can be called in order to predict the next value.

Our approach was to use 12 hidden layers, one output layer, and 3400 data to train the neural network and predict the next value based on 3 past measurements. In every iteration, we have 3 inputs that are being applied on the network and we apply back propagation to train the weights and biases of every neuron of the hidden and output layer. The network is then trying to find the optimal weights and biases that describe our dataset.

An illustration of the neural network is shown below.

When the training is done, we apply the trained biases and weights of the neural network on the lagged data matrix. We achieved a correlation of 98.93%. The model that describes the dataset is like the linear version of the regression training:

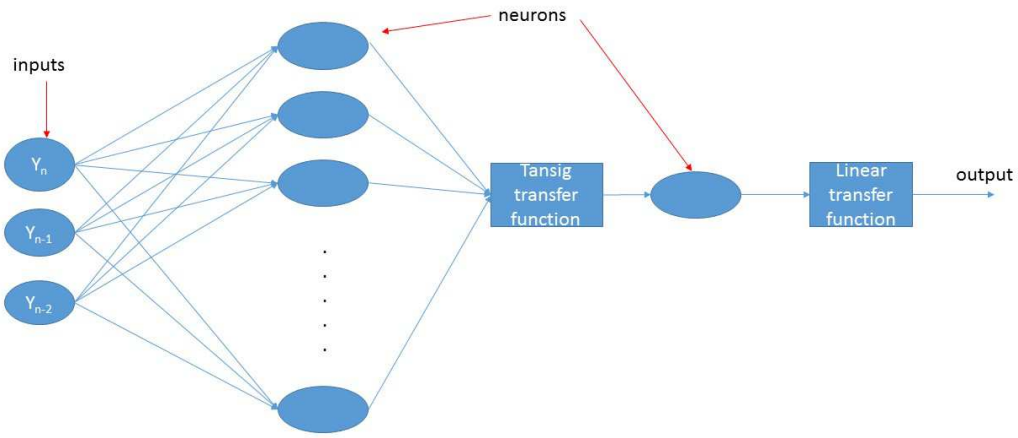

Figure 42: Neural network topology.

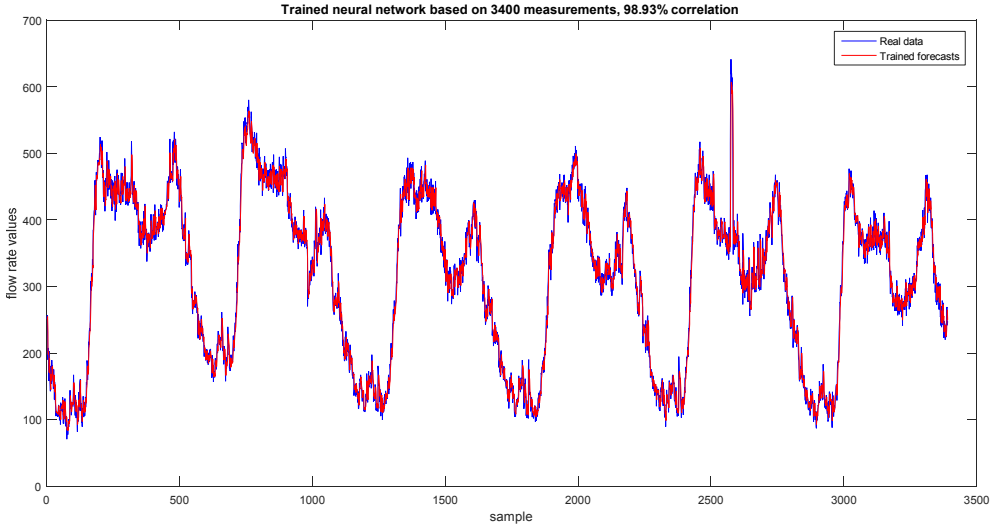

Figure 43: trained neural network predictions.

In-WMS extrapolation can also incorporate an algorithm based on **Nearest Neighbours Time Series** that when applied to a current output and its nearby previous values, it searches for past patterns with similar current and previous values; the predicted next output will be the value followed after the pattern similarity has been matched. This algorithm may be used to predict next few outputs after the pattern similarity matching.

4.3.3 Demonstration of smart operational software

The design phase of both the Operational System Software and the Smart Application Software will comprise the design of an evaluation based on testing and demonstration. The demo topology and the storyline are illustrated in Figure 44. The Local PC is used for connectivity reasons and communication purposes of the MCU that embeds the Operational System Software (state machine) and the Smart Application Software (regression model for in-PNODE extrapolation), while the Remote PC represents the WMS for issuing commands and performing in-WMS extrapolation.

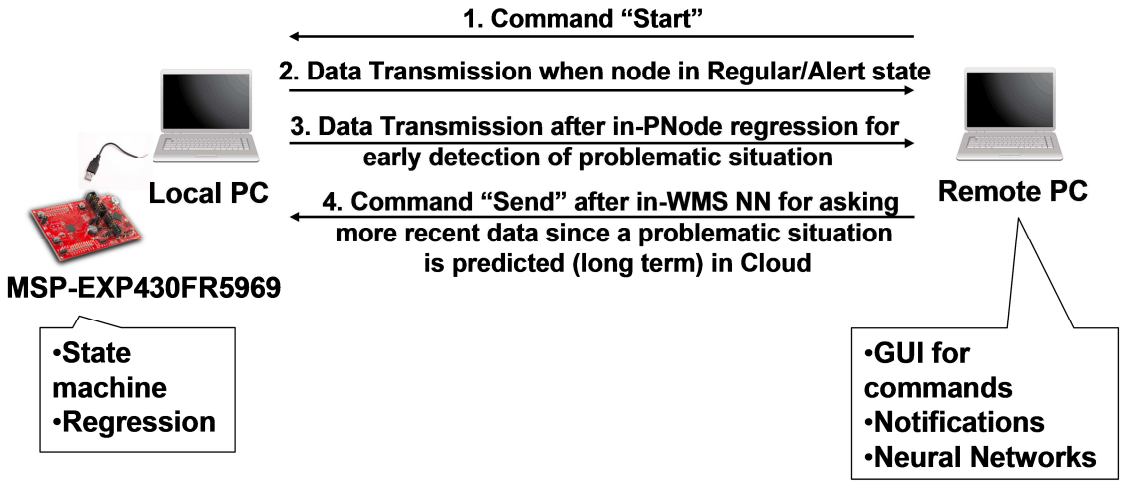

Figure 44: Design of Operational System Software and the Smart Application Software evaluation for the first run

This evaluation comprises the following steps:

1. Command "Start" from Remote PC to Local PC and MSP-EXP430FR5969 to show the GUI for command; the MSP-EXP430FR5969 starts running and is fed by fake data based on what sent by SMAS.

2. Based on this data, after some time, the MSP-EXP430FR5969 goes from Regular to Alert state and sends after the predefined consecutive similar observations data to the Remote PC.

3. After a period, one of the conditions for triggering regression is true in the state machine of the MSP-EXP430FR5969, regression is run (short term prediction) and data or notification (via a flag indicator) is sent to Remote PC immediately for early detection of problematic situation (violation of a sensing parameter threshold bound to a specific event e.g. sensing parameter flowrate violation bound to an overflow event in rain water use case).

4. After a period, in Remote PC Neural Networks makes a long term prediction that a problematic situation (violation of a sensing parameter threshold bound to a specific event) may occur in MSP-EXP430FR5969; command "Send" is sent from Remote PC to MSP-EXP430FR5969 to ask for recent data for further processing and validation in Remote PC.

5 Energy Budget and Power Management

One of the key requirements for the PROTEUS Node (PNODE) is related with its power dissipation and energy consumption profile. Attending to the limited quantity of energy that energy harvester may collect and the limited capacity of the energy storage unit, the PNODE must operate under an optmized power management strategy.

The total amount of energy spent by the PNODE is determined by the voltage, current supply and timing profile of the operation, resulting in the generic and well known equation given by,

$$\text{Energy} = \int_{t1}^{t2} p(t)\,dt = \int_{t1}^{t2} v(t)\,i(t)\,dt \qquad [J] \qquad \text{Eq. 8}$$

where p(t) represents the electrical power consumption, in watt, of the PNODE. An analysis of (9) reveals that an effective power reduction can be achieved not only by optimizing the voltage-current product but also by reducing the time when the PNODE is effectively in full operation.

Therefore, the design must integrate a range of techniques applied both at circuit and system levels, including:

- reducing the voltage power supply, designing circuits able to operate under 1 volt supply,
- designing low power circuits by using lower currents,
- defining the minimum number of operations needed for each state, to reduce the total current,
- optimization of the timing profile through an extensive use of duty cycling. This aspect is of crucial importance since it involves not only the PNODE per se but also the smart application algorithm profile.

As previously presented, the PNODE architecture includes both digital and analog building blocks, which can be powered at different voltage supply. The analog front end (AFE) is used for the sensor-interfacing step and it also performs the analog signal conditioning before the digitization done by the analog-to-digital converter (ADC). The resulting digital data is further (if needed) processed by the digital part, which may include a direct memory access (DMA) scheme, a digital hardware accelerator (ACC) and the microcontroller (MCU). The later is responsible for the operation of the PNODE, including the control of the power duty cycling strategy and algorithm, through the energy and power management unit (EPMU). The energy for the device operation is collected by the harvesters units, as analysed previously and, as a project option, always stored in a short-term energy buffer (supercapacitor) complemented or not by a long-term energy storage (battery). Therefore, the design strategy for the powering the PNODE:

- a short term but rapid charge storing electrical energy element (e.g., supercapacitor) is always used between the harvesters and the main circuits. This supercapacitor will serve as the input of the previously described DC-DC converter.

- a slow charge but with high energy density element, a battery, may be also added to the system as a long-term storage unit. This device is charged through the harvester whenever excess energy from the harvester is available.

The energy consumption profile heavily duty cycled is of major importance for the design of the PNODE. Before tracing a model to estimate the total energy consumed per day, a duty cycle timing profile has to be assumed/defined. A candidate for the timing diagram is presented in Figure 45, where the three major PNODE states are considered. It assumes that when the PNODE enters into alert mode, the measurement frequency increases. The node return to the previous mode after the alert condition disappears.

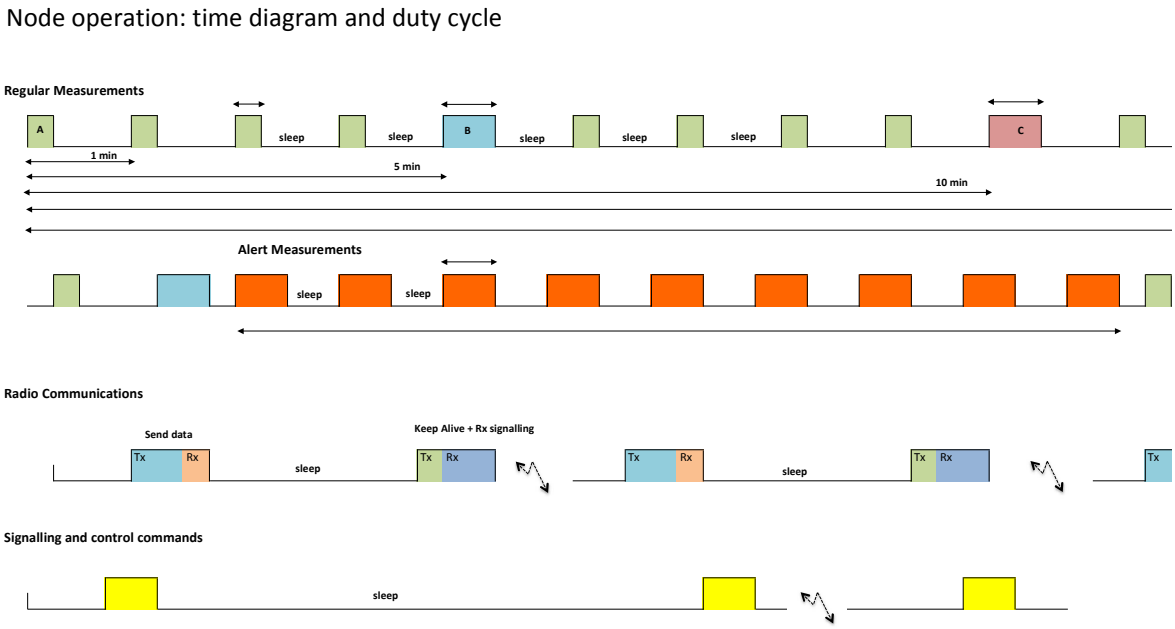

Figure 45: Timing profile diagram of the PNODE.

Based on the timing diagram, an energy budget model was defined which is presented in Figure 45. The energy consumed in each time slot is simply determined by the duration, average current and supply voltage. An assumption concerning the number of alerts and false alarms per day is also included in the model.

The simulation of the energy budget for the PNODE is detailed in Figure 46. The estimated energy consumed in one day is, in average, 0.1 Wh. Therefore, a battery of 1000 mAh can maintain the operation of the PNODE during 10 days. The model also shows that the sleep mode current has to be minimized since the equipment remains in this state more than 90% of the time. The estimated peak instantaneous power has to be lower than 100 mW for a voltage supply of 1 V.

Energy budget analysis

Assumptions				
voltage supply	1	volt		
Major window cycle	24	hours	86400000	ms
storage capacity	1000	mAh		
energy harvested	2	J		

	item/Type	Time Duration (ms)	Time Period (min)	Number of slots	Current consumption (Average; mA)	Total time in major window cycle (daily)		% time	current contribution	
Regular Measurements (RM)	A	5000	1	48	50	5760000	ms	0.06667	3.333	mA
	B	1000	5	6	60	144000	ms	0.00167	0.100	mA
	C	1000	10	4	60	96000	ms	0.00111	0.067	mA
	D	1000	30	1	60	24000	ms	0.00028	0.017	mA
	E	1000	60	1	60	24000	ms	0.00028	0.017	mA
						6048000	ms	0.07		

Alert mode measurements (AM)	Duration of one alert mode (min)	Time Duration (ms)	Time Period (min)	Number of slots	Current consumption (Average; mA)	num of alert per day	num of false alerts	total time in major window cycle (daily)		% time	current contribution	
	60	1000	1	60	60	5	2	420000	ms	0.00486111	0.29166667	mA

Communication mode	Type	Time Duration (ms)	Time Period (min)	Number of slots	Current consumption (Average; mA)	total time in major window cycle (daily)		% time	current contribution	
	Tx(Rx) - Regular	1000	720	2	50	2000	ms	2.31E-05	0.00116	mA
	Tx(Rx) - Alert	1000	1	420	50	420000	ms	4.86E-03	0.24306	mA
	Rx(Tx)	500	60	24	30	12000	ms	1.39E-04	0.00417	mA
						434000	ms	0.00502315		

Sleep mode	Total time (min)	average current (mA)	% time	current contribution	
	1324.966667	0.2	0.920	0.184023	ma

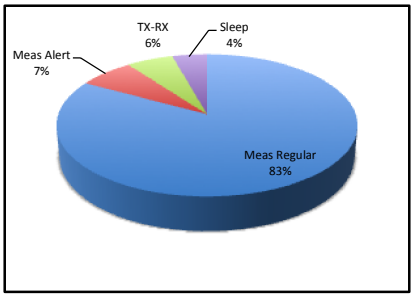

Node average current in 1 day	4.2574 mA
Total charge in 24 hour	102.18 mAh
Average power during one day	4.257402778 mW

Total energy per day	**367.84 J**	**0.10**	**Wh/day**

Figure 46: Energy budget model.

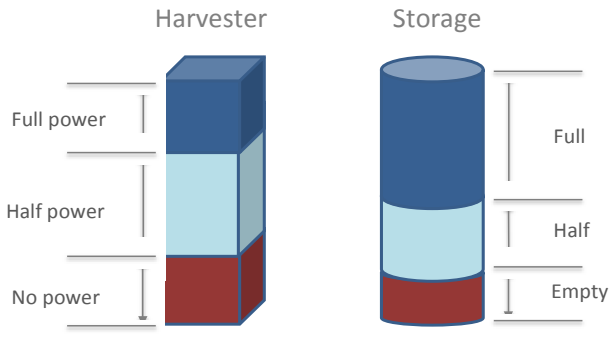

Figure 47: Power and Charge levels.

The PNODE state characterization and respective transitions, implicitly demands that the operation must be energy aware. This means that the information about the available energy needs to be known during the node operation. This information will also contribute for the definition of scenarios for the node power consumption.

Harvester	Energy storage		Power consumption Modes (node states)						Observation
	State	State of stored energy	Regular Meas (RM)	Alert Meas (AM)	Control/signalling (CS)	Communication (COM)	Panic	Sleep	
Active	Charging	Full	Nominal Pwr	Nominal Pwr	Nominal Pwr	Nominal Pwr	-	ULP	Harvester has enough power
		Half	Nominal Pwr	Nominal Pwr	Nominal Pwr	Nominal Pwr	-	ULP	Harvester has enough power
		Empty	Nominal Pwr	Nominal Pwr	Nominal Pwr	Nominal Pwr	-	ULP	Harvester has enough power
	Discharging	Full	Nominal Pwr	Nominal Pwr	Nominal Pwr	Nominal Pwr	-	ULP	Part of the energy from storage
		Half	Reduced Pwr: reinforce duty cycle	Reduced Pwr: reinforce duty cycle	Reduced Pwr: reduce signalling, block some operations	Reduced Pwr: reinforce duty cycle, decrease TX power	-	ULP	Part of the energy from storage
		Empty	go to panic	go to panic	-	-	prepare node to sleep and send panic msg	ULP	Harvester is not enough to sustain node operation
Inactive	Discharging	Full	Nominal Pwr	Nominal Pwr	Nominal Pwr	Nominal Pwr	-	ULP	Running from energy storage
		Half	Reduced Pwr: reinforce duty cycle	Reduced Pwr: reinforce duty cycle	Reduced Pwr: reduce signalling, block some operations	Reduced Pwr: reinforce duty cycling, decrease TX power	-	ULP	Running from energy storage
		Empty	go to panic	go to panic	-		prepare node to sleep and send panic msg	ULP	Running from energy storage

Table 10: Power consumption scenarios (ULP – Ultra Low Power).

In Table 10 several combinations involving the harvesters, short-term energy buffer (e.g. supercap) and long-term energy storage (e.g. Lithium battery) are summarised and related to the power consumption profile associated with each node state. Two states have been identified for the harvester, which are divided in “inactive” and “active”. In active state the harvester can be in maximum nominal power or below it. Regarding the energy storage elements in the PNODE, the possible states are “charging” or discharging. Additionally, it is also relevant to monitor their charge state, which may, in a first approach, be divided in “Full”, “Half” or “Empty”, see Figure 47, The instantaneous power of the PNODE is subject to intermittence and variables levels of available power (depending on the physical and environment aspects where the harvester is immersed). Therefore, it also important that the PNODE may monitor the available power level of the harvester which may also, in a first approach, follow the same classification which is “Full Nominal Power”, “Half power” and “Not Enough Power”.

The above analysis and description, resumed in Table 10, may define at least three power consumption cases that the node shall support.

The “Nominal Power” represents the case when the harvester and/or energy storage do not impose extra restriction to the microsystem operation. However, the circuits should maintain their power optimized functioning. Each PNODE state determines its own “Nominal Power” level, reflecting the loaded configuration.

The second power state, named as “Reduced Power”, is applied whenever the harvesters and/or energy store cannot sustain enough energy for a long-term operation period. In this case the PNODE state shall determine the subtasks that can be stopped. More specifically, an extra reduction of power should be achieved by reinforcing the duty cycle, i.e. increasing the sleeping time, and/or reduce the number of primary sensors. The number and type of sensors to be disconnected should be reconfigurable.

Finally, the Ultra Low Power mode (ULP) is activated each time the PNODE enters into Sleep State. In this mode the AFE is powered off, the MCU operates at a very low power level (namely by reducing its clock frequency) and also a low power Real Time Clock (RTC) is running to trigger the wake-up of the PNODE. The power management may be active to charge the energy storage elements.

To demonstrate how the PNODE should proceed, Table 11 and Table 12 show the case for the Regular Measurement Mode, in which the measurements frequency is decreased when it enters in Reduced Power state.

Parameter	Read	send to SCADA	Regular Meas State : Nominal Power (60 minutes window)
Drink Water Network			
Conductivity	1/5min	2/day	
Chlorine	1/5min	2/day	
pH*	1/10min	2/day	
Temperature	1/10min	2/day	
Pressure	1/min	2/day	
Flow rate	1/min	2/day	
Chloride	1/30min	1/day	
Nitrates	1/30min	1/day	
Calcium	1/hour	1/day	
Magnesium	1/hour	1/day	
Rain Water Network			
Flow rate	1/5min	1/day	
pH*	1/15min	1/day	
Salinity	1/15min	1/day	
Pressure	1/5min	1/day	
Waste Water Network			
pH	1/15min	1/day	
Flow rate	1/5min	1/day	
Temperature	1/15min	1/day	
Pressure	1/5min	1/day	
Dissolved oxygen	1/15min	1/day	
Salinity	1/15min	1/day	
Redox potential	1/15min	1/day	
Conductivity	1/15min	1/day	
Nitrates	1/15min	1/day	

Table 11: regular Measurement @ Nominal Power. The PNODE enters Sleep state after Measurements.

Parameter	Read	send to SCADA	Regular Meas State : Reduced Power (60 minutes window)
Drink Water Network			
Conductivity	1/5min	2/day	
Chlorine	1/5min	2/day	
pH*	1/10min	2/day	
Temperature	1/10min	2/day	
Pressure	1/min	2/day	
Flow rate	1/min	2/day	
Chloride	1/30min	1/day	
Nitrates	1/30min	1/day	
Calcium	1/hour	1/day	
Magnesium	1/hour	1/day	
Rain Water Network			
Flow rate	1/5min	1/day	
pH*	1/15min	1/day	
Salinity	1/15min	1/day	
Pressure	1/5min	1/day	
Waste Water Network			
pH	1/15min	1/day	
Flow rate	1/5min	1/day	
Temperature	1/15min	1/day	
Pressure	1/5min	1/day	
Dissolved oxygen	1/15min	1/day	
Salinity	1/15min	1/day	
Redox potential	1/15min	1/day	
Conductivity	1/15min	1/day	
Nitrates	1/15min	1/day	

Table 12: Regular Measurement @ Reduced Power. The PNODE enters Sleep state after Measurements.

6 Energy Harvesting

Figure 48 shows schematics of a self-powering wireless sensor node integrated with a harvesting system and temporary energy storage. The energy sources available in the environment of the water network (SMAS, Almada, Portugal) include mainly solar, kinetic energy from vibrations and traffic and water flux, as described in deliverable D1.2. Thermal energy and electromagnetic energy at radio frequency (RF) are also present but in smaller amount. In fact, temperature differences located around the monitoring points, for instance inside and outside manholes, or between pipes, do not reach more than 40 degrees, on average; thermoelectric generators are not efficient within this range[6,7]. On the other hand, electromagnetic waves from WIFI, GSM have very low power density (Figure 48).

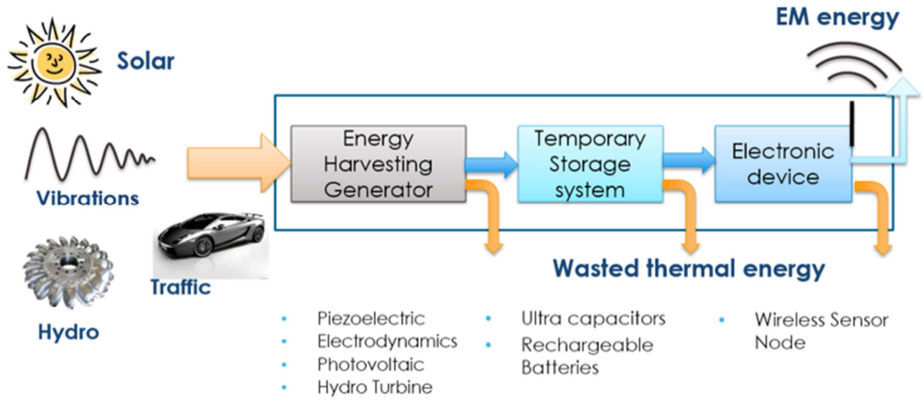

Figure 48: Available energy sources and self-powering wireless sensor.

Energy Source	Characteristics	Efficiency	Harvested Power
Light	Outdoor Indoor	10~24%	100 mW/cm² 100 µW/cm²
Thermal	Human Industrial	~0.1% ~3%	60 µW/cm² ~1-10 mW/cm²
Vibration	~Hz–human ~kHz–machines	25~50%	~4 µW/cm³ ~800 µW/cm³
RF	GSM 900 MHz WiFi	~50%	0.1 µW/cm² 0.001 µW/cm²

Figure 49: Texas Instruments, Energy Harvesting – White paper 2009.

Depending on the energy type, the electrical generator can be based on piezoelectric, electromagnetic, photovoltaic cell or micro hydroelectric turbine. As the power sources are variable in time, depend on the location and have different output characteristics (AC, DC), a temporary storage system that collects the generated electricity is necessary. Once rectified, the electrical signal

[6] http://thermoelectric-generator.com/thermoelectric-power-generator-module-selection/
[7] Harb, Adnan. "Energy harvesting: State-of-the-art." Renewable Energy 36.10 (2011): 2641-2654.

recharges the storage system (for example, battery or ultra-capacitor) and then the power may flow from it to the end user device (wireless node) when required. For these reasons, power electronics is required to interface one or more generators to the storage system and then to manage the delivery of the electrical energy to the sensor node. The use of a battery, both as stand-alone power system or temporary storage, presents the inherent problem of limited recharging cycles (typically 300 - 500). As it can be seen from Figure 50, after a couple of years, the battery power density and capacity is drastically reduced. For this reason, super-capacitors will be considered as valid alternative, even if at the cost of lower energy density[8,9].

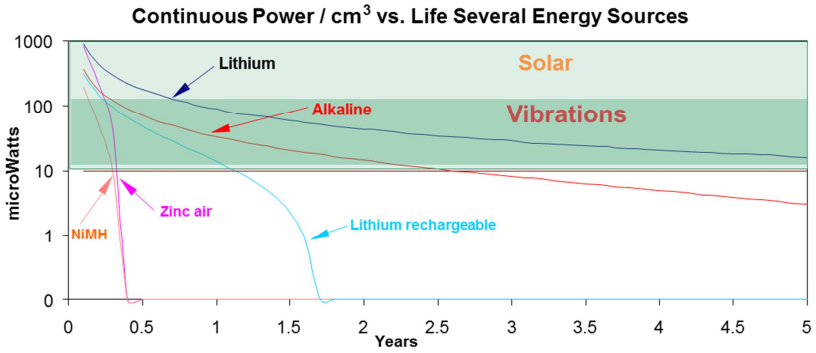

Figure 50: Power density of energy harvesting systems and batteries. S. Roundy et al. [10].

In general, the energy required by the wireless node depends on the use cases: sensor type and sampling frequency, transmission frequency and distance, remote intervention etc. Based on the exact characteristics of the monitoring points and sensing functionality, one or a combination of several power sources will be implemented. The main criteria that will guide this choice will include:

- energy reliability,
- physical robustness,
- device lifetime,
- cost-effectiveness,
- ease and cost of installation.

Most of the energy harvesting mechanisms are intermitent by nature. Therefore, a multi-source energy harvesting approach will constitute a convenient way to achieve a high level of availability, which will be further reinforced by the addition of rechargable storage element(s), namely a supercap and/or battery.

In the following paragraphs, we show some reference examples of harvesting technology with physical characteristics comparable to PROTEUS application in order to provide a comparison based on the mentioned features. In particular, for each generator type, the produced energy is estimated over a time interval of 5 years. Within this period, the cost and lifetime cycles are taken into account.

[8] Van Voorden, Arjan M., et al. "The application of super capacitors to relieve battery-storage systems in autonomous renewable energy systems." *Power Tech, 2007 IEEE Lausanne.* IEEE, 2007.
[9] Chu, Andrew, and Paul Braatz. "Comparison of commercial supercapacitors and high-power lithium-ion batteries for power-assist applications in hybrid electric vehicles: I. Initial characterization." *Journal of power sources* 112.1 (2002): 236-246.
[10] S. Roundy, P. K. Wright, and J. M. Rabay, “Energy Scavenging For Wireless Sensor Networks with special focus on Vibrations” *Kluwer Academic Publisher*, 2004.

6.1 Energy harvesting from traffic

The energy from traffic can be harvested by using both piezoelectric (PZ) or electromagnetic (EM) conversion technique. Piezoelectric material has the ability to convert traffic pressure into voltage, whereas electromagnetic transducers make use of permanent magnets that moves against fixed coils. Depending on the choice of piezoelectric material and transducer shape, the Young's modulus E can be stiffer or softer that asphalt. For example, for Lead Zirconate Titanate (PZT), E_p=69 GPa, whereas, typical asphalt pavement has E_a = 5 GPa. PZ method is more expensive than EM because of the cost of piezoelectric material, but it's relatively easy to implement. On the other hand, electromagnetic transducers could lower the cost but carrying more complexity related to the need for moving mechanical parts. In addition, the installation cost could vary a lot depending on the type of integration with the road. Examples of installation that we intend to test are shown in **Erreur ! Source du renvoi introuvable.** for a) embedded under the surface of the asphalt or b) integrated into road speed humpers upon the surface.

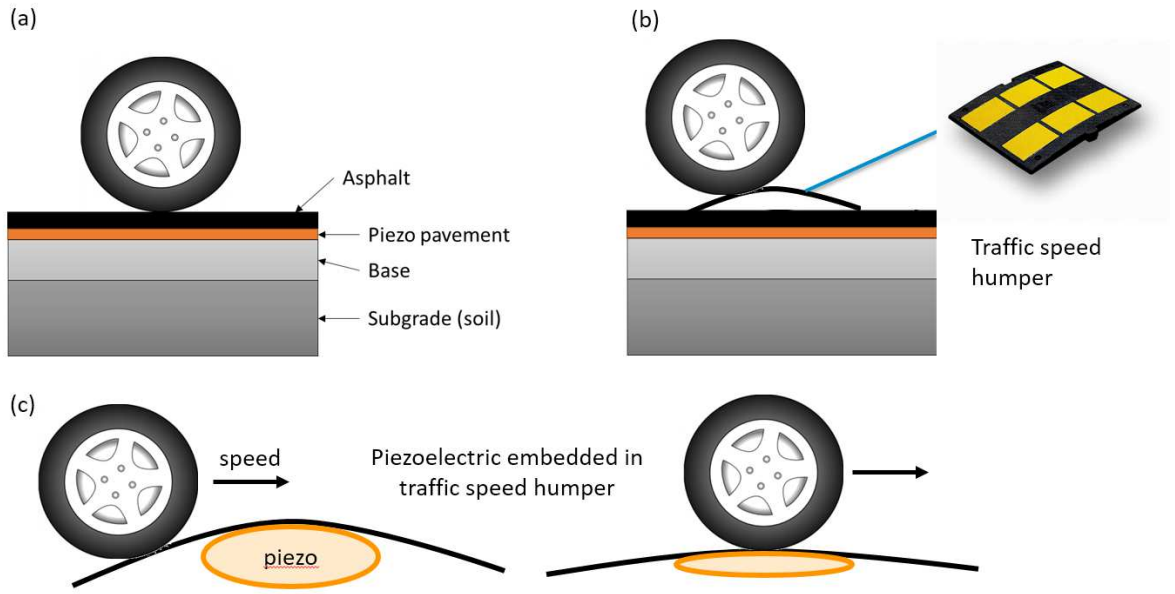

Figure 51: Example of piezoelectric pavement (a) under or over (b) the asphalt with speed humper type shape for traffic energy harvesting. (c) Drawing of compression sequence of the transducer under the speed humper.

As first prototype, we will target a device with standard shape of speed humper sizing 600 x 490 x 30 mm^3. For the PZ version, we select PZT and PVDF (PolyVinylidene DiFluoride) as materials to be used for the mechanical to electrical energy transduction. The cost per unit is estimated to be around 50 euros, but mostly depends on the transducer configuration: cantlever, rods, rubber-type. The EM version of the harvester will make use of commercial NdFeB permanet magnets that will be set either as fixed or movable part with respect to a coil. In principle, the limited displacement of the membrane (around few millimeters) will not allow high conversion efficiency and as the output voltage is expected to be much lower than PZ. This could be raised by applying a frequency-up conversion mechanism such as multiplying gears or pinched cantilever concept.

Direct compressive force exerted by a vehicle onto the road surface is typically F=15 kN per wheel, and the tyre contact pressure can reach 700 kPa, depending on the type of vehicle: trucks or cars. If we imagine a compression length Δz = 2 mm, the mechanical work done by one wheel is E_m=$F\Delta z$ = 15 J, while the power over an impulse duration of Δt=0.2 s is E_m /Δt = 750W. It is clear that if we target a conversion efficiency of 1% we should be able to harvest 0.15 J of electrical energy for each passing

wheel and 7 W of average power during the pulse. However, although the typical piezoelectric voltage obtained by direct compression is about *V*=100-400 V for each wheel, the electric current is often around *I*=0.35 mA, and the electrical power is thus *P* = 0.14 W. In case of 400 vehicles per day (that is 1 vehicle each 3.6 minute), the daily energy produced is 3.11 x 10^{-5} Wh/d per vehicle per module, and the total daily energy produced per module results 11.2 J or 1.24 x 10^{-2} Wh/d. Nevertheless, the mechanical energy can be first accumulated in form of elastic potential energy and then converted in longer scale time and with higher efficiency.

In this project, we will focus on both lowering the cost and increasing the conversion efficiency by comparing various piezoelectric materials, design optimization and, in case, using electromagnetic transducer in place of piezoelectric layer.

6.2 Energy harvesting from photovoltaic cells

Where sunlight is present, photovoltaic (PV) cells will be integrated in manholes covers to provide solar energy as main or complementary power source. After a short evaluation on the market, for the first prototype, we decided to test OEM small thin film PV cells by PowerFilm Solar Inc. In particular, the model SP4.2-37 sizes 3.6 x 8.4 cm^2 of area and 0.22 cm of thickness and generates 4.2 V and 22 mA at 100% of sunlight, it is lightweight and suitable to be attached onto the covers. However, the efficiency of ground-located cells can be affected by dust, crushed by transportations or subjected to hursh weather conditions. Along with these, we will purchase and assemble also specific outdoor models, such as the PT15-75 which is designed to resist to weather attacks. It measures 9 x 27 cm^2 and produce a peak voltage of 15.4 V and current of 50mA, thus 0.7 W of peak power. **Erreur ! Source du renvoi introuvable.** shows a potential installation scheme of the PV cells on the manhole cover.

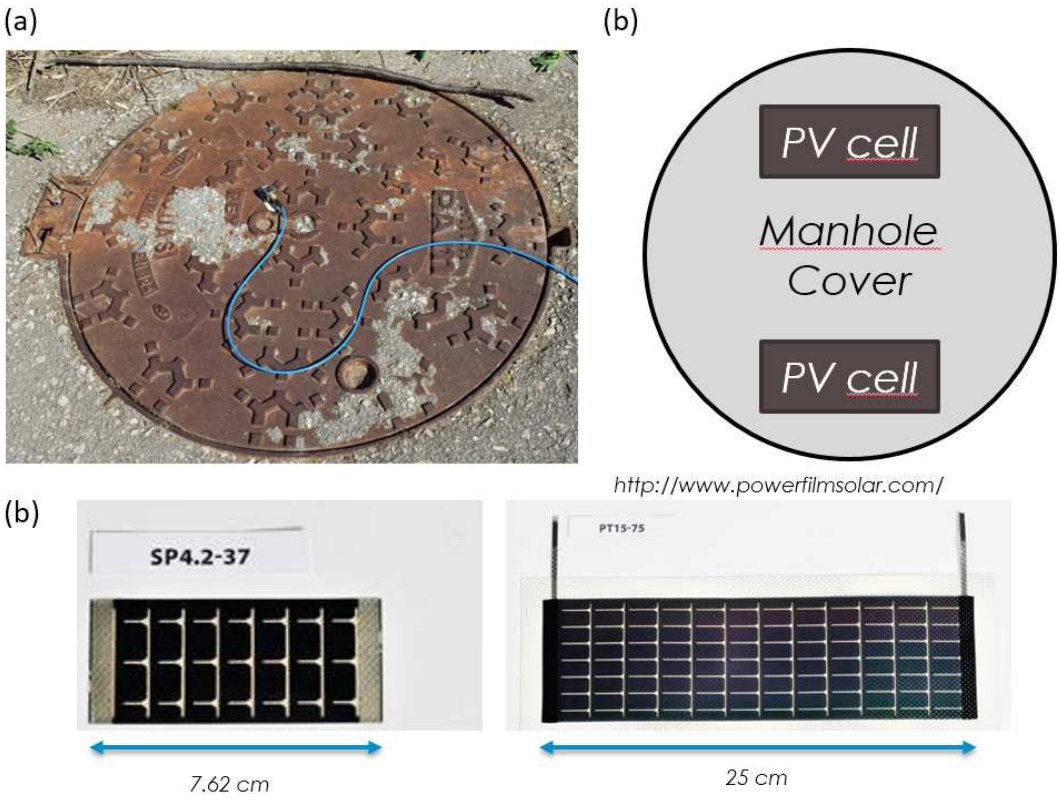

Figure 52 – a) Photograph of a manhole cover of SMAS Almada, b) Installation configuration of PV cells.

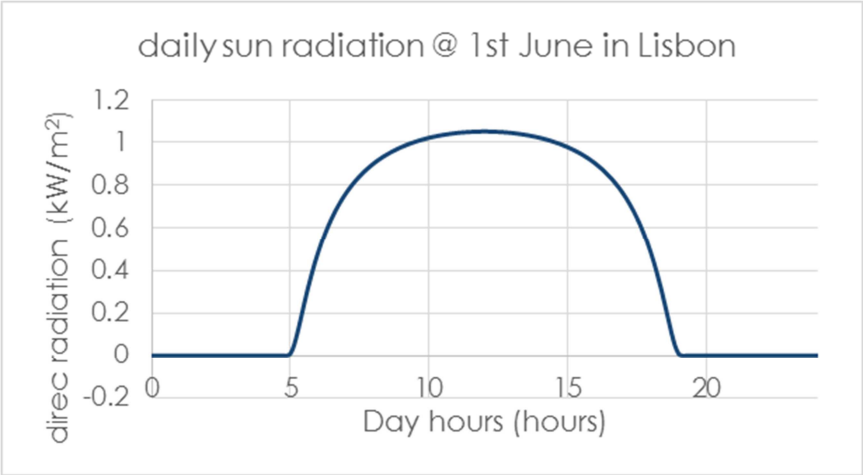

Figure 53: a) Daily sun radiation power density in Lisbon [11,12,13].

In order to make an estimation of the average daily energy generated by the PV cells, we normalized the peak power by the average solar radiation at Lisbon coordinates (latitude 38.7° N, longitude 9.13° W) during the month of June taken as in **Erreur ! Source du renvoi introuvable.**. The resulted energy generated by is 0.97 Wh/d and 8.1 Wh/d with a cost of 3 € and 7 € for the SP4.2-37 and PT15-75 respectively.

6.3 Energy harvesting from water flux

The high power density of the water flux, mostly due to its kinetic energy ($W \quad \frac{1}{2}\rho v^3 \sim 1\ W \cdot cm^{-2}$, for an average water speed equal to 2-3 m/s) can be partly exploited for powering the sensor without significantly affecting the overall flux both in pipes and in non confined wastewater/rain conduits. According to Betz' Law, the theoretical maximum of efficiency of energy extraction is limited to 59%, even if actual design of the harvester wil further decrease this figure. As a general design strategy, in order to reduce the installation costs and favor device integration, it would be preferrable inserting the harvester head in the main pipe (see Figure 72), directly connected to the Proteus – node. We will investigate two designs for the harvester head: one based on turbines and one based on vortex induced vibrations.

[11] http://pveducation.org/pvcdrom/properties-of-sunlight/calculation-of-solar-insolation
[12] http://re.jrc.ec.europa.eu/pvgis/apps4/pvest.php?lang=en&map=europe
[13] http://solargis.info/doc/free-solar-radiation-maps-DNI

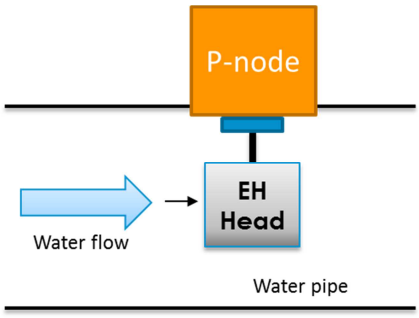

.*Figure 72 Scheme of the harvester deployment.*

6.3.1 Micro Hydro Turbine

Micro hydro turbines (MHTs) usually operate in a strongly conditionated flow, where all the water is injected into a channel and pushed against the turbine blades. This can be obtained both with an axis of rotation parallel or perpendicular to the fluid velocity. However in the case of the scheme of figure 72, a rotation axis perpendicular to the flow is preferrable in order to drive the alternator, placed in the water sealed part of the P-node, directly by the turbine rotor, with no mechanical transmission required. This scheme is also preferrable for reducing installation costs, as we avoid conditioning the water flow. Figure 73 shows two realizations of this principle, the first based on a modified Pelton turbine (a) with a suitable protection to enhance the force difference between the two sides of the wheel and the second on a Darrieus turbine, exploiting the lift difference on the sides of the wing shaped blades.

In a non conditioned flow the Darrieus turbine, which can be installed “naked” appears the logical choice even if the efficiency for a straight blades turbine is limited to about 20%. In any case, a relatively small turbine with 1 cm long blades and arms will provide a maximum of about 400 mW power, much more than the required one and also allowing some relaxing in the design specifics. For prototypation, the generator will be fabricated at the NiPS Laboratory; in particular suitable blades will be produced in PLA or ABS polymers by using a 3D printer. Note that for the final device, both materials are food safe, once appropriate fabrication procedures are used. The conversion from mechanical to electrical energy will be realized by a standard alternator followed by a conditioning circuit feeding the temporary energy storage (battery/supercap).

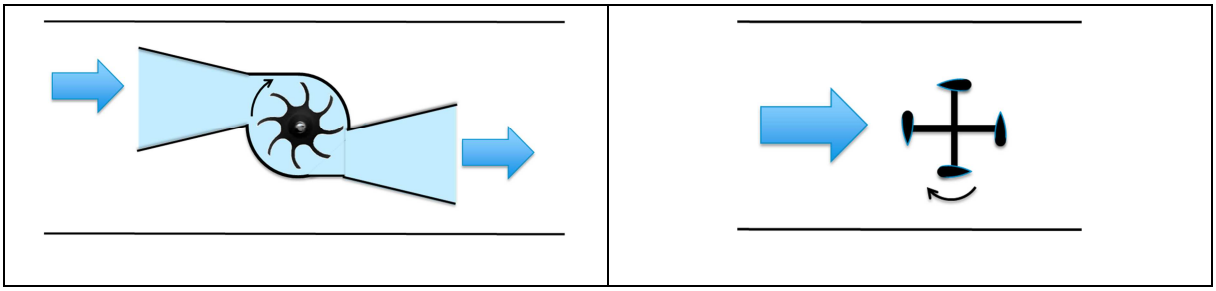

Figure 73: Harvester head employing two different vertical axis turbines: (a) Pelton, (b) Darrieus. The P-node, not sketched, is above the turbine and directly connected with the turbine axis.

6.3.2 Vortex Piezoelectric Generator

A different approach to capture the energy of a fluid flow is using a piezoelectric generator driven by turbulent Von Karman vortex (Vortex Piezo Generator - VPG). In fact, blunt bodies placed in a fluid flow, generate vortices behind them by for a wide range of Reynolds number; in turn, the vortices induce a periodic lift force on the immersed body. In our design, the body, for instance a cylinder, is anchored at the end of a piezoelectric slender beam which is fixed to the P-node. The piezoelectric generator is immersed into the water with insulated electrical connection. Figure 74 shows a scheme of the VPG attached to the P-node in a) horizontal and b) vertical direction respectively. As the water flows around the cylinder, it produces two variable lift forces on the two sides due to the vortex effect. As a result, the cylinder oscillates along transverse direction with respect to the water flow. The vibration of the VPG is then converted into electrical current, which, through a conditioning circuit, feeds the temporary storage (super capacitor, battery).

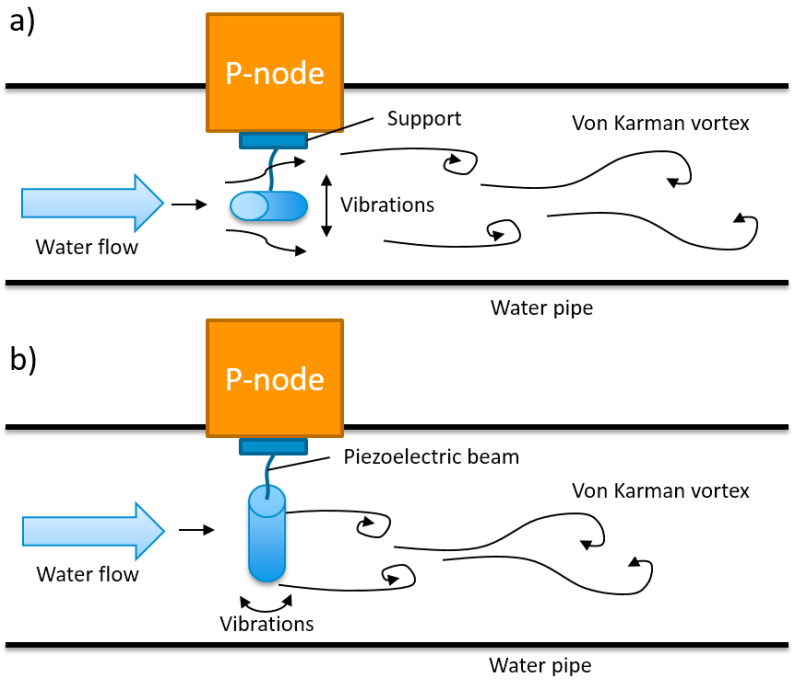

Figure 54: Scheme of the VPG in A) horizontal and b) vertical direction versus pipe configuration.

In order to carry on a preliminary analysis, we can assume a uniform velocity profile at the inlet along the direction of the water flow and zero velocity all along the pipe walls (no slip). The fluid is considered incompressible. Only the relative pressure difference around the cylinder is important to determine the lift force variation. The Reynolds number of the fluid is determined by the formula

$$\mathrm{Re} = \frac{\rho v \mathrm{D}}{\mu} \qquad \text{Eq. 9}$$

where *v*, ρ, μ and *D* are the velocity, density, dynamical viscosity and characteristic length (diameter of the cylinder) respectively. In our case, assuming a diameter of 2 cm and velocity of 2.5 m/s, the Reynolds number reaches 5.6 x 10^4. We performed a simulation of the Karman vortex using a freeware licenced version of SimFlow software. The flow velocity pattern and drag and lift force coefficient are shown in **Erreur ! Source du renvoi introuvable.**.

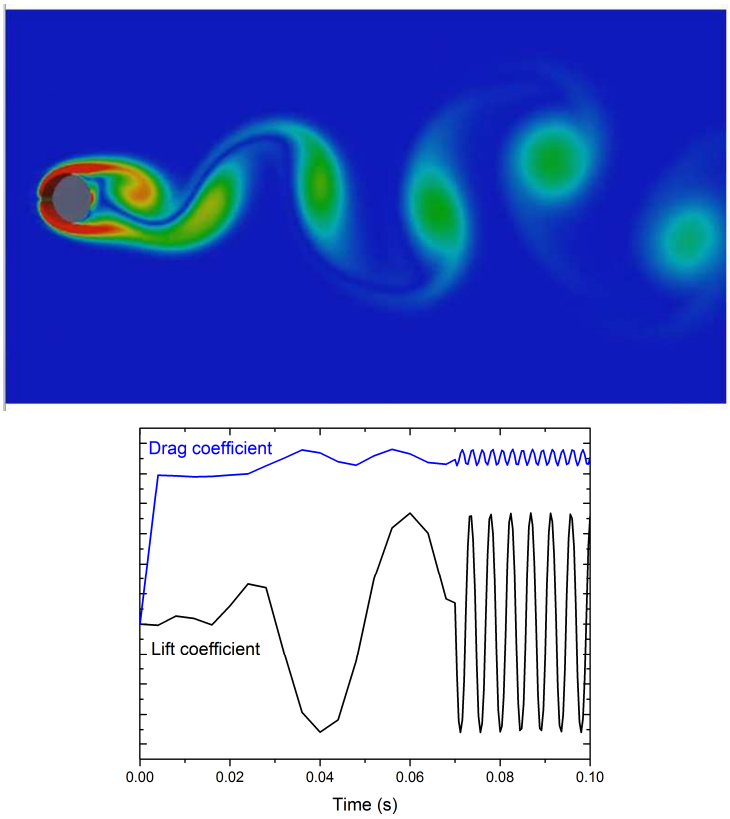

Figure 55: (left) Simulation of the velocity profile around a cylinder with resulting (right) Drag and lift force coefficient.

The vibration frequency of the cylinder is about *f*=20 Hz, so that the piezoelectric beam should be designed to have a resonant frequency equal to this. The mechanical power transferred to the vibrating cylinder can be estimated as about 25%. About 15% of this power can be converted into electrical power by a piezoelectric beam operating at resonance. For a cylinder with height and diameter equal to 2 cm, this corresponds to about 40 mW. Even if this value is still more than enough to power the device continuously, it is about 20 time less than a Darrieus turbine of comparable size. However, this design is intrinsically sturdier than a turbine, so that it should give lower durability problems. Moreover, its rounded shape could be an asset when used in waste waters as it will be less prone to stop and collect solid residuals. For the fabrication of the prototypes suitable PZT beams will

be acquired. The oscillating cylinder will be designed in order to tune the oscillating frequency of the lift force with the mechanical resonance of the mass + beam system.

6.4 Summary

In conclusion, for the first version of the PNODE prototype, a mult-source energy harvesting system will be developed by combining photovoltaic, traffic and fluid generators. In particular, the PV cells will be purchased among those available on the market (PowerFilm ® as a first choice, other alternatives will be evaluated), whereas, traffc and fluid energy harvesters (Piezoelectric Vortex Generator and Micro Hydro Turbine) will be designed and fabricated at NiPS laboratory at University of Perugia. The PV cells and the Traffic Harvester (TH) will be installed, where possible, upon or nearby the manholes covers. Instead, the fluid energy harvesters will be designed to be directly attached to the PNODE, so that immersed in the water flux. Here below the flow diagram of the prototype development actions.

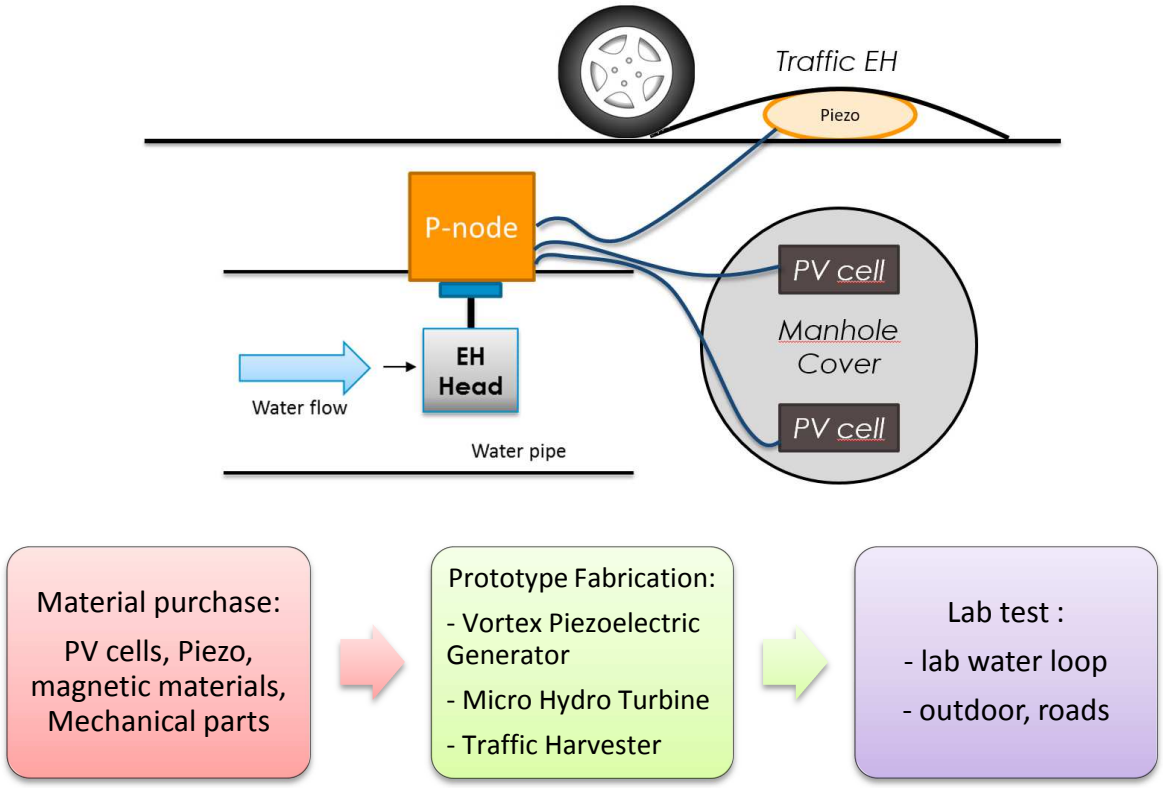

Figure 56 – (Upper) Final scheme of the multi-source energy harvesting system and (lower) flow diagram of development and validation.

Energy budget comparison

The following plot in Figure 57 shows the comparison of the different power sources versus the energy required by the PNODE, according to the estimated consumption. The analysis is taken considering an operating period of 5 years, including the comparison with a stand alone rechargeable battery which is taken as a reference (High Power Polymer Li-Ion Cell model 9759156-10C from www.batteryspace.com, capacity of 37 Wh, voltage of 3.7V @ 40 €). By assuming no recharging (free-maintenance) to compare with other power sources, 1 charge over 5 years, the battery produce 844 µW of average power, that is 0.02 Wh/d. The use of a non rechargeable battery (lithium or alkaline) could lower the price but with small impact on the total energy available. It can be noted that best solutions are the PV combined with water energy harvesters (MHT and VPG). Therefore, these technologies represent our target for the development of the harvester with added innovative concepts. For example, the design of the PVG will be tailored to work in nonlinear bistable dynamical regime in order to be efficient even for noisy flux rate and rain/waste water conditions. While, the MHT will be reshaped starting from the basic design of the Arrhenius turbine. In addition, as an alternative and secondary choice, we also point at development of a piezoelectric Traffic EH demo. This type of technology is indeed at an early stage and there is lots of room for the efficiency improvement.

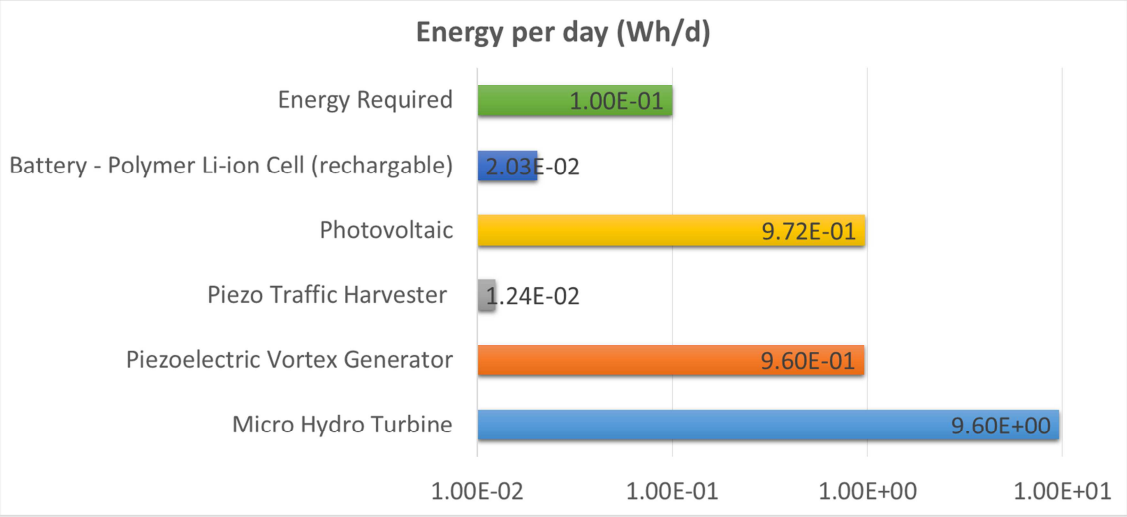

Figure 57: (Top) Daily energy generated by different power sources. (Bottom) Power density per device volume.

7 Mechanical and packaging aspects

7.1 Prerequisites

The packaging should comply with production requirements and regulatory standards suitable for this first version scenario, which were covered in D1.2 and D1.3.

7.2 Main elements of the prototype in first version

As shown in

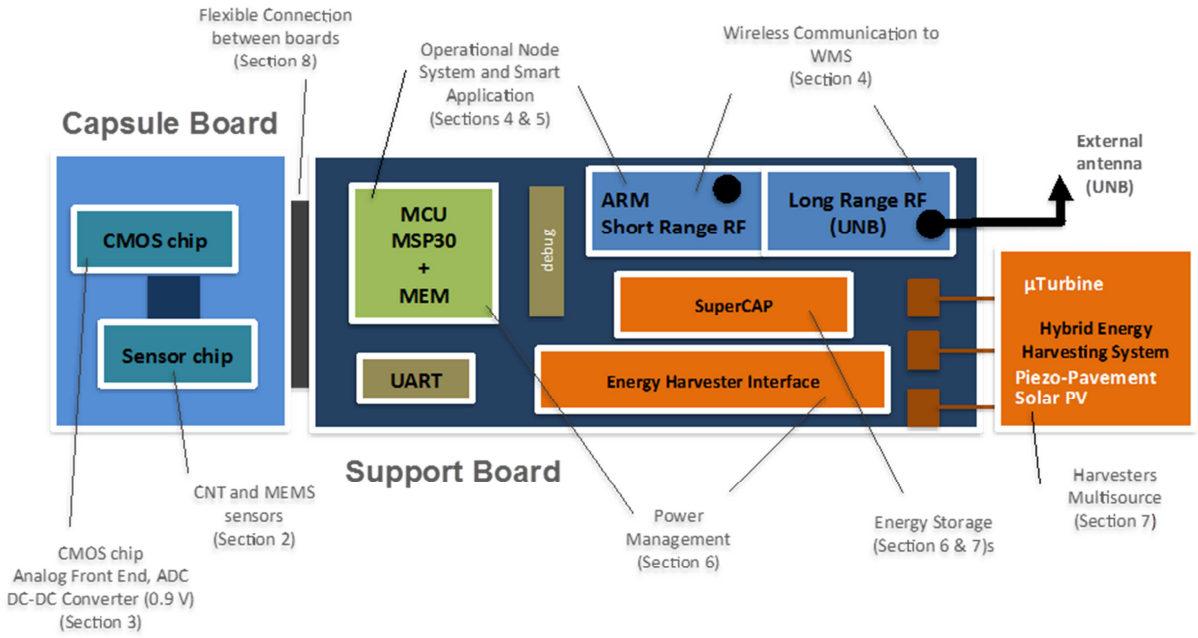

Figure 3, the sensor node (PNODE) comprises two parts: the sensor capsule and the support board. These two parts will exchange energy and data using a flexible flat cable and respective connectors.

At the stage of the project, we suppose that each sensor chip, which combine physical sensors and chemical sensors, will not deliver exactly the same signals than another chip processed in the same time on one wafer. Consequently, factory coefficients' should be associated to each multi-parameter sensor chip included in a sensor cap. In this case, a duo composed by a sensor cap and all these coefficients exists. It is necessary to identify each sensor cap with a serial number. The serial number printed on the body of the cap and included in a CMOS memory, are related to calibration coefficients in a data base.

The node could read the serial number of the cap and check the compatibility of this cap and the coefficients memorized. This strategy of management of spare parts could be validated with the electronics and firmware of the first prototype.

During laboratory trials, various sensor chip from a batch could be associated to a unique electronics, named support board of the node, in order to evaluate the variability of signals and the long term behaviour.

7.2.1 Mechanical housing of the sensor cap:

Considering the environment in which the first version of prototype will be installed, the design of the active sensing part has to include waterproof property. In this way, a strategy of coating will be defined in WP3 combining the design of the cap housing and the use of selected epoxy or polyurethane resin.

A cylindrical geometry of the sensor node is required. At this stage, the size of the prototype is not critical. Nevertheless, the external diameter of the prototype should be in the range of 30 to 40 mm. This diameter will impact the size of the top of the testbench.

The size of the capsule board is directly related to MEMS, CNT and CMOS chips size. Sensors chips will be directly wirebonded to a printed circuit board to reduce parasitic capacitance and inductance.

7.2.2 Mechanical housing of the node (electronic part):

In the first version, the printed circuit board of the node should have a 20mm width and no constraint for the length. A shield will be introduced all around the board in order to protect the electronic against electromagnetic interferences. The system design for the first version of the prototype include:

- Wire connection in order to power supply the prototype without using energy generator,
- Wire connection for local access to measurements (TTL signals and values after computing). RS485 communication and Modbus protocol already validated by Aqualabo could be implemented in MSP microcontroller.

7.2.3 Connectivity between capsule and support boards

The connection type between the support and capsule boards will be selected among three possible configurations, shown in Figure 58.

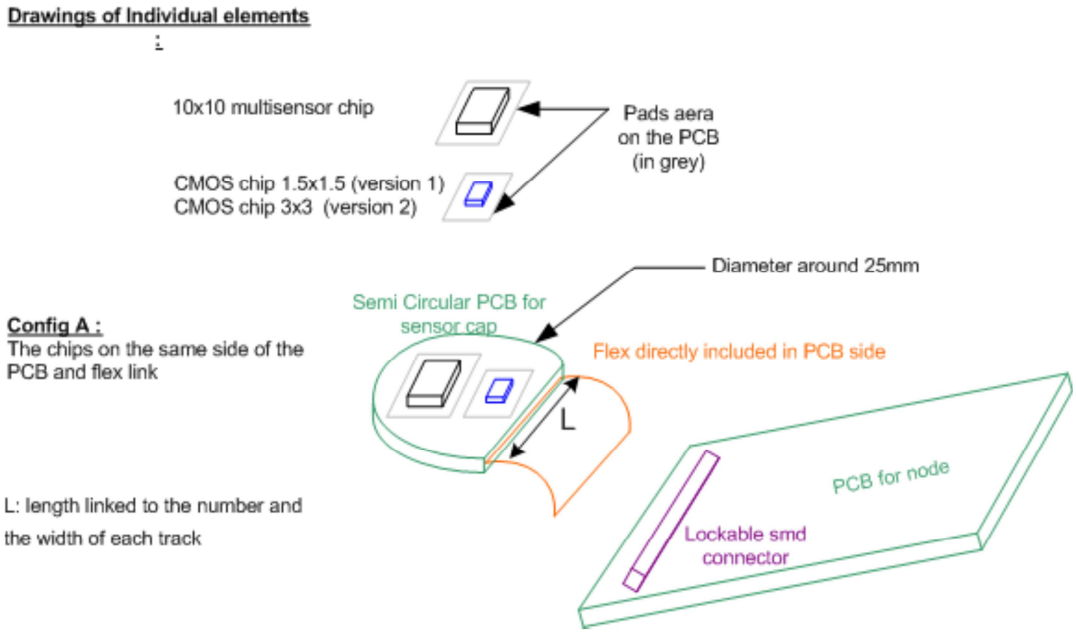

a) Config A

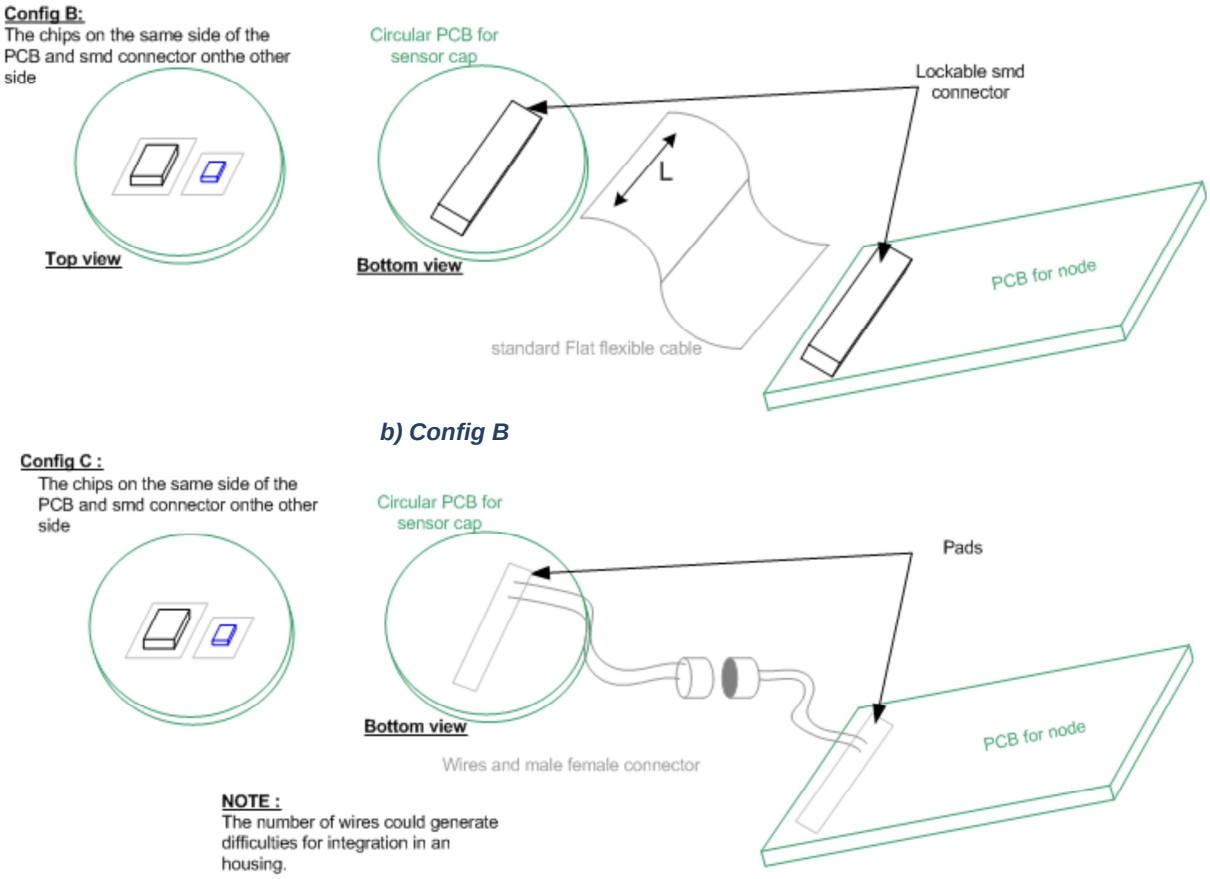

b) Config B

c) Config C

Figure 58: - Possible connections between boards (Top) Config A (Middle) Config B (Bottom) Config C .

8 Conclusions and D1.2-D2.1 cross-reference requirements

The complexity and heterogeneity of the Proteus system is addressed by the project by splitting the design phase into intermediate steps in order to optimize the interaction between all system building blocks, ranging from hardware to software.

For each of the major system blocks, the technology and design options has been addressed, including:

- Sensor chips:
- CMOS chip:
- Energy harvester
- PNODE “encapsulation”
- Communications and Software

The design considerations included in this document reflects the requirements previously identified and report in the Deliverables D1.1 to D1.3. The following tables shows the cross-reference between the requirements gathered in D1.2 and the various sections of this document.

Table 13: Mapping and cross-link to D1.2 Requirements.

D1.2 Ref	D1.2 Section	Description	**D2.1 Section**	Comments
FR-01	4.2	The system MUST measure the 5 critical parameters listed in Table 2 of D1.2.	2.1-2.4	Task of Sensor Chip with CNT and MEMS sensors + CMOS chip.
FR-02	4.2	The system MUST measure the 5 critical parameters listed in Table 2 of D1.2.	2.1-2.4	Task of Sensor Chip with CNT and MEMS sensors + CMOS chip.
FR-03	4.2	The system SHOULD cover the measurement range and precision of the parameters as expressed in tables 1 and 2 of D1.2.	2.1-2.4	Task of Sensor Chip with CNT and MEMS sensors + CMOS chip.
FR-04	4.2	The system SHOULD measure 4 physical/rheological parameters and 5 chemical parameters	2.1-2.4	Task of Sensor Chip with CNT and MEMS sensors + CMOS chip.
FR-05	4.2	The PNODE MUST be able to detect itself (without off-node processing) an alert or alarm based on sensors’ measurements.	4	Guaranteed by the system operational software.
FR-06	4.2	The PNODE MUST be able to carry out thresholding as well as averaging or trend detection over 5 data points.	4, 5	Mostly guaranteed by the smart application software. Although some function are in the system operational software
FR-07	4.2	In their regular range of operation, critical parameters MUST be acquired once per minute, non-critical parameters, once per 5 minutes	4.1, 6	Part of the operational system software and related with available energy.
FR-08	4.2	When a single parameter enters a non-regular level (above or below alert level) all the correlated parameters MUST be acquired once every 30s, and the non-critical parameters SHOULD be acquired once every 2 min	4, 5	Mostly guaranteed by the smart application software. Although some function are in the system operational software.
FR-09	4.2	All the collected data MUST be transmitted to the WMS at least once a day	4.1-4.2	First version, PNODE support board with radio module to access WMS.

FR-10	4.2	The time of sending data to the WMS SHOULD be defined within the configuration	4.1-4.2	First version, PNODE support board with radio module to access WMS and receive configuration
FR-11	4.2	The PROTEUS node MUST have enough memory to store all the sensor measurements made between communications	1	In first version, guaranteed by the memory associated with the MCU of the PNODE support board. In final version intended to be in-chip.
FR-12	4.2	If a critical or non-critical parameter passes alarm threshold for 4 consecutive measurements, the information MUST be transmitted immediately to the SCADA	4.1-4.2	First version, PNODE support board with radio module to access WMS.
FR-13	4.2	If a critical parameter remains above alert threshold for 10 consecutive measurements, the information MUST be transmitted immediately to the SCADA.	4.1-4.2	First version, PNODE support board with radio module to access WMS.
FR-14	4.2	If a non-critical parameter remains above alert threshold for 15 consecutive measurements, the information MUST be transmitted	4.1-4.2	First version, PNODE support board with radio module to access WMS.
FR-15	4.2	In case of alert/alarm transmission, the transmitted information SHOULD be the measurements of all correlated parameters (Table 4), during the full alert/alarm period plus the last measurements before alert/alarm.	4.1-4.2, 5	First version, PNODE support board with radio module to access WMS. Correlation performed by the smart application stack.

D1.2 Ref	D1.2 Section	Description	**D2.1 Section**	Comments
PR-P-01	5.1	The Proteus Node MUST be able to operate without connection to a power supply network	1, 6 and 7	PNODE equipped with energy harvesters (multisource) and Power management unit including energy storage element(s)
PR-P-02	5.1	The PNODE MUST have an autonomy at least two years, between battery changes	1, 6 and 7	PNODE equipped with energy harvesters (multisource) and Power management unit including energy storage element(s)
PR-P-03	5.1	The PNODE MUST include an energy harvesting system integrated with a temporary energy storage device (either short or long term storage such as battery or ultra-capacitor) for enabling self-powering capability.	1, 6 and 7	PNODE equipped with energy harvesters (multisource) and Power management unit including energy storage element(s)
PR-P-04	5.1	The energy harvesting system SHOULD support the use of more than one type of local energy sources	1, 6 and 7	PNODE equipped with energy harvesters (multisource) and Power management unit including energy storage element(s)
PR-P-05	5.1	The Proteus Node device operation MUST monitor the available energy	6	PNODE equipped with Energy and Power management unit
PR-P-06	5.1	The Proteus Node MUST provide at least three modes of power consumption: Nominal, Reduced and Panic mode	6	PNODE equipped with Energy and Power management unit
PR-P-07	5.1	The Sleep mode SHOULD be ultra-low power	3, 6	PNODE equipped with Energy and Power management unit. Circuits selected and designed for low power consumption and have distinct power states (e.g, power – down)
PR-P-08	5.1	The PROTEUS node MUST warn the WMS in the event of low power and send the last critical data after moving to the lowest energy consumption state (Panic mode)	4.1-4.2	Part of the operational system software and related with available energy.
PR-S-01	5.2	The system MUST be compliant to safety standards	2.4.6, 8	Identified and included in the design.
PR-S-02	5.2	The PNODE SHOULD have 2 year life time	1, 3, 8	Reflected in the chosen technology for each “component”, e.g, CMOS chip

PR-S-03	5.2	The PNODE body MUST comply to European regulation	8	Identified and included in the design.
PR-S-04	5.2	The PROTEUS Node SHOULD operate 24/7	1, 3, 4	Included in the design process and reflected in the implementation phase
PR-C-01	5.3	The PROTEUS Node MUST feature a target size of 1/10 of the state of the art comparable market devices.	1, 3	Both sensors and electronics integrated in micro and nano scale dies.
PR-C-02	5.3	In the visit chamber, the PNODE MUST NOT be directly in the flow axis	8	To avoid obstruction. Issue addressed during the implementation phase.
PR-C-03	5.3	The geometry of the sensor housing MUST be designed in order to prevent occlusion in the pipe	8	Issue addressed during not only in the system conception but mostly in the implementation phase.
PR-C-04	5.3	The system in waste and rain water MUST be in contact with water	8	Issue addressed during not only in the sensor design but mostly in the implementation phase.
PR-C-05	5.3	The parts of the PNODE body in contact with drinking water MUST be in materials approved for contact with this type of water	2.4.6, 8	Issue addressed during the implementation phase.
PR-C-06	5.3	The parts of the system inside the visit chamber of waste water MAY be approved for ATEX certification	8	Considered in the implementation phase
PR-C-07	5.3	In-pipe installation of sensors MAY be acceptable when no occlusion risk exist and installation is compatible with the pipe diameter, age and material.	8	Considered in the implementation phase
PR-C-08	5.3	The specific gravity of the sensor MUST be over one.	8	Considered in the implementation phase
PR-C-09	5.3	The sensor SHOULD be defined in two parts. The sensor cap which is the spare part active for sensing. The node which is the major electronic part. The two housings MUST be linked by a watertight connection.	8	Considered in the implementation phase
PR-R-01	5.4	The PNODE MUST be water resistant IP68	8	Considered in the implementation phase
PR-R-02	5.4	The system to waste water MUST resist to corrosive environment	8	Considered in the implementation phase
PR-R-03	5.4	When mounted into a visit chamber or a drink water pipe, the PNODE and its mounting in the pipe/chamber MUST be able to withstand mechanically the maximum flow rate and pressure likely to occur in the system.	8	Issue addressed during the implementation phase.
PR-R-04	5.4	The part of the PNODE not exposed to water MUST withstand exposure to H2S	8	Considered in the implementation phase
PR-R-05	5.4	The storage temperature range MUST be extended from -5 to 60°C.	2,3,8	Considered during the design and circuit dimensioning phase

D1.2 Ref	D1.2 Section	Description	**D2.1 Section**	Comments
SR-01	6	The PROTEUS node MUST offer hybrid processing capabilities with predictive, reactive and cognitive capabilities spanning across analog domain, dedicated logic-digital circuit and MCUs	1,3, 4, 5	In the 1st version Digital processing performed by the support board while the key analog conditioning circuits are integrated in the CMOS SoC. The 2nd version of the chip will include the digital part.

SR-02	6	The PROTEUS system MUST provide a trade-off between energy consumption and communication overhead (also affecting energy) when selecting processing mode	1,3, 4.2	All the building blocks included in the SoC have power-down modes
SR-03	6	The PNODE MUST provide the PROTEUS system with the ability to support several operation modes of the PNODE through an operational system software (state machine implementation) running in an ultra-low power microcontroller (MCU)	1, 3, 4	All the building blocks included in both the SoC and support board have distinct power states levels which are selectable. This is accessible by the operational system software running at the MCU.
SR-04	6	The PROTEUS system MUST be able to run smart application software algorithms (e.g. value or pattern extrapolation)	1, 3, 5	Done by the support board in the MCU and/or ARM.
SR-05	6	The PROTEUS system MUST provide the PNODE with the ability to adapt the monitoring profile of each critical and non- critical parameter in terms of measurement frequency and data transmission time	1, 3, 5	Done by the support board in the MCU.
SR-06	6	The PNODE MUST execute each processing function in the domain where its “power usage footprint” is lower	3, 4	Part of the power consumption optimization strategy.
SR-07	6	The PNODE MUST adjust its operation mode based on its energy state	6	Part of the power consumption optimization strategy.
SR-08	6	The PNODE MUST be able to feed the processing units with decoupled signals based on the commands of these units to the sensor elements	1, 3	Available from the API.
SR-09	6	The PROTEUS system MAY provide filtering means to reduce the noise from measurements	3	First Version of the SoC already includes programmable filter.
SR-10	6	The PROTEUS system MUST BE ABLE TO handle the {Name, Criticality, Minimum, Maximum, CurrentValue, Precision, MinAlarm, MinAlert, MaxAlert, MaxAlarm, MeasurementFrequency, TimeToTransmit} of each measurable parameter based on the current use case	5	Protocol and messaging format related.
SR-11	6	The PROTEUS system MUST offer bidirectional communication between PNODE and the WMS	4.2	All communication are considered to be bidirectional.
SR-12	6	The PNODE SHOULD offer bidirectional communication RS 485, Modbus RTU protocol	1,8	This is for the production phase.
SR-13	6	The PROTEUS system MUST be able to change the Monitoring Profile of each parameter independently in case of Alert or Alarm event	4	Overall System level related.
SR-14	6	The PROTEUS system MUST extrapolate sensing data for at least one parameter (the more critical one) upon user or system request	5	Protocol and API related.
SR-15	6	The PROTEUS system MAY provide short term (time) extrapolation in PNODE and long term (time and space) and more precise in the WMS	5	Due to limited resources (e.g, energy) available in the PNODE.
SR-16	6	The PROTEUS system MAY PROVIDE the WMS with the ability to train the smart application software algorithms for extrapolation and then to send to PNODE their parameterization	4,5	Overall System level related.
SR-17	6	An Analog Front-end API MUST be provided to PROTEUS nodes for abstraction of the complexity of the Analog Front- end	3, 4	API is part of the Operational System Software.
SR-18	6	Communication APIs MUST be defined to specify the communications between the PNODEs, the PROTEUS WMS	4.2	Protocol and messaging related.

SR-19	6	A data model MUST be defined to specify how data (measurement data and corresponding metadata e.g. parameter name, timestamp, etc.) is stored and read in PNODE.	4	Protocol and memory format related.
SR-20	6	The PROTEUS node MUST be able to generate all the signals to configure the Analog Front-end without the need for external tools	3, 4	I should be also available via short range radio communication.
SR-21	6	The Analog Front-end MUST be re-configurable in runtime	3, 4	Included in the low-level API.

D1.2 Ref	D1.2 Section	Description	**D2.1 Section**	Comments
LR-S-01	7	The WMS MUST produce data in modbus/profibus	1	Implementation related.
LR-S-02	7.1	The system MUST support connectivity to SCADA	2.1	Implementation related.
LR-S-03	7.1	Each PNODE sensor part MUST be replaceable easily and independently from the rest of the PNODE	8	Implementation related.
LR-C-01	7.2	The system MUST be factory-calibrated.	8	Implementation related.
LR-C-02	7.2	The system MUST compensate for pH and temperature variations.	3,4	Background and Foreground calibration processes.
LR-C-03	7.2	The drift of the system during PNODE lifetime MUST be known and compensated.	3,4	Background and Foreground calibration processes.
LR-C-04	7.2	The PNODE should not require frequent calibration	3,4,5	Implementation related.
LR-C-05	7.2	The calibrations SHOULD be friendly and in situ	8	Can be also made wirelessly using short range technology.
LR-C-06	7.2	The PNODE SHOULD provide a RS485 modbus RTU cabled access	8	Production related.
LR-M-01	7.3	PNODE SHOULD NOT need maintenance at a frequency higher than once a year	8	Implementation related.
LR-M-02	7.3	The battery replacement MUST not decrease the IP protection	8	Implementation related.
LR-M-03	7.3	The PNODE MUST be easy to withdraw from a pipe under pressure	8	Implementation related.
LR-T-01	7.4	An electronic auto-test SHOULD be implemented in the node to check each parameter in a specific mode.	3,4	Implementation related.
LR-T-02	7.4	It SHOULD be possible to specify the order of the parameters test sequence	3,4	Implementation related.

APPENDIX A - Behavioural Diagrams

In this annex, behavioural diagrams of the devices used for communication testing are provided in order to allow an easier understanding of the automation methodology, as well as extending the information related with the internal actions of each device.

To accomplish this fact, the Behavioural Diagrams are implemented in a state machine form, allowing to establish the synchronism across the devices more quickly, as it can be seen in the following Figure 59 and Figure 60. The majority of the existing states in the diagrams are common to both devices, coordinator and end device, even so there are states specific to each of the existing devices. In the following behavioural diagrams, the transitions between states are represented with a black closed line. To prevent deadlock case scenarios, it was added to the architecture some fail-safes, as it can be seen in the diagrams as a red open line.

Auxiliary Device

Start: Although it is an obvious state, this state cares for a small explanation. The state represents the initial state of the device, the manual action of turning on the device.

Analysis: The analysis state is unique to the Auxiliary device, Figure 59. This state is continuous loop responsible for the data acquisition power consumption values during the entire test execution, stopping when the signal End Analysis is received.

Store Data: This state is responsible for the storage of the data acquired in the analysis state, due to the nature of the state it only can be found in the Auxiliary device, Figure 59.

Wait: The current state will maintain a loop until any input exists, in the Coordinator case a manual input generated by the user, a Configuration message in the case of the End device or in the auxiliary device case a start command generated by the end device.

Completed Test: Although this state it is not used in the Auxiliary device this state will be used in the other devices that composes this automation methodology. The state in question do not execute any function, being included only add some visual perception to the behaviour and provide an easier deployment.

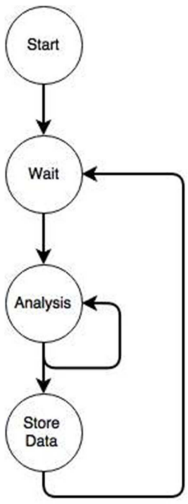

Figure 59 - Auxiliary Device behavioural diagram

Coordinator Device

TxConfig: This state is used exclusively by the Coordinator device, Figure 60, this state is responsible for the acceptance of the testing parameters from the user and consequently its validations. After the parameters validations, the state generates a configuration message with validates testing parameters and transmits it to the end device.

RxACKc: As well as the previous state, this state appears exclusively in the Coordinator device behavioural diagram. This state is responsible for the reception of a confirmation from the end device stating that the configuration message was received successfully. After such confirmation, this state is responsible for the next state correct according to the initial parameters received from the user.

TxTest: This state is used in both, coordinator and end, devices, working as a finite loop state. The operations done in this loop are the generation of testing messages with the defined parameters and conditions set by the user or by the configuration message.

RxTest: As it can be expected this state is the exact opposite of the previous state. It is a loop state with the reception objective, receiving testing messages sent by the other device. The state keeps track the number of received messages comparing it to the number of expected messages established in the configuration message. In case of an exception event occur, the device can detect the reception of a message that does not correspond to a test message. If the message received in this exception situation is an End-of-Test message, the device will automatic generate an exception forcing the test termination and jump to the wait state.

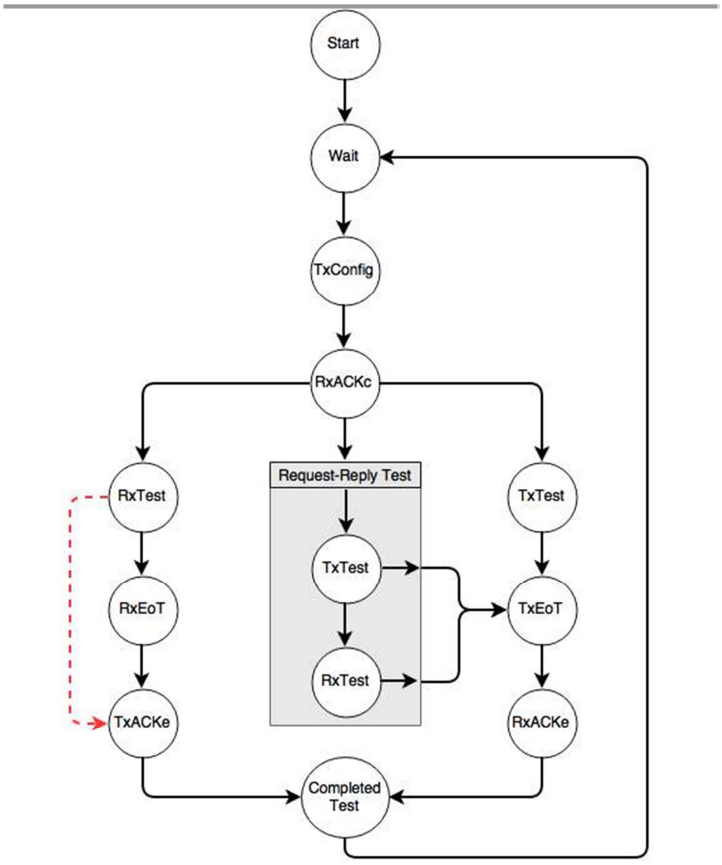

Figure 60 - Coordinator Device behavioural diagram

Request-Reply Test: In this state, both devices will be tasked with the transmission and reception of test messages. In this state the first testing message is always sent by the coordinator device and received by the end device. After a successful reception in the end device, this device is responsible for the transmission of the second testing message, being the coordinator device obliged with the reception, and so on until the end of messages. Similarly to the RxTest, this state also counts the number of test messages comparing it to the number of expected messages.

The deadlock control was also added to this state being only applied in the end device, since the coordinator is always the first to initialize the test communication. The behaviour of this exception is absolutely the same as the RxTest exception.

TxEoT: This state is used in both devices, Coordinator and End device, being the state responsible for the transmission the information that the test was ended. In order to maintain the architecture free of deadlocks, the transmission this synchronism message is the solely responsibility of the device that start the transmission of the testing messages.

RxEoT: As it can be expected this state is responsible for the reception of a message representing the End-of-Test, being used in both devices.

TxACKe: In order to maintain the synchronism between the Coordinator and End device, this state is responsible for the transmission of one acknowledge confirming the end of test.

RxACKe: As it can be expected, this state is in the architecture to allow the reception of the confirmation of the acknowledge generated by the previous state.

End Device

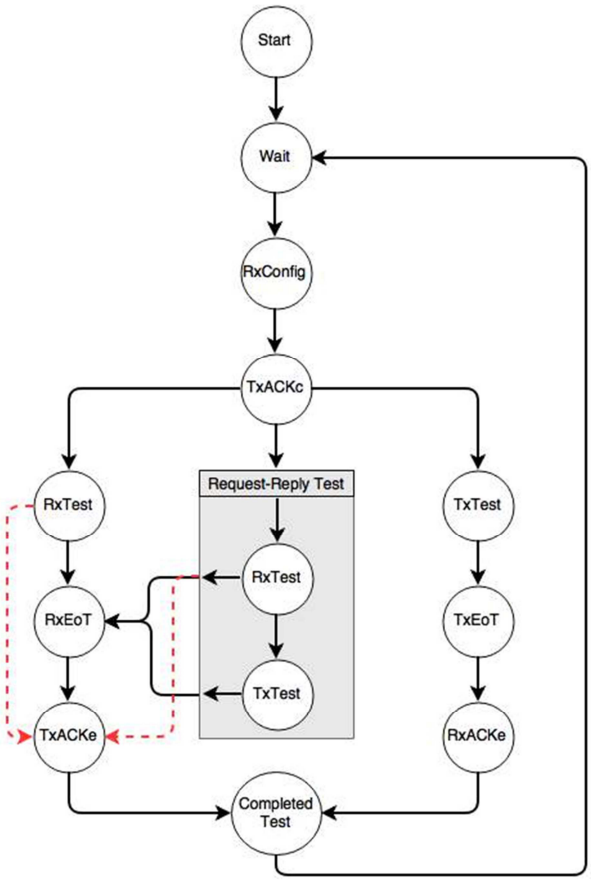

Figure 61 - End Device behavioural diagram

RxConfig: The interaction with the end device, Figure 61, begins with this state. This state is responsible for the reception of the configuration message from the coordinator device and consequently its validations.

TxACKc: The existence of this state is exclusive to the end device to maintain the synchronism level. In case of a successfully configuration message reception this state is responsible for the transmission, to the coordinator device, of one acknowledge indicating a successful reception. After send this confirmation the state is responsible to make the choice of the adequate next state to the architecture based on the received configuration message.

APPENDIX B - CNT-related health risk

Legislative frameworks are being built worldwide to deal with nanomaterial-based issues. These frameworks address the whole chain of values of nanomaterials, from definition (what is a nanomaterial?) to labeling (which products should be labelled as containing nanomaterials?) to life cycle analysis (what happens to nanomaterials during the life cycle of products containing them?) to risk assessment (what is the heal risk for workers? And for the general public?). The intense public interest on this topic has given rise to a plentiful literature which covers a wide range of societal, technical and scientific topics. The document[14] "Current legislative framework for nanomaterials Introduction to the impact assessment on transparency measures", by Maurits-Jan Prinz, 2014, summarizes clearly the 2014 status of this topic and lists the relevant EU legislations.

Among this plentiful of topics, the following section provides a state-of-the-art-based insight into the topic of CNT-related health risks, with a focus on the risks that might be relevant to Proteus goals and a discussion on how to address them. The SOTA evolves quickly, so the analysis will be updated regularly during the course of the project.

Toxicity of CNT

The toxicity of CNT has been widely studied. The comprehensive paper "Understanding the Toxicity of Carbon Nanotubes", Liu et al., Accounts of chemical research, 2013, 702-713, provides one of the many reviews on the topic. Roughly summarized, depending on the mode of exposure, CNT may reach any kind of cells in the body, from skin and lungs to heart and kidneys. Once in the body, they may cause a wide range of reactions, from no effect at all to cell damage and inflammation, even to genotoxicity and cancer ("Genotoxicity and carcinogenicity risk of carbon nanotubes", Toyokuni, Advanced Drug Delivery Reviews 65 (2013) 2098–2110).

These elements are only generality. Very importantly, the actual toxicity strongly depends on the specific morphology of the CNT under study: length, diameter, surface area, tendency to agglomerate, bio-durability, presence and nature of catalyst residues as well as chemical functionalization of the CNT. The publication "Determinants of carbon nanotube toxicity", Lanone et al., Advanced Drug Delivery Reviews 65 (2013) 2063–2069, provides a detailed analysis of these factors. Of course, the toxicity also depends on the intensity of the exposure, namely the duration of exposure and the quantity of CNT.

In our present project, we are considering multi-walled carbon nanotubes with diameter 9.5nm and length 1.5µm (from datasheet; the aqueous dispersion process may reduce the average length of the MWNTs). A next stage of the study (for instance for required the M18 review) could include a more detailed study from the bibliography on the impact of such types of MWNTs compared to other types, to determine whether switching to another type of CNT might be relevant on the short term (PROTEUS duration) and on the long term (industrialization)

[14] http://ec.europa.eu/DocsRoom/documents/5716/attachments/1/translations/en/renditions/native

Scenarios of exposure to CNT

Though there are results on toxicity of CNT, the effective risks depend on actual exposure (frequency and duration of exposure, quantity of products). Three types of exposure are usually considered, dermal contact, ingestion and inhalation, for two types of population, the workers involved in the manufacturing process (occupational hazard[15]) and the general public/end users. In Proteus (as well as in most nanomaterials related products), the worker category may be divided into two subcategories, the workers directly manipulating CNTs and the workers manipulating CNT-containing intermediate and end products. The post-use phase (end-of-life/recycling) raises specific concerns which are also quickly covered here[16].

1. Worker directly manipulating CNTs

a. inhalation

Regarding to worker exposure, inhalation may occur when CNT are fabricated (for instance when opening the fabrication chambers) or in powder form (when opening the containers containing CNT powder). Inhalation is the most problematic type of occupational exposure in the field of CNTs, as a contamination of air by CNTs is not easily contained; the equipment options to protect against it are also expensive and inconvenient to use.

As we use prefabricated, commercial CNT in PROTEUS, we are not directly concerned by the inhalation exposure during CNT fabrication. However, this type of exposure should be accounted for in a full-scale life cycle analysis of PROTEUS products.

In PROTEUS however, we are directly concerned by risk of inhalation of CNT when weighing them in solid form before putting them in liquid. Indeed, because of their low weight, CNT are easily suspended in air in the presence of air currents, typically the vertical aspirations encountered in chemical hood. For this reason, weighing of CNT is carried out in a (airtight) glove box, preventing any risk of inhalation of CNTs during weighing.

b. Dermal contact and ingestion

Workers could be exposed via dermal contact or ingestion to CNT in powder form and liquid dispersion. Traditional safety rules in chemical lab are specially designed to prevent this kind of exposure to chemicals: obligatory use of gloves and safety googles, interdiction of food and beverage in the lab. Like any other chemical, wrongful application of these rules might lead to exposure. The usual methods for mitigation should be implemented in case of accidental exposure.

[15] Occupational Exposure Assessment in Carbon Nanotube and Nanofiber Primary and Secondary Manufacturers: Mobile Direct-Reading Sampling, Dahm et al., Ann. Occup. Hyg., Vol. 57, No. 3, pp. 328–344, 2013

[16] Identification of starting points for exposure assessment in the post-use phase of nanomaterial-containing products, Ostertag et al., Journal of Cleaner Production 16 (2008) 938-948

A next stage of the study (for instance for required the M18 review) could include a more detailed study of lab precautions that have been proposed for handling nanomaterials (see for instance [17]), and the current practices in case of accidental worker exposure to nanomaterials.

2. Worker manipulating CNT-containing intermediate and end products

a. Assembly and characterization of sensor nodes including CNT

After CNT have been deposited on a substrate, CNT are not manipulated directly anymore. They are manipulated via a substrate (in Proteus either Silicon or glass). This substrate may be submitted to subsequent cleanroom processes, particularly in Proteus to packaging operations to yield a SoC (System On Chip). Then the SoC including the CNT on their substrate is integrated into a full sensor node.

For both these steps (from substrate to SoC, and from SoC to sensor node), exposure to CNT may only occur when the active area covered by CNT is touched by the worker and this only in the case where no glove is worn (dermal exposure). Directly touching the CNT-covered area may result into damaging the sensing device itself so it is to be avoided. It is expected to occur only as a rare, accidental event. Henceforth, to prevent accidental dermal exposure, the CNT substrate and then the SoC should always be manipulated with gloves (which is current practice anyway). No inhalation risk has ever been considered in this configuration.

When the chips are tested in liquid phase, the CNT are exposed to liquid. There is a risk that CNTs are released from the substrate and remain in the liquid phase (see section 2.4.6.3 for more details on this topic). As such, the liquid solutions used for benchmarking may be contaminated by CNT and should be treated following the common practices of the company regarding to waste chemicals incorporating nanomaterials. Some companies deal with them as with regular chemicals. Others have implemented specific guidelines. Whenever available in the company, these practices should be used. There does not appear to be a dedicated legal framework on these topics, only recommendations. Please note that the separation of the CNTs from the surface is detrimental for the operation of the sensors; as such, the sensors will be designed to minimize this loss of CNTs and the actual release is expected to be very small.

b. Manipulation of sensor nodes including CNTs

During service life, the risk of exposure to the workers manipulating the sensor nodes lies in them accidentally touching the active CNT area with bare hands. As this type of contact to the sensors is detrimental to the sensor function anyway, the sensor outer packaging should be designed to prevent such accidental contact.

3. General public

[17] "Safe handling and use of carbon nanotubes in the workplace", Information sheet, 2012, www.safeworkaustralia.gov.au

For the general public, exposure would exclusively be by ingestion of CNTs released from the surface of the sensor and dispersed in the drinkwater. This scenario of exposure can only be prevented by covering the CNT layer by an additional layer, which would remove the risk of CNT release from the surface. However, this layer would be drastically detrimental to the sensor sensitivity (though the use of a porous layer material may also proposed). On the other hand, considering the small surface area of CNT coverage, it appears likely that the quantity of CNT released over the lifetime of the devices is very low compared to threshold levels of health risk via ingestion.

We propose to go into more details into this topic in the next stage of this study due M18, with a detailed analysis of CNT mass expected to be released into the water over the lifetime of the sensors, to compare them to toxicity threshold of other drinkwater pollutants.

4. End-of-life/recycling operations

The end-of-life procedures for electronic products constitute an ongoing debate[18]. Disposal of sensor nodes including CNT and more generally nanomaterials should be discussed within this framework.

Roughly speaking, two options might be considered, though we are too early in the project to anticipate which might be implemented for Proteus nodes:

- Nodes go through the recycling chain for electronic products: in this case, the sensor part could be separated from the rest of the node and destroyed separately in a nanomaterial-compatible process.
- Waste disposal of the node (generic waste disposal): there is a risk that the CNTs are released in time from the substrate under the effect of water, and contaminate the water. If this water is not contained (in unauthorized dump sites), the CNT may enter the environment. The environmental life cycle of nanoparticles and CNTs is a widely studied topic (see for instance [19]), as the general public may in turn be exposed to the nanoparticles stored in the environment.

Note that the quantities of CNT involved here are extremely weak compared to already existing, commercialized CNT (and more generally nanomaterial-based) products, so the environmental impact of Proteus node is expected to be very limited.

Release of CNT from a surface

From the previous section, it appears clear that the main risk related to CNT in the present project is associated to uncontrolled release of CNT from the substrate surface (glass or silion) in the presence of water.

This release should be quantified as much as possible from theoretical consideration. A series of reference paper are available today to analyze and quantify the mechanics of CNT release, most

[18] Recycling of WEEEs: An economic assessment of present and future e-waste streams, Cucchiella et al., Renewable and Sustainable Energy Reviews, Volume 51, November 2015, Pages 263–272
[19] Potential Release Pathways, Environmental Fate, And Ecological Risks of Carbon Nanotubes, Petersen et al., Environ. Sci. Technol. 2011, 45, 9837–9856

recently the papers „Influence of Solution Chemistry on the Release of Multiwalled Carbon Nanotubes from Silica Surfaces“, Environ. Sci. Technol. 2013, 47, 12211−12218; and „Release Kinetics of Multiwalled Carbon Nanotubes Deposited on Silica Surfaces: Quartz Crystal Microbalance with Dissipation (QCMD) Measurements and Modeling“, Environ. Sci. Technol. 2014, 48, 4406−441, both by P. Yi and K. L. Chen.

These papers rely notably on earlier research from the microelectronics industry developed over 30 years ago to optimize the cleaning process for SiO2 substrates, for instance „Particle Adhesion and Removal in Model Systems. Part V. Interpretation of the Kinetics of Particle Detachment“, Nelligan et al. Journal of Colloid and Interface Science, Vol. 89, No. 1, September 1982; or more recently „Describing hydrodynamic particle removal from surfaces using the particle Reynolds number“, Burdick et al., Journal of Nanoparticle Research 3: 455–467, 2001.

In the next stage of this study by M18, we will go into more details on this topic.

Summary and next stage of the study

There are consistent reports on toxicity of CNTs in the literature, with effects ranging from mild to intense. The actual health risk however depends both on the actual morphology and chemistry of the CNTs under study, and on the specificity of the exposure (duration and concentration of particles). It can be drastically reduced by minimizing exposure, and by selecting types of CNTs with low toxicity.

Exposure scenarios for the workers manipulating the CNTs and or manipulating the final Proteus nodes are easily described and easily prevented by using classical operating rules for chemistry and electronics labs.

Exposure of the general public is a more complex topic. In case of Proteus, it may occur via release of the CNT from the surface and contamination of the drinkwater, either directly for drinkwater nodes, or indirectly after environmental storage of the CNTs. To mitigate this risk, one has to mention that the quantity of CNTs involved in Proteus process are extremely low compared to most nanomaterial-based products.

Based on this first analysis, in the next stage of the study of CNT health impact due M18, we propose to study the following aspects:

- Detailed analysis of toxicity (including threshold) for non-functionalized MWNTs with 10nm diameter and less than 1.5µm length.
- Analysis of release mechanisms of CNTs from silica and glass substrates, in order to assess the potential volume of CNTs released in the drinkwater and in the environment from Proteus nodes.
- SOTA of current practices in terms of occupational handling of nanomaterials.